UNIVERSITY OF MINNESOTA
ST. ANTHONY FALLS HYDRAULIC LABORATORY

Project Report No. 304

RESERVOIR SEDIMENTATION AND SEDIMENT SLUICING: EXPERIMENTAL AND NUMERICAL ANALYSIS

by

Rollin Hull Hotchkiss

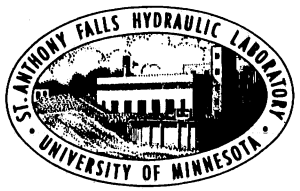

Prepared for

Legislative Commission on Minnesota Resources
State of Minnesota

January 1990

Minneapolis, Minnesota

University of Minnesota
St. Anthony Falls Hydraulic Laboratory

Project Report No. 304

RESERVOIR SEDIMENTATION AND SEDIMENT SLUICING: EXPERIMENTAL AND NUMERICAL ANALYSIS

by

Rollin Hull Hotchkiss

Prepared for

Legislative Commission on Minnesota Resources
State of Minnesota

January 1990

ABSTRACT

Reservoir sedimentation and sediment sluicing are simulated in laboratory and numerical experiments.

The laboratory experiments are conducted in a 12.2 meter long, 0.38 meter high, 15 centimeter wide flume. The flume was later modified by adding a 2 meter expanding section at the downstream end. A sluice gate extending completely across the flume width was installed about 9 meters downstream from the entrance for the first set of experiments. Later this sluice gate was replaced with a simulated dam 1.5 meters into the expanding section. The dam was fittedwith three sluice gates, each 0.15 meters wide. All gates were manually operated; each gate could be set separately.

All experiments were performed with lightweight sediment consisting of crushed walnut shells with a mean diameter of 0.67 millimeters, gradation coefficient of 1.3, porosity of 0.53, and specific gravity of 1.35.

Steady water discharges ranged from 1.5 to 4.25 liters per second and sediment feed rates (input at the upstream end of the flume) ranged from 50 to 570 grams per minute.

Upon lowering the sluice gate(s) more than about fifty per cent of the flow depth, all incoming sediment deposited near the flume entrance in response to the rise in water surface. Deposition continued until the flow depth at the entrance decreased sufficiently to produce adequate velocity for sediment transport. This process formed a delta, characterized by a steep foreset front with a slope near the submerged angle of repose. Sediment was transported over the delta lip and deposited on the foreset slope, thus moving the delta forward in the flume. Near uniform depth and slope were maintained upstream of the delta lip. The delta stopped moving forward near the sluice gate, and all incoming sediment passed over the delta lip and under the sluice gate(s). At this time the flow field in the flume appeared exactly as before lowering the sluice gate(s), except that the the bed had risen as much as the water surface and a delta was in place in front of the sluice gate(s).

Upon raising the sluice gate(s) after a delta had reached equilibrium, the water surface dropped at the dam and sediment transport was increased significantly. The drop in water surface and increase in sediment transport proceeded upstream, causing upstream progressing degradation of the bed. This process continued until a new equilibrium condition was established, consisting of uniform flow with a water surface parallel to the previous condition but lower by an amount equal to the drop in water surface at the dam.

A one dimensional numerical model was developed for aggradation and sediment sluicing in reservoirs. The quasi-steady, one-dimensional St. Venant equations were used to represent the flow field; the sediment continuity equation supplemented by a form of the sediment transport equation due to Parker (1976) described sediment movement. All computations were corrected for flume sidewall and bedform influences. The equations were solved in a decoupled fashion by first computing a backwater profile and

then adjusting the bed elevations accordingly. Subcritical flow is maintained at all times in the model.

In the numerical model, the delta was simulated by a vertical shock face, fittedto the bed at a location where the steepening bed slope exceeded the original slope by at least five times. The shock face was moved forward each time step an amount equal to the volume of sediment passing the face divided by the cross-sectional area of the face. Computed water surface and bed profiles compare very well with the experimental data. The computed shock face moved forward 27 per cent faster than observed, due to a 22 per cent higher-than-observed computed sediment transport rate for the flume.

Sediment sluicing for the flume was simulated by lowering the water surface at the downstream boundary of the model in discrete steps so as not to cause supercritical flow. Agreement with observed experimental results was good.

The model was applied to the Granite Falls Dam on the Minnesota River as an example of field case application. The dam was first closed in 1871 and was completely full of sediment from 20 to 58 years later. Model results with three different lengths of backwater zones predicted complete sedimentation in 35 to 48 years from closure. Sluicing was modeled by initially drawing down the water surface at the dam to within one per cent of critical depth. Subsequent water surface elevations were lowered as much as the bed at the dam was eroded, thus preserving the near-critical flow condition at the dam. Results showed that the bed near the dam was eroded to pre-closure conditions in less than three months, and that the upstream progressing degradation was nearly complete after about ten years of simulation.

The equations of motion for gradually-varied flow were examined for steady-state equilibrium conditions, and algebraic equations were developed describing the response of the streambed to changes in channel width. The equations, applicable to a rectangular channel, include inertial and pressure effects, but do not account for sidewall or bedform influences.

Equations were also developed for the case of a rectangular channel with a sinusoidal pertubation in width. The first order solution of the pertubation expansion shows the bed response lags the width pertubation as a function of sediment transport and Froude number. As an example of the effects such a channel produces, the equations were applied to the Minnesota River for a low discharge, the mean annual discharge, and bankfull discharge. Perturbation amplitude was equal to ten percent of the uniform channel width. Results show that the location of maximum bed scour migrates downstream for increasing discharge. Specifically, the location of maximum scour for bankfull discharge is at the narrowest section of the channel. This result explains the field observation that scour problems appear to be worst at narrow channel sections where most bridges, crossings, and stream gage stations are located.

CONTENTS

LIST OF FIGURES

LIST OF TABLES

LIST OF SYMBOLS

A	cross-sectional flow area [L^2]
a	reference elevation in Rouse equation for suspended sediment concentration [L]
a_1,b_1,c_1	coefficients in Li, Mussetter, and Grindeland equation (1988) for sand wave celerity
B	phase lag or lead, degrees
b	stream width; half-width in Chapter 5 [L]
C	Chezy coefficient [$L^{0.5}T$]
c_2	coefficient in Parker equation (1976)
c_3	coefficient in Woolhiser and Lenz equation (1965)
c_4	coefficient in sediment transport power law
C_a	suspended sediment concentration at reference elevation, a [MM^{-1}]
C_d	sluice gate discharge coefficient
C_f	total friction factor
C_n	sand wave celerity [LT^{-1}]
C_y	suspended sediment concentration at depth y [MM^{-1}]
d	distance upstream of sluice gate the bed is scoured to the bottom of the flume [L]
d_{50}	median sediment diameter [L]
Dk	pertubation amplitude = D times k, where k is a wave number = $\frac{2\pi}{\lambda}$
E_c	capacity ratio
E_s	scouring efficiency
E_t	time factor
f	Darcy-Weisbach friction coefficient
F_r	Froude number
G	bed material transport, [lb/sec], in Woolhiser and Lenz equation (1965)
g	gravitational acceleration [LT^{-2}]
H	total energy head [L]
h	cross-sectionally averaged depth above mid-dune [L]
h_g	sluice gate opening [L]
h_N	normal flow depth [L]
k	wave number = $\frac{2\pi}{\lambda}$
k_s	roughness height [L]
m	slope of the line expressing how the laboratory flume diverges with increasing x
ν	kinematic viscosity [L^2T^{-1}]
n	Manning's coefficient
p	wetted perimeter
Q	stream discharge [L^3T^{-1}]
q	water discharge per unit width [L^2T^{-1}]
q_s^*	dimensionless sediment transport per unit width
Q_f	volume of water used in flushing [L^3]
q_s	volumetric sediment transport rate per unit width [L^2T^{-1}]
R	submerged specific gravity

r	hydraulic radius [L]
r_N	hydraulic radius pertaining to normal flow [L]
Re	Reynolds number
S	deviation from normal slope
S_f	energy slope
S_o	channel slope
t	time [T]
τ_r^*	dimensionless critical shear stress in Parker equation (1976)
T_f	fraction of a year used in flushing
T_r	fraction of a year that a river's sediment load will take to refill V_a [T]
U	velocity of delta apex parallel to original bed [LT^{-1}] in Ashida equation (1980)
u	cross-sectionally averaged velocity [LT^{-1}]
u_*	shear velocity [LT^{-1}]
u^*	$u^* = \frac{u^2}{\rho g R d_{50}}$
V	velocity of delta apex perpendicular to original bed [LT^{-1}] in Ashida equation (1980)
V_a	storage volume added by flushing [L^3]
V_o	original live reservoir capacity [L^3]
w	width of sluice gate opening [L]
X	velocity correction factor in Einstein-Barbarossa equation (1952)
x	horizontal distance [L]
y	water depth above mid-dune elevation [L]
z	exponent in Rouse equation for suspended sediment concentration

Greek letters

α	$\alpha = D k (\frac{2N-3}{2N})(1 + \beta^2)^{\frac{1}{2}}$ in pertubation expansion
β	$\beta = \frac{2Nk}{\varepsilon(2N-3)}(\frac{Fr_o^2(1-2N)-1}{2N})$ in pertubation expansion
Δ	change in a variable
δ	$\delta = \frac{11.6\nu}{u_{*g}}$ = laminar sublayer thickness [L]
Δt	time step in finite difference method [T]
Δx	distance step in finite difference method [L]
ε	aspect ratio times friction factor = γC_f
ϕ	weighting factor in finite difference method
γ	aspect ratio = $\frac{b}{h}$

η	cross-sectionally averaged bed elevation [L]
κ	von Karman constant
λ	wavelength of perturbed channel or meandering channel
λ_p	porosity of sediment
θ	momentum flux correction factor
ρ	density of water [ML^{-3}]
τ_b	total bed shear stress [$ML^{-1}T^{-2}$]
ω	$\omega = Dk \cdot sinkx$ in pertubation expansion
ξ, ξ_R, ξ_T	water surface, headwater, and tailwater elevations, respectively [L]
ψ	$\psi = (\frac{2N-3}{2N})Dk$ in pertubation expansion
ζ	ratio of water to sediment discharge

Superscripts

*, ^	dimensionless notation

Subscripts

b	pertaining to the bed
g	pertaining to a grain (skin)
w	pertaining to the wall
*	pertaining to shear values
o	equilibrium values
i	distance node in finite difference method
j	time node in finite difference method

Units

L	length
M	mass
T	time

ACKNOWLEDGEMENTS

This research described in this report was funded by the Legislative Commission on Minnesota Resources. Computer funding was provided by the University of Minnesota Academic Computing Services and Systems center.

This report is based on a thesis submitted to the University of Minnesota Graduate School by Rollin Hotchkiss as partial fulfillment of the requirements for the degree of doctor of philosophy. This report was prepared under the advisorship and auspices of Dr. Gary Parker, Department of Civil & Mineral Engineering, University of Minnesota.

1. INTRODUCTION

The purposes of the Introduction are to discuss the extent and effects of reservoir sedimentation, to state the objectives of the research, and to describe the remainder of the thesis.

1.1 Extent of Reservoir Sedimentation

All streams and rivers carry sediment - particles of clay , silt, sand, or gravel. When streams or rivers enter a reservoir, the cross-sectional flow area increases, water velocity decreases and sediments begin to deposit. The largest sediment particles settle farthest upstream, followed by progressively smaller and smaller particles downstream. The deposition process forms a delta in the headwater area of the reservoir that extends further into the reservoir as deposition continues (see Figure 1.1). Over time, the delta can essentially fill the reservoir with deposited sediments and eliminate the benefits for which the dam was built.

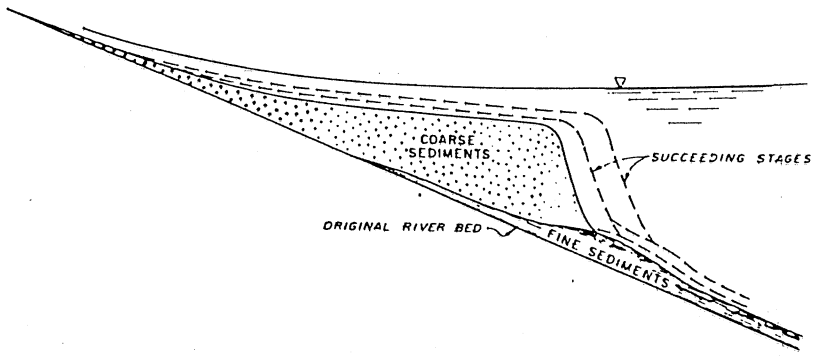

Figure 1.1 Profile of typical reservoir delta (from Vanoni, 1975, p. 349. With permission ASCE)

Vanoni (1975) estimates the original capacity of large reservoirs in the United States was 0.4 billion acre-feet (494 km^3) and that about 1 million acre-feet (1.23 km^3) is occupied by deposited sediment each year. The annual cost of replacing this lost storage capacity has been estimated at 150 million dollars (Mahmood, 1987). Areas in the midwest and southeast experience higher rates of deposition. Thirty-five percent of dams built in these areas of the United States before 1935 had lost between 1/4 and 1/2 of their original storage capactiy by 1970. Fourteen percent of the dams lost between 1/2 and 3/4 their original capacity, while 10 percent had been converted to run-of-river projects - essentially full of deposited sediment (Vanoni, 1975).

Mahmood (1987), describing average worldwide deposition, estimates about 41 million acre-feet (50 km^3), or roughly 1 percent of worldwide gross storage capacity, is lost each year. Annual storage replacement costs would be more than 6 billion dollars.

1.2 Effects of Reservoir Sedimentation

In addition to the economic cost of replacing storage capacity, reservoir sedimentation also has negative impacts on other project benefits. Evrard (1983) and Garde and Ranga Raju (1985) discuss the following examples:

1. reduction in upstream navigational bridge clearance,
2. increase in upstream flood levels,
3. increase in upstream water table elevations, thus encouraging marsh growth and loss of land,
4. increase in water losses due to evaporation and transpiration,
5. blockage or clogging of upstream water intakes,
6. rise in base levels on tributary streams and a subsequent increase in aquatic growth,
7. reduction of water supply for irrigation, industry, and recreation, and
8. reduction of flood control benefits

1.3 Purpose and Organization of Thesis

The purpose of the investigation described herein is to perform basic research on sediment sluicing as a method to restore or maintain reservoir storage capacity. The objectives are a) to understand the nature of reservoir aggradation and degradation in simple cases using laboratory models, and b) to develop a one-dimensional mathematical model to describe the physical processes involved.

The remainder of the thesis is organized as follows: first a literature review describes the process of reservoir sedimentation in detail, including methods of preserving reservoir capacity and sediment sluicing effectiveness. The review also discusses experimental and mathematical modeling approaches used in past reservoir sedimentation investigations. The experiments are then described, including the setup, procedure, and results. Development and testing of the numerical model are then presented including an illustration of a field-scale case. This is followed by the development of equations for the bed slope and elevation of rectangular channels of varying width.

2. LITERATURE REVIEW OF RESERVOIR SEDIMENTATION

The purpose of this chapter is to describe the process of reservoir sedimentation and how it has been modeled experimentally and numerically.

2.1 Description

Forces responsible for moving sediment include gravity, turbulence, and flow forces such as drag and lift. As water and sediment enter the backwater reach of a reservoir, the velocity decreases, the turbulent fluctuations are damped, and particles begin to settle out.

2.1.1 Deposition Pattern

The sediment depositional pattern depends on the size and size distribution of the sediment, the shape of the reservoir, the reservoir operation plan, and previous deposition. The coarsest particles settle in the upstream reach initially affected by backwater. Subsequent coarse particle (i.e. bedload) deposition extends in both the upstream and downstream directions as the initial backwater zone responds to the increase in bed elevation level. The coarse deposits form a delta . The delta width usually increases in the downstream direction except in narrow, gorge-like reservoirs. Based on observations made of wider reservoirs, the flow concentrates in a width slightly larger than the incoming channel, periodically shifting laterally by avulsion to spread across the reservoir width (Bondurant, 1955, and Mahmood, 1987).

The delta topset slope in storage reservoirs of varying width, representative of the delta in its growth stage, is most commonly observed to be between one-half and two-thirds the original river bed slope (Borland, 1971).

Aside from storage reservoirs, several researchers have investigated the equilibrium channel slope attained upstream of debris reservoirs and gully control structures (Johnson and Minaker, 1944, Woolhiser and Lenz, 1965, Sugio, 1966, and Sugio, Hashino,and Sasaki, 1973). These are generally small structures designed to trap sediment or stabilize stream channels. Observations of hundreds of these structures generally show flatter channel slopes than in the original channels. Johnson and Minaker believe the upstream channel slope should eventually equal the original slope, and argue that the observed channels had not yet reached equilibrium. Woolhiser and Lenz, however, show that the equilibrium channel slope may indeed be flatter if the final channel is wider than the original one.

If S is the equilibrium slope of a channel in which the characteristic width, roughness, and discharge vary from a channel with slope S_o, they showed

$$\frac{S}{S_o} = \left(\frac{G}{G_o}\right)^{\frac{5}{7}} \left(\frac{c_3}{c_{3o}}\right)^{\frac{5}{7}} \left(\frac{Q_o}{Q}\right)^{\frac{6}{7}} \left(\frac{n_o}{n}\right)^{\frac{6}{7}} \left(\frac{b}{b_o}\right)^{\frac{1}{7}} \qquad (2.1)$$

using the DuBoys sediment transport equation where G = bed material transport [lb/sec], c_3 = coefficient, Q = stream discharge [ft^3/sec], n = Manning's coefficient, and b =

stream width [ft]. Note that if b is greater than b_o, S is less than S_o. Their field data showed ranges in the ratio of debris channel slope to original slope from 0.3 to 0.95.

The downstream depositional face of the delta is called the foreset slope. Strand and Pemberton (1982) find the foreset slope in storage reservoirs of varying width is most often about 6.5 times that of the topset slope, with variations of up to 100 times the topset slope. No descriptions of the sediment material (i.e. fine, coarse, cohesive, etc.) were given in the study.

The finer sediment particles, including the washload, continue in suspension longer and deposit more uniformly throughout the reservoir. These sediments form bottomset beds and are often composed of cohesive and small non-cohesive particles (Graf, 1977). The role of fine sediment in reservoir deposition ranges from negligible, as reported by Graf in describing alpine reservoirs, to important, as reported by Chen (1988) in describing a Chinese reservoir. Some of the fine particles pass over the reservoir spillway or through intermediate outlets without depositing in the reservoir. Certain hydraulic conditions produce density currents consisting of fine suspended particles which plunge with the flow and move toward the dam as an underflow. If not released through sluice gates, the fines deposit in front of the dam. Fine particle deposition and transport is not considered in this thesis.

Mukhamedov (1981), describes rare observations of the sedimentation process in small, narrow, run-of-the-river projects in Russia. He explains that in projects with heads of 3 - 4 meters, deposition is from bedload, which forms a "bank" that advances slowly towards the dam. After the dam is filled with sediment, which usually takes 2 - 3 years, Mukhamedov observes "the hydraulic regime of the river almost approaches that of the free flow."

2.1.2 Experimental Investigations

Temporal and spatial scales of reservoir deposition are usually so large, typically encompassing years of time and spans of several kilometers, that field observation of the deposition process is difficult. Past laboratory experiments have provided insight into the basic mechanics of deposition. While mostly qualitative, they give a general picture of the sedimentation process, particularly for the coarser sediments.

Garde and Ranga Raju (1985) perform the following thought experiment on reservoir deposition. They explain (for a vertical-walled reservoir) that

> "Because of backwater formation the velocity reduces as water flows towards the dam...Hence the coarser material deposits farther away from the dam, while finer material is deposited closer to the dam. With continuous deposition of material on the bed the level rises up to C3 [top of dam]. Ultimately the new profile passes through C3 and is parallel to AC [the original bed]."

Thus in the ultimate condition where sediment completely fills the reservoir, the upstream bed has been raised uniformly by an amount equal to the dam height, and the influence of the reservoir extends infinitely far upstream.

Insight into the actual process is provided by other researchers. Chee and Sweetman (1971) and Chee (1983) performed a series of laboratory experiments simulating a dam in a gorge-like setting. The purpose of their studies was to test various

bedload transport formulae in a depositional environment. Upon causing a rise in the downstream water surface, Chee and Sweetman describe the sedimentation process:

> "At the commencement of the introduction of sediment flow, a mound of sediment initially formed at the inlet to the reservoir. The sediment bank filled the full width of the channel and gradually increased in size until stable hydraulic conditions were attained. Sediment is then transported on the surface of the bed as bedload and deposited on the steep leading face. The sediment bed advanced rapidly in this manner until the entire reservoir was filled. Further addition of sediment resulted in its transportation over the outlet weir. The disposition of the sediment was always very regular."

Bhamidipaty and Shen (1971) conducted general experiments on degradation and aggradation. For the aggradation studies, a straight, narrow flume with a sand bed in equilibrium was surcharged with an additional constant sediment load at its upstream end. They describe the results:

> "If the sediment supply is suddenly increased at a given section, A, the stream cannot carry the excess sediment because the sediment transport capacity of the stream is exceeded. First, the excess sediment is deposited at Section A, and the flow condition continues to change until a new equilibrium slope is reached at Section A over which the stream can transport the supplied sediment without either deposition or scour. The entire stream behaves as if it consists of two entirely different reaches, an upstream aggrading reach and a downstream reach (where the flow condition is more or less undisturbed by the excess sediment supply) with a short transition reach in between. The upstream aggrading reach extends gradually downstream."

The foreset slope was observed to be between 31° and 34 °, which is very nearly the submerged angle of repose for the sands used.

Sugio (1972), in a discussion of Bhamidipaty and Shen, describes his experiments using a 20 mm high dam in a long, narrow flume with sand as the sediment. Holding the inflow of water and sediment constant, he states "a definite sediment front was formed...increasing its size and decreasing its advancing speed. The water surface...rose almost as much as the aggraded height."

For small ratios of sediment to water discharge Sugio concludes that the aggrading profile can be considered to be almost in an equilibrium state even if the sediment front is advancing.

Chitale, Galgali, and Appukuttam, (1975), in a scale model study of reservoir deposition on the Beas River, observed that the slope of the depositional delta was the same as the original river bed after 10 simulated flood seasons.

In summary, for coarse sediments, i.e. those likely to be transported as bedload rather than suspended load, a depositional delta forms and is composed of two parts: the foreset slope, equal to or near the submerged angle of repose, and the topset slope, which approximates the original bed slope. The delta gradually moves downstream into the reservoir, maintaining its shape (in narrow channels). The delta eventually approaches

the dam, where further inflowing sediment passes over the dam (in the simple model described above).

2.1.3 Methods of Preserving Reservoir Capacity

Since the primary purpose of a reservoir is to provide for the storage of water, preserving and maintaining storage capacity is very important. Fan (1983) discusses four different approaches to maintaining storage capacity: watershed management, preventing sediments from entering the reservoir, mechanical means of removing sediment, and sediment sluicing.

The goal of watershed management for reservoir sedimentation is to reduce soil erosion at its source. Techniques available for erosion control include

1. reforestation,
2. grazing control,
3. changing local industry,
4. grass planting,
5. terracing with or without agriculture,
6. constructing check dams and drop structures,
7. crop rotation, and
8. contour farming.

Preventing sediments, once eroded, from entering the reservoir necessitates either natural or man-made sediment traps in the reservoir upper reaches, or bypassing the incoming sediment through diversion works.

Once deposited, sediment may be removed mechanically or may be flushed through sluice gates. Mechanical methods of sediment removal include dredging and hydraulic siphoning. According to Annandale (1987), dredging is not often an economical solution to the sediment storage problem. He concludes that it is usually more economical to build a new reservoir to replace the lost storage than to dredge the sediment. Siphoning sediment over or through the dam is documented in Fan (1983), and is a relatively new approach to sediment removal.

Sediment sluicing is defined as the evacuation of sediment from a reservoir by passing water and sediment through sluice gates located at or near the bottom of a dam. Sediment sluicing increases storage capacity by 1) completely scouring deposited sediment in the vicinity of the sluice gates and 2) lowering the general level of deposits upstream. The first of these processes decreases granular transport through the turbines and thus reduces damage to the turbine blades. However, since the scour is local, restored reservoir capacity is minimal. The second process, by lowering the general level of deposits upstream, can restore significant storage capacity.

White and Bettes (1984) used potential flow theory to simulate flow under a sluice gate for static (zero inflow) conditions. They showed, using a critical erosive velocity approach, that the distance from the outlet at which the velocity falls below critical is relatively short. This means that complete scouring is limited to the local vicinity upstream of the sluice gate. They further showed that water levels must be lowered significantly upstream to move sediment to the sluice gate area.

Sediment sluicing is usually performed via flow regulation during floods or by drawing the reservoir down using the sluice outlets.

Flow regulation during floods using sluice gates is practiced regularly in China. The Chinese philosophy of sediment management is to store clean water and to discharge muddy water for downstream diversion to agricultural lands (Xia and Ren, 1980). This philosophy is a necessary part of sediment management in a country where commonly 80 to 90 percent of the annual sediment enters the reservoir in a 2 month flood season (Zhang, Xia, Chen, Li, and Xia, 1976).

Drawdown flushing is performed by completely draining the reservoir through the sluice gates. High water velocities in the resulting shallow flows are effective in eroding a channel within the reservoir deposits. Drawdown flushing can be economically performed in irrigation reservoirs that have a dependable inflow volume each year. It is performed at the expense of hydroelectric benefits.

2.1.4 Sluicing Effectiveness

In 1975, Vanoni stated that the removal of material by sluicing is seldom, if ever, practical, resulting only in a deep, narrow channel through the deposited sediment which he deems restores only insignificant reservoir capacity. White, quoted in Annandale (1987), says sediment sluicing can be effective if performed by drawdown flushing, but that it is prudent for only very small reservoirs. The restriction to very small reservoirs concerns the reliability of the natural water supply. Since drawdown flushing largely depletes the stored water supply, he suggests the annual inflow should be 50 times larger than reservoir capacity to ensure a dependable supply of water to the reservoir.

Many others, however, have demonstrated that sluicing can be effective in restoring and preserving significant reservoir storage. Recently, Paul and Dhillon (1988) reviewed the sediment sluicing experience of 6 countries and concluded "hydraulic flushing is an efficient technique for the removal of sediment deposits, not only from small reservoirs (with capacities of less than 100 million m^3) but also from large-scale reservoirs (with capacities of up to 10,000 million m^3)." They go on to suggest, based on existing literature, that the optimum height of the sluice gate is 1.5 to 2.5 meters, and that the required sluicing area can be obtained from Figure 2.1. They comment that the required sluice area should be obtained by increasing the sluice gate width rather than height. They also plot the variation in the volume of sediment flushed with the volume of water used for the flushing, reproduced here in Figure 2.2.

Sediment sluicing is practiced routinely in China, where high sediment loads necessitate regular flushing operations. Several researchers have reported that sediment sluicing, especially practiced by drawdown flushing, can be very successful (Fan, 1983, Zhang, Long, and Jiao, 1980, Yan and Xu, 1980, Cao and Chen, 1980, Xia and Ren, 1980). Xia and Han (1980) report that from 11 to 71 percent of the original storage capacity can be restored depending on the shape of the reservoir. Wide reservoirs with extensive floodplain deposits are not as amenable to sluicing as narrow, gorge-like reservoirs.

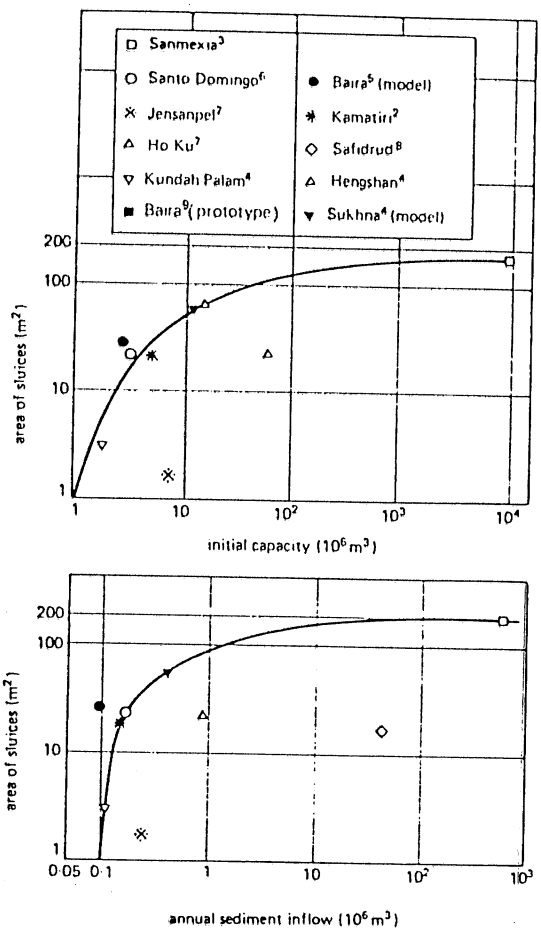

Figure 2.1 Suggested design curves for flushing sluices (from Paul and Dhillon, 1988)

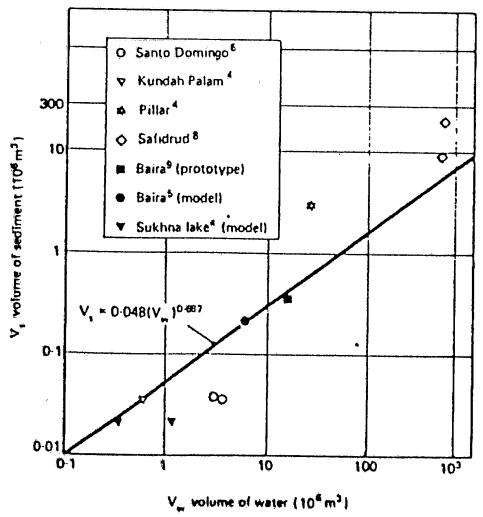

Figure 2.2 Variation of sediment flushed with water used (from Paul and Dhillon, 1988)

According to Bogardi (1974) sluicing will in general be more effective if:

1. water depths are low and discharge is high,
2. sluice gates are wide and located near the bottom of the dam,
3. the original streambed is steep and the reservoir has a short, straight bottom, and
4. the reservoir is in an advanced stage of siltation and the deposits consist of fine grained, recently settled material.

Mahmood(1987) summarizes sediment sluicing techniques and adds that sediment sluicing is not effective unless the reservoir is drawn down to an extent that flow conditions over the deposits approach those of the original river and remain low for up to several months. He cautions that clay layers just a few years old can constitute a sediment control section and effectively retard sediment flushing.

During sluicing operations, there can be a danger of massive slides of sediment blocking the gated outlets. This was observed by Mikhalev (1971) during experimental studies of sluicing from mountain reservoirs. A siphon inlet was built in the Santo Domingo reservoir, Venezuela, to cope with the blockage problem (Mahmood, 1977).

Finally, Mahmood introduces terms to evaluate reservoir sediment sluicing effectiveness. These are:

1. scouring efficiency, E_s, defined by

$$E_s = 100 \cdot \frac{V_a}{Q_f} \qquad (2.2),$$

2. capacity ratio, E_c, defined by

$$E_c = 100 \cdot \frac{V_a}{V_o} \qquad (2.3),$$

and

3. time factor, E_t, defined by

$$E_t = \frac{T_r}{(1-T_f)} \qquad (2.4),$$

where V_a = volume added by flushing, Q_f = volume of water used in flushing, V_o = original live reservoir capacity, T_r = fraction of a year that the river's sediment load will take to refill V_a, and T_f = fraction of a year used in flushing.

Note that if E_t is less than or equal to 1.0, it will be possible to increase available storage from year to year. If E_t is greater than 1, the annual capacity will decrease and flushing will not be effective in the long term.

2.2 Numerical Models

Methods for predicting sedimentation in reservoirs can be classified into 2 broad categories: empirical and mathematical (Mahmood, 1987). Empirical methods are based on an understanding of physical processes, but rely on inductive analyses of data for the development of predictive relationships. A well known empirical method for predicting trap efficiency, for example, was developed by Brune (1953). Discussion of this and other empirical relationships may be found in Annandale (1987) and Fan (1983). The remainder of this literature review focuses on mathematical models.

2.2.1 Governing Equations

For this investigation, the bedload sediment transport and deposition of cohesive, uniform material is to be modeled for a variable-width, vertical-walled reservoir with a longitudinal dimension that far exceeds the lateral dimension. A one-dimensional mathematical model should be adequate except in the immediate vicinity of a steep delta or near the sluice gates.

The problem has five unknowns, each a function of distance and time: velocity, depth, sediment movement, friction slope, and bed elevation (see Figure 2.3). Channel width is known at all locations. The unknowns may be found using the three partial differential equations that govern water and sediment movement, and two constitutive relations. Under the conditions described above, the appropriate one-dimensional equations are the St. Venant equations for momentum and continuity:

$$\frac{\partial(u\,h\,b)}{\partial t} + \frac{\partial(u^2\,hb\theta)}{\partial x} = -g\,b\,h\frac{\partial \xi}{\partial x} - p\,C_f u^2 \qquad (2.5);$$

$$\frac{\partial(h\,b)}{\partial t} + \frac{\partial(u\,h\,b)}{\partial x} = 0 \qquad (2.6);$$

the conservation of mass equation for sediment:

$$\frac{\partial(\eta\,b)}{\partial t} + \frac{1}{1-\lambda_p}\frac{\partial(q_s\,b)}{\partial x} = 0 \qquad (2.7);$$

a functional relationship for sediment transport such as

$$q_s = f(\tau_b) \qquad (2.8);$$

and an equation relating friction slope to flow and sediment characteristics:

$$S_f = f(u,h,q_s...) \qquad (2.9),$$

where u = cross-sectionally averaged velocity [LT^{-1}], b = channel width [L], t = time [T], x = horizontal distance [L], θ = momentum flux correction factor for non-uniform velocity distributions, g = gravitational acceleration [LT^{-2}], h = cross-sectionally averaged depth [L], ξ = water surface elevation [L], p = wetted perimeter [L], C_f = friction factor, S_f = friction slope [1], η = bed elevation [L], λ_p = porosity of bed sediment [1], q_s = volumetric sediment transport rate per unit width [L^2T^{-1}], and τ_b = bed shear stress [$ML^{-1}T^{-2}$]. In addition, recall that $\tau_b = \rho\,C_f\,u^2$, where ρ = density of water [ML^{-3}], and that $S_f = \frac{C_f u^2}{rg}$, where r = hydraulic radius [L].

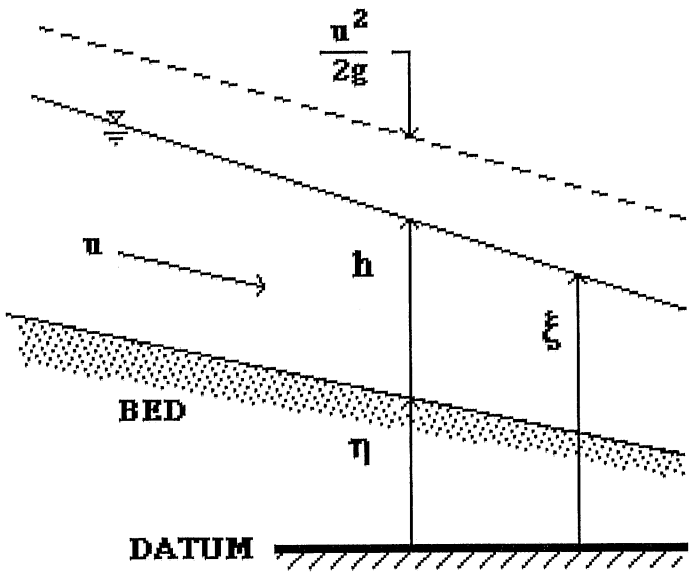

Figure 2.3 Definition sketch for governing equations

Assumptions necessary for the derivation of the St. Venant equations are (Chow, Maidment, and Mays, 1988):

1. The flow is one-dimensional; depth and velocity vary only in the longitudinal direction. This implies that for a particular section perpendicular to the longitudinal axis the velocity is constant and the water surface is horizontal.
2. Flow varies only gradually along the channel so hydrostatic pressure prevails and vertical accelerations may be neglected.
3. The longitudinal axis of the channel can be approximated by a straight line.
4. The bottom slope of the channel is small and does not change significantly during a modeled time step.
5. Resistance coefficients for steady, uniform flow (taken as turbulent heren) are applicable.
6. The fluid is incompressible and of constant density.

2.2.1.1 Quasi-steady approximation.

It has been shown by deVries (1973) that for Froude numbers less than about 0.7, a quasi-steady approximation of equations (2.5) and (2.6) according to which the temporal terms $\frac{\partial(uhb)}{\partial t}$ and $\frac{\partial(hb)}{\partial t}$ may be neglected is valid. This approximation is based on the relatively slow propagation speed of bedforms compared to the overlying water wave celerity. It means that the water surface and velocity adjust "instantly" to changes in

channel bed elevations. An alternate approach will be taken here to demonstrate the validity of this assumption.

Assume a constant roughness, unit width channel for simplicity (i.e. p = b = 1), and assume the momentum flux correction factor is equal to 1.0 (normal values range from 1.03 to 1.06). Equations (2.5) through (2.7) are made dimensionless by introducing the variables $\hat{u} = \frac{u}{u_o}$, $\hat{h} = \frac{h}{h_o}$, $\hat{x} = \frac{x}{h_o}$, $\hat{\eta} = \frac{\eta}{h_o}$ and $\hat{q_s} = \frac{q_s}{q_{so}}$, where u_o, h_o, and q_{so} are values of velocity, depth, and bedload sediment transport, respectively, under uniform flow conditions. It is also necessary to introduce two time scales, one based on water flow parameters, $\hat{t} = \frac{t}{h_o/u_o}$, and the other based on sediment transport parameters: $\hat{t}^* = \frac{t}{h_o^2/q_{so}}$. Equations (2.5) through (2.7) become:

$$\frac{\partial(\hat{u}\hat{h})}{\partial\hat{t}} + \frac{\partial(\hat{u}^2\hat{h})}{\partial\hat{x}} = -g\frac{h_o\hat{h}}{u_o^2}\left(\frac{\partial\hat{h}}{\partial\hat{x}} - S_o\right) - C_f\hat{u}^2 \qquad (2.10),$$

$$\frac{\partial\hat{h}}{\partial\hat{t}} + \frac{\partial(\hat{u}\hat{h})}{\partial\hat{x}} = 0 \qquad (2.11),$$

and

$$\frac{\partial\hat{\eta}}{\partial\hat{t}} + \frac{1}{1-\lambda_p}\frac{q_{so}}{u_o h_o}\frac{\partial\hat{q_s}}{\partial\hat{x}} = 0 \qquad (2.12).$$

Now express the dimensionless time scale in terms of $\hat{t}^* = \frac{t}{h_o^2/q_{so}}$.

Note that

$$\hat{t} = \hat{t}^*\frac{h_o^2 u_o}{q_{so} h_o} = \frac{\hat{t}^*}{\zeta} \qquad (2.13),$$

where

$$\zeta = \frac{q_{so}}{u_o h_o} \qquad (2.14)$$

and is the ratio of water to sediment discharge. Parker (1976) showed that $\zeta << 1$ for natural rivers and laboratory flumes. Substituting into (2.10) through (2.12) yields

$$\zeta\frac{\partial(\hat{u}\hat{h})}{\partial\hat{t}^*} + \frac{\partial(\hat{u}^2\hat{h})}{\partial\hat{x}} = -g\frac{h_o\hat{h}}{u_o^2}\left(\frac{\partial\hat{h}}{\partial\hat{x}} - S_o\right) - C_f u_o^2 \qquad (2.15),$$

$$\zeta\frac{\partial\hat{h}}{\partial\hat{t}^*} + \frac{\partial\hat{u}}{\partial\hat{x}} = 0. \qquad (2.16),$$

and

$$\frac{\partial \hat{\eta}}{\partial \hat{t}} + \frac{1}{1-\lambda_p}\frac{\partial \hat{q_s}}{\partial \hat{x}} = 0 \qquad (2.17).$$

Now for an order one (O(1)) change in dimensionless variables, the terms $\zeta\frac{\partial(\hat{u}\hat{h})}{\partial \hat{t}^*}$ and $\zeta\frac{\partial \hat{h}}{\partial \hat{t}^*}$ are <<1 and may be neglected. That is, for small changes in water velocity, depth and sediment transport capacity, the momentum and continuity equations can be cast in a quasi-steady dynamic form. Care must be taken, however, that in using the quasi-steady approximation, the assumption that $\frac{\partial h}{\partial t} = 0$ is not violated. Cunge, Holly, and Verwey (1983) and Chen (1979) warn that using very long time steps in a model where the bed is actively aggrading may result in a violation of the water continuity equation and may significantly affect the solution of the hydraulic variables.

A quasi-steady approximation is well-suited to an explicit finite difference formulation and also allows the equations of water and sediment transport to be decoupled. Most models in use today are of this type.

2.2.1.2 One-dimensionality.

Equations (2.5) through (2.7) are cast in one-dimensional form, and do not account for variations in the lateral or vertical directions. This may be a limitation in areas such as expanding reservoirs where lateral velocity and sediment distributions are not necessarily uniform. Equation (2.7), for example, has no provision for varying the lateral extent of deposition or erosion. Early numerical models for reservoirs (Annandale, 1987) tried to overcome this limitation by using two dimensional jet theory to simulate the spreading velocity field in a diverging zone. Sediment is distributed laterally using lateral diffusion coefficients. Chen, Lopez, and Richardson, (1978) and Lopez (1978) used this approach and tested the equations with experiments of sediment transport in sudden expansions. Wang, Scarlatos, and McAnally (1983) used a similar approach to describe delta growth in the Atchafalaya-Mississippi river region. Other models simply distribute deposition in horizontal layers across a two-dimensionally defined cross section (Chang, 1984), or adjust all cross section coordinates vertically (Cunge, 1988, Thomas, 1977). Lateral variations in conveyance or tractive force are sometimes used (Chang, 1984, Li, Mussetter, and Grindeland, 1988) to estimate distribution of scour. Sanoyan (1971) distributed lateral sediment using a normal probability distribution.

All of these methods attempt to overcome limitations of one-dimensional modeling by modifying the lateral distribution of sediment. Cunge, Holly, and Verwey (1983), however, discourage using semi-empirical schemes to distribute sediment laterally using one-dimensional models. Since the precise distribution of deposition is unknown, they suggest using rectangular cross sections in one-dimensional models. This suggestion is adopted for this investigation.

2.2.1.3 Sediment transport law.

Equation (2.8) is a general representation of sediment transport capacity as a function of shear stress. Many specific equations describing sediment transport are

available, such as those using critical thresholds of velocity or tractive force, and those based on roughness as a function of sediment grain size and/or bedform amplitude (See Graf, 1971, for a discussion of several sediment transport functions). Equation (2.8) shows the basic relationship and will be used for illustrative purposes. Flume-specific transport relationships are derived in Chapter 3.

Equation (2.8), like other sediment transport equations, are equilibrium relationships based on flume and field data collected under equilibrium flow conditions in shallow water bodies. Thus non-equilibrium sediment transport and transport in deep-water conditions, i.e., reservoirs, are not included. Mahmood (1987) points out there is no available bedload function tested on deep reservoirs, while Nordin (1988) leads the way in advocating use of non-equilibrium sediment transport laws for reservoir models. Bell and Sutherland (1983) describe "a nonequilibruim state exists under steady water flows when the sediment transport rate changes with time and position so that there is no balance between input and output of sediment." They further comment that nonequilibruim conditions can exist, for example, "when the upstream sediment transport supply is changed, e.g., introduction of man-made sediment barriers." Such a situation is described with different time scales. When aggradation (or degradation) is occuring, the fluvial system is clearly in disequilibrium. This does not mean, however, that equilibrium sediment transport relationships cannot be used. Let T_a be the characteristic time scale for significant aggradation and T_r be a relaxation time, or time required for the sediment transport to adjust to actual conditions. If $\frac{T_a}{T_r} >> 1$, an equilibrium sediment transport relationship can be used to describe disequilibrium profiles.

Han (1980) used the concept of non-equilibrium sediment transport in the study of suspended load transport in Chinese reservoirs. Chen (1988) recognized the meaning of the concept applied to reservoirs when he explained "if upstream sediment transport rate is greater than the equilibruim sediment transport capacity, then a portion of this upstream load will be carried farther downstream." He approximates this process, as did Bell and Sutherland, with an exponential decay factor applied to the upstream transport capacity. Chen explains, "This differs from the equilibrium approach, which assumes that all excess bed material load is deposited in the next downstream reach." The exponential decay serves as a damping or lag factor to the equilibruim transport relationship. The non-equilibrium approach is still under development and requires the use of experimentally derived or calibrated delay coefficients. Since the lag length is very short in most cases (Bell and Sutherland, 1983), equilibruim sediment transport equations are used in this research, and model results are compared to experimental observations to test compatibility.

Finally, equation (2.8) is a relationship for uniform sediments, which, with an appropriate generalization, may be applied separately to graded sediments by means of a hiding function.. Research herein is based on the assumption that the sediments are uniform and noncohesive, thus eliminating the complexities introduced by non-uniform or cohesive sediments. Hence armoring, hiding, sorting and consolidation are not considered herein.

2.2.2 Solution Techniques

Mathematical solutions to equations (2.5) through (2.7) may be classified as analytic or numerical. Numerical methods include finite element and finite difference schemes, and the method of characteristics . Finite difference methods and the method of characteristics may be either implicit or explicit.

2.2.2.1 Analytic solutions.

The St. Venant equations constitute a pair of first order, partial differential equations of hyperbolic type. When coupled with sediment continuity, analytic solutions are available only for special cases. For example, Gill (1988) and Ribberink and van der Sande (1985) found linearized solutions for the problem of sediment overloading in a channel. In this case a sediment front forms at the influx point, but diffuses as it progresses downstream. Similarly, exact solutions using simplified forms of equations (2.5) through (2.7) have been found for degradation below dams (Jaramillo and Jain, 1984). In this case, an initial negative step in the streambed extends downstream in a diffusive process. Reservoir sedimentation, however, produces an increasingly steep front in the downstream direction until a delta forms with a foreset slope at the submerged angle of repose. Analytic solutions to the linearized reservoir sedimentation problem have not yet been found.

2.2.2.2 Finite element.

The finite element formulation is appropriate for two- or three-dimensional modeling. It requires mesh generation and tracking techniques that use relatively large amounts of computer time. The method also re-formulates the governing equations into an extremal problem, such that the components of the equations are no longer easily associated with physical flow parameters. No finite element models of reservoir deposition were found.

2.2.2.3. Finite difference.

In the finite difference formulation, the governing differential equations are written in finite difference form and solved at a discrete number of grid points. The discretization may be explicit or implicit. The implicit method seeks the simultaneous solution of the difference equations for the entire computational domain for each time step, requiring large amounts of computer resources. The explicit method solves for each grid point successively without using simultaneous equations. Fully dynamic models must use the implicit solution technique. Decoupled models may employ either or both. The implicit method allows for larger time and distance steps than the explicit approach, thus offsetting the larger amounts of time required for each time step solution. More details on the explicit method follow.

2.2.2.4 Method of characteristics.

Using the method of characteristics first requires the transformation of the partial differential equations into ordinary differential equations. The numerical solution may then proceed using either implicit or explicit methods. A necessary condition for the use of this method is the existence of characteristics.

2.2.2.5 Explicit finite difference formulation.

The sediment continuity equation for a uniform-width channel is used to illustrate the explicit finite difference formulation. Equation (2.7) may expressed in finite difference form as

$$\Delta\eta_i = \frac{1}{1-\lambda_p}\frac{\Delta t}{0.5(\Delta x_{i+1} + \Delta x_i)}[(1-\phi)\,(q_{s,i+1} - q_{s,i})] + [\phi(q_{s,i} - q_{s,i-1})] \tag{2.18}$$

where $\Delta\eta_i$ is the change in bed elevation at node i during the time period Δt, $\Delta x_{i+1}$is the

interval between nodes i+1 and i, Δx_i is the interval between nodes i and i-1, and ϕ is a weighting factor with a value between 0 and 1 (see Figure 2.4 below).

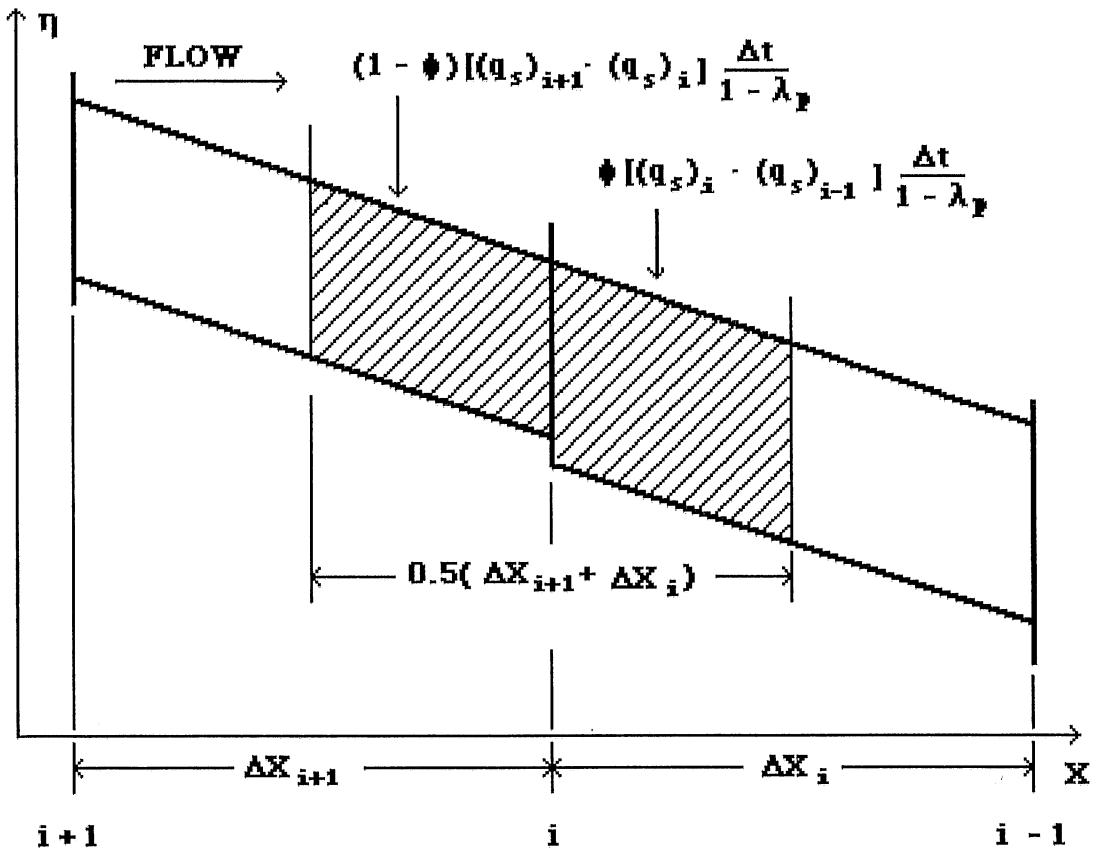

Figure 2.4 Schematic diagram for explicit finite difference scheme

The finite difference formulation of equation (2.18) is known as a forward difference scheme if $\phi = 1$, a centered-difference scheme if $\phi = 0.5$, and a backward difference scheme if $\phi = 0$. A Taylors series expansion of equation (2.7) shows that the forward and backward difference schemes are accurate to $O(\Delta x)$, while a centered-difference scheme is accurate to $O(\Delta x^2)$ (Street, 1973). The accuracy of all solutions increases with smaller time and distance steps

Explicit formulations may be unstable if called the Courant number, a function of the ratio $\frac{(1-\lambda_p)\Delta x}{\Delta t}$, becomes too large. Various researchers have given expressions for the function and use it as a surrogate for Courant number. For example, Li, Mussetter, and Grindeland (1988) derive the following expression for sand wave celerity C_n:

$$C_n = 2.33 [a_1(b_1 - c_1)u^{b_1}h^{c_1-1}]^{0.96} \quad (2.19)$$

where a_1,b_1, and c_1, are coefficients in the generalized sediment transport expression $q_s = a_1 q^{b_1}(\xi-\eta)^{c_1-b_1}$. Here h is the local water depth, η is the local bed elevation, ξ is the water surface elevation, and q is the water discharge per unit width. They suggest that the reach length should be longer than the distance the sand wave would travel in the selected time step using the celerity from (2.19).

2.2.3 Specific Models

Some models developed specifically for reservoir sedimentation are now briefly discussed.

2.2.3.1 Yucel and Graf (1973).

In 1973 Yucel and Graf developed a one-dimensional reservoir mathemaatical model using a Schoklitsch-type equation for sediment transport. Since the Schoklitsch equation was derived using uniform flow conditions and a critical velocity for scour, two modifications to the equation were made. First, recognizing the inequality of the water surface and bed slopes in reservoirs, they used an averge of the two to represent the friction slope in the equation. Next, since their model was for aggradation only, they modified the critical velocity factor in the equation to represent a deposition velocity limit instead of a scour velocity limit. Their results show a delta-like front forming but with a maximum slope of 0.4 per cent, very far from the submerged angle of repose.

2.2.3.2 Cao, Fang, Liu, and Chen (1988).

A model that simulates the type of aggradation and degradation commonly encountered in Chinese reservoirs was presented by Shuyou, Duo, Xinnian, and Jiayang. Drawdown flushing is used at many Chinese reservoirs to evacuate stored sediment. Often the water surface temporarily drops below the delta lip and exposes the deposited sediment. Their model uses an implicit scheme for computing degradation in such cases, and an explicit scheme for computing aggradation. Since much of the sediment is carried in suspension, they include field-calibrated equations for the suspended load. Results are compared on a gross scale to several reservoirs; the agreement is quite good.

2.2.2.3 Ashida (1980).

In 1980, Ashida discussed tracing the movement of the delta apex (lip) in a reservoir. He combined the equations of motion to derive an approximate expression for the movement of the apex:

$$U = \frac{q_{sf}}{(1-\lambda)\eta_f} \quad (2.20)$$

and

$$V = (\frac{\partial \eta}{\partial t})_f + U(\frac{\partial \eta}{\partial x}) \quad (2.21)$$

where U is the apex velocity parallel to the original bed, V is the apex velocity perpendicular to the bed, and the subscript f describes functional values at the apex. Without giving specific comparisons, Ashida states these theoretical values are very close to values observed during experiments.

2.2.2.4 Cavor (no date).

A mathematical model for flushing was developed by Cavor for use in simulating the process in an Iranian reservoir. The pattern of rainfall and irrigation in Iran is such that some expendable water remains in reservoirs at the end of the irrigation season. Bottom outlets are opened and the reservoir is drained to an established minimum level. The gates are suddenly closed, water partially fills the reservoir, and the gates are then opened again. This process is repeated several times. The unsteady terms in the momentum and continuity equations are retained by Cavor to simulate the opening and closing cycle of the gates. Close to the dam, the velocity field is approximated by a two-dimensional jet equation, similar to the models previously described by Lopez (1978) and Chen, Lopez, and Richardson (1978). Since suspended sediment is dominant, diffusion coefficients and source/sink terms representing erosion and deposition are derived from field data when applied to a specific reservoir.

2.2.2.5 Other models.

Other models exist for purposes different from those identified for this investigation, Razvan, and Ramos (1981) and Bouchard (1987) consider erosion of cohesive sediments in their models. Mukhamedov (1981) and Karaushev, Bogoliubova, and Tabakaeva (1981) describe reservoir models developed in Russia that consider suspended sediment in one case and provide empirical predictions of flushing factors in the other. Asada (1973) describes a model developed for mountainous rivers in Japan; it involves carefully monitoring the change in bed level during computations so deposition during any one time step will not exceed the water depth.

3. EXPERIMENTAL ANALYSIS

The purpose of this chapter is to describe the setup, procedure, and results of the research experiments.

3.1 Experimental Facilites

Experiments were performed in a 12.2 meter long, 0.38 meter high, 15 centimeter wide flume (Figure 3.1) at the St. Anthony Falls Hydraulic Laboratory. The flume was later modified by adding a 2 meter expanding section at the downstream end (Figure 3.2). Water enters the flume from a city water supply through a 0.0508 meter diameter orifice meter in a 0.0762 meter pipe. The orifice meter operates with a standard manometer setup for measuring discharge. The exit from the flume is controlled by a hand-operated tailwater gate set to maintain near-uniform flow conditions in the flume when the sluice gates are fully open. In the first set of experiments in the uniform width flume, a sluice gate extending completely across the flume width was installed about 9 meters downstream from the entrance. Later this sluice gate was removed and replaced with a simulated dam 1.5 meters into the expanding section. The dam was fitted with three sluice gates, each 0.15 meters wide. The gates were manually operated; each gate could be set separately.

The sediment for the experiments consisted of quasi-uniform crushed walnut shells with a mean diameter of 0.67 millimeters, a gradation coefficient of 1.3 (see Figure 3.3 for the particle size distribution), and a porosity of 0.53. This lightweight material (specific gravity 1.35) simulates suitable full-scale sediment transport (Vries, Hartman, and Amorocho, 1980, and Parker, Martinez, and Hills, 1982). Using the walnut shells repeatedly did not change the size distribution. Sediment was fed into the flume using a mechanical auger which had been calibrated for input rates of between 80 and 450 gramsper minute. The sediment was collected in a settling box downstream of the flume exit, dried and used again.

3.2 Purposes of the Experiments

Experiments were conducted in both the uniform width flume and the flume with the expanding channel upstream of the dam. The purposes of the experiments were:

1. To check the validity of previous statements that flow in the flume consisted of two distinct zones: one upstream of the depositonal delta lip, where near-uniform conditions are said to prevail, and one downstream of the delta, where flow is basically unaffected by upstream conditions.
2. To observe general characteristics of aggradation and degradation for different flow, sediment, and sluice gate settings.
3. To determine the characteristics of the depostional delta and its equilibrium position in relation to sluice gates of different openings.
4. To gather data on the time needed to achieve equilibrium in the flume once the sluice gate settings change.
5. To examine the properties of the bed slope in the laterally expanding reservoir-like portion of the flume upsteam from the dam.

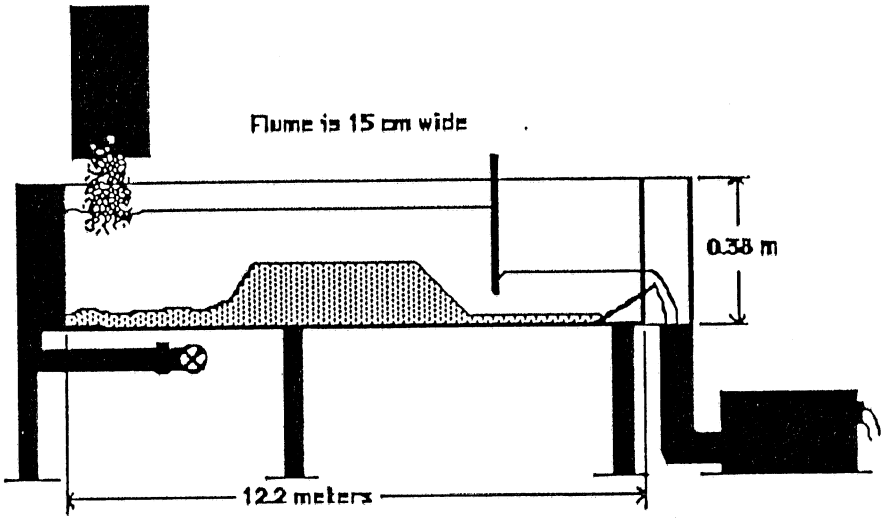

Figure 3.1 Uniform width flume (not to scale)

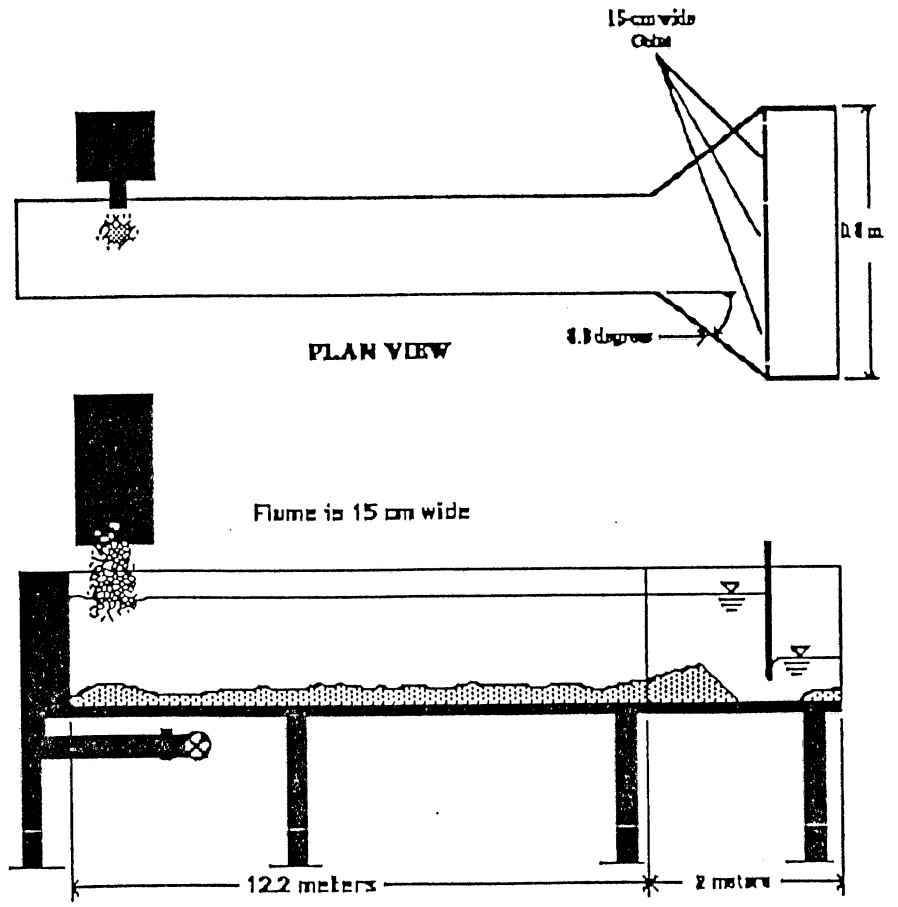

Figure 3.2 Flume with expansion upstream of dam (not to scale)

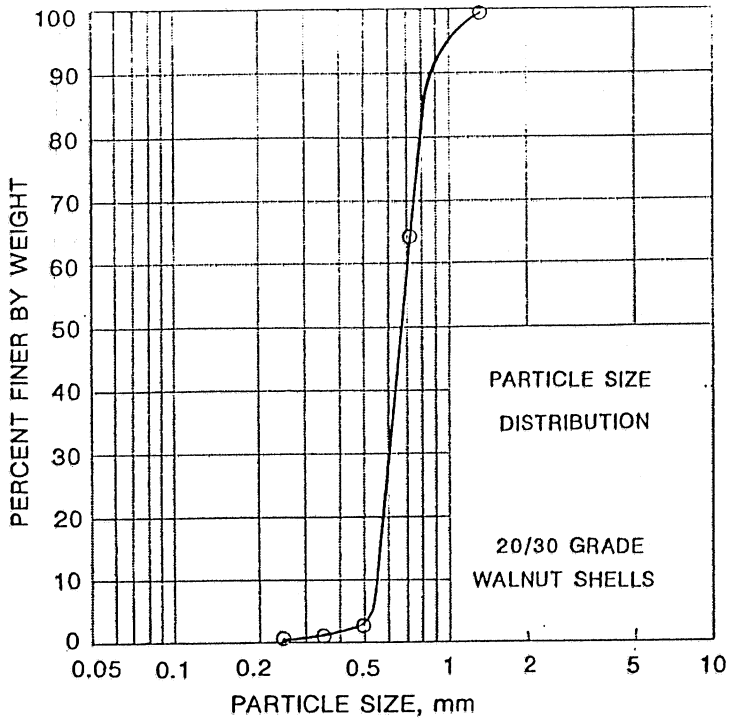

Figure 3.3 Crushed walnut shell particle size distribution

3.3 Measurements and Data Collection

The flume was fitted with a moving carriage mounted with equipment to measure flow field properties in the vertical and lateral directions. The glass walls of the flume provided easy access for observations and measurements. An Apple II-C computer was used with data acquisition software and an A-to-D (analog to digital) converter card to collect velocity and sediment concentration data.

3.3.1 Non-computer Measurements

Measurements taken during experimental runs included:

1. water temperature,
2. longitudinal profiles of the bed and water surface upstream of the dam,
3. bedform amplitude, wavelength, and speed/frequency,
4. equilibrium location and shape of the depositional delta,
5. water surface elevations upstream and downstream of the sluice gate and at the exit of the flume, and
6. time to reach equilibrium after changing sluice gate settings.

Equilibrium was assumed to prevail when there was no measurable difference between water surface and bed elevation profiles in two readings, usually taken 1 hour apart.

3.3.2 Computer-collected Measurements

3.3.2.1 Velocity.

A Prandtl tube 1.59 millimeter in diameter (1.17 millimeter diameter dynamic port and 0.46 millimeter diameter static ports) and a pressure transducer were used to measure water velocity. Measurements were taken at 8 points on centerline vertical profiles at

several locations upstream of the sluice gates. For one run using the uniform width flume, vertical profiles were also taken at locations corresponding to 25 per cent and 75 per cent of the channel width. For runs in the flume with the expanding section upstream from the dam, lateral profiles at mid-depth were taken at several stations. Accuracy at the smallest measured velocity (about 0.20 meters per second) is about ±3 per cent. Sampling intervals, frequencies and locations are shown in Figure 3.4.

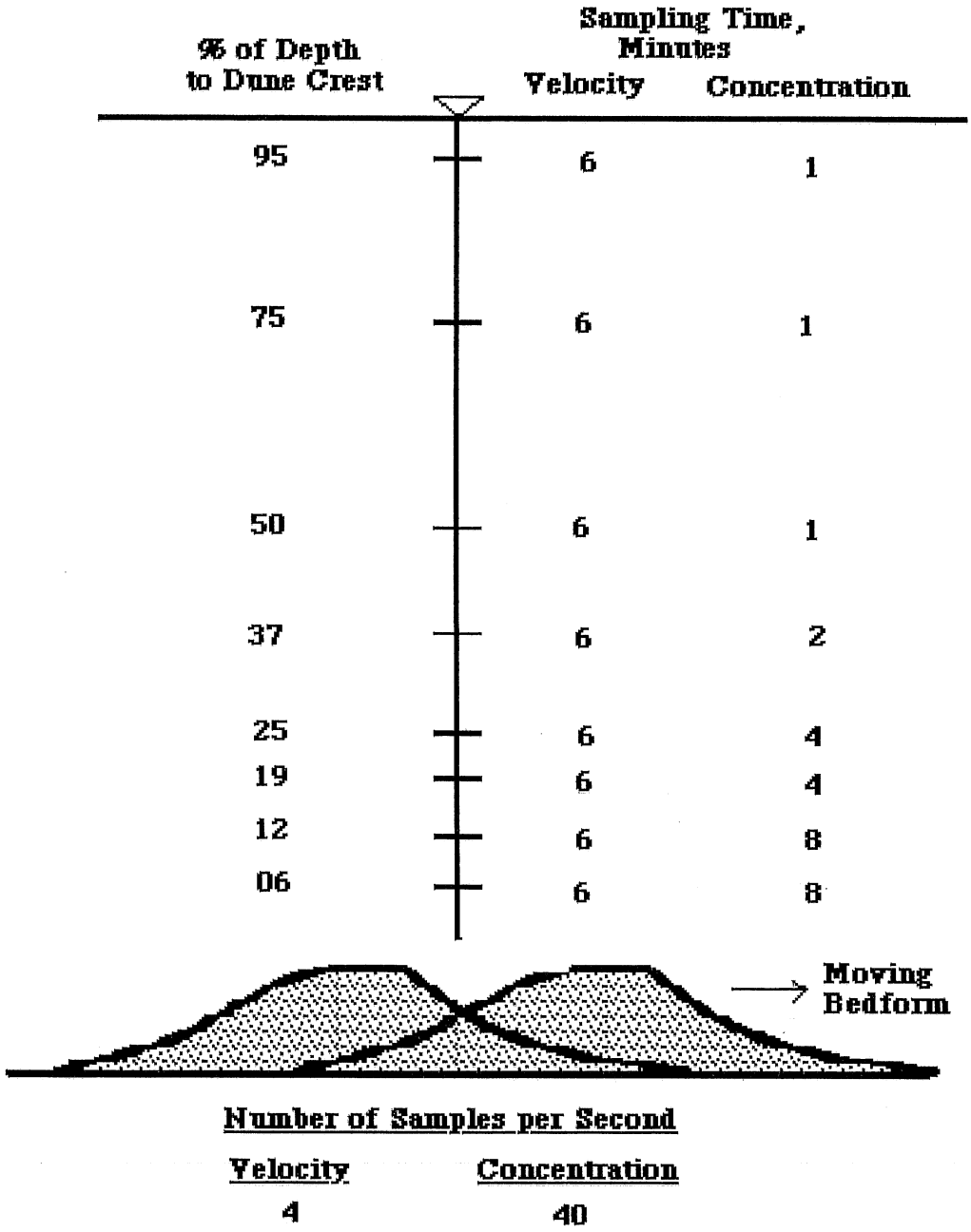

Figure 3.4 Velocity and sediment concentration sampling intervals, frequencies, and locations

3.3.2.2 Sediment concentration.

Suspended sediment concentration was measured using an electro-optical concentration meter. This kind of device has been successfully used to measure concentrations of uniform quartz sand (Ikeda and Asaeda, 1983). Water and sediment particles pass throught the submerged probe light beam, which is 2 millimeters in diameter and 1 centimeter wide. The sediment particles, or portions thereof, passing through the sample space block a portion of the light beam. Registered voltage is directly proportional to the percentage of the light beam blocked by the sediment. A predictive relationship (Figure 3.5) based on this principle agreed well with calibration tests using known concentrations of walnut shells. Measurement accuracy decreases with sediment concentration. Expected accuracy is +/- 90 percent at concentrations of 100 ppm, and +/- 2 percent at 5000 ppm. Sampling intervals, frequencies, and locations are shown in Figure 3.4.

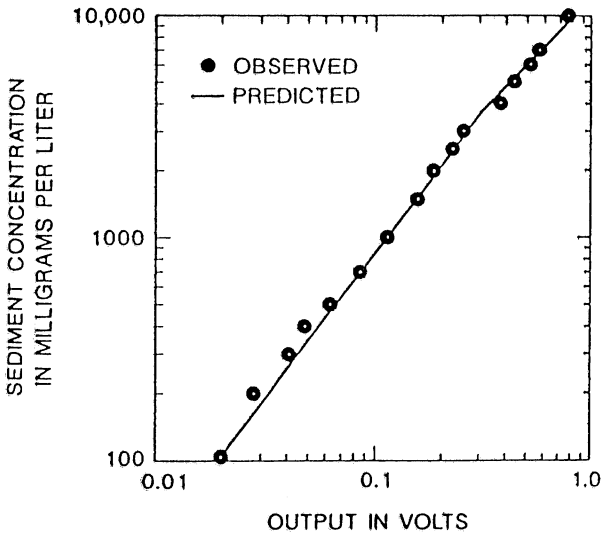

Figure 3.5 Calibration of electro-optical concentration meter

3.4 Experimental Procedure

Several runs were made in the uniform width flume and the flume with an expanding channel upstream from the dam. A typical run consisted of the following steps:

1. Select the desired water and sediment discharge rates. Water discharge varied from 1 to 3 liters per second (16 to 48 gallons per minute) and sediment discharge varied from 150 to 300 grams per minute (0.33 to 0.66 pounds per minute).
2. Estimate the bed slope for uniform open channel flow. The Engelund-Hansen equation (Engelund and Hansen, 1967) was used for this purpose because it accounts for changes in form roughness with increasing discharge, a common phenomenom in mobile-bed channels.
3. Set the tailwater control gate to produce near-uniform flow throughout the flume for open channel flow conditions.
4. Set the desired sluice gate elevation if the sluice gate is to be used.

An experiment was run until equilibrium conditions prevailed in the flume. Measurements and data were taken as described above. After all pertinent data were collected, the sluice gate elevation was changed and the run repeated. A typical experiment took more than 12 hours.

3.5 Results

Experimental results for the uniform width flume and the flume with an expanding channel upstream from the dam are summarized in Tables 3.1 through 3.5. Entries in the tables are explained below.

3.5.1 Hydraulic Data

Each depth shown in Table 3.1 includes one-half the bedform amplitude, and is the average of several depth and bedform measurements taken throughout the length of the flume. The calculated velocity is simply the discharge divided by the cross-sectional flow area. The total friction factor was computed from the relationship $C_f = \frac{grS}{u^2}$, where C_f is the total friction factor, r is the measured hydraulic radius, equal to the cross-sectional flow area divided by the wetted perimeter, S is the normal slope, and u is the mean cross-sectional velocity. Values of bed and wall friction factors were found using the Johnson sidewall correction technique found in Vanoni, 1975, and explained in Appendix 1.

3.5.2 Bedform and Sediment Data

Bedform amplitude (taken as the height from crest to trough), wavelength, and wave speed were measured repeatedly during the experiments and averaged for each run. Values are shown in Table 3.2. The bedforms were observed to be fairly regular downstream of a point about 3 meters from the flume entrance. They were also two-dimensional, extending the full width of the flume. This observation is consistent with the conclusions of Hwang and Divoky (1971) who discussed the effect of flume width on bedform characteristics. The dimensionless Chezy coefficient, $\frac{C}{\sqrt{g}}$, is given by the relation $C = \frac{1}{\sqrt{C_b}}$, where C_b is.the bed friction factor in Table 3.1 corrected for sidewall influences. The values of $\frac{C}{\sqrt{g}}$ correspond to lower regime dunes that have bed material concentrations of 200 -2,000 ppm according to Graf (1971).

"Bedform load" is defined as that portion of sediment load traveling as a defined bedform; it is calculated as the product of bedform speed, width, and volume, where the volume is the product of the shape factor, amplitude, and volume of solids (1 - porosity). The shape factor for roughly triangular bedforms is 0.5. This calculation is similar to that found in Crickmore (1970). Since the bedform is composed of individual grains that are rolling, sliding, and briefly saltating, bedform load is typically equivalent to bedload when bedforms are present.

The suspended load concentrations were negligible at total transport rates of 150 gr/min. Suspended loads for a total transport of 300 gr/min were found by numerically integrating point measurements over the vertical profile and multiplying the result by the mean velocity. While this kind of numerical integration is not as accurate as integrating

Run Number	Channel[a]	No. of gates open	Discharge l/s	Sediment discharge gr/min	Normal depth cm[b]	Normal Slope	Calculated velocity cm/s[c]	Froude Number	Water Temperature Degrees Celsius	Friction Factors[d] Total	Bed	Wall	Dimensionless Bed Shear Stress[e]
1	U	1	1.5	150	3.64	0.0020	27.5	0.46	26	0.0064	0.0078	0.0034	0.256
6	U	1	1.5	300	3.25	0.0025	30.8	0.54	26	0.0059	0.0070	0.0037	0.287
13	U	1	3.0	150	6.18	0.0017	32.4	0.42	3	0.0054	0.0071	0.0034	0.322
14	U	1	3.0	150	6.13	0.0017	32.6	0.42	16	0.0053	0.0071	0.0031	0.326
15	U	1	3.0	300	5.66	0.0019	35.3	0.47	12	0.0048	0.0061	0.0031	0.332
16	U	1	3.0	300	5.40	0.0019	37.0	0.51	3	0.0043	0.0051	0.0032	0.302
17	D	1	3.0	150	6.30	0.0017	31.8	0.40	25	0.0057	0.0079	0.0030	0.345
20	D	3	3.0	150	6.30	0.0017	31.8	0.40	25	0.0057	0.0079	0.0030	0.345
21	U	1	1.5	300	3.07	0.0030	32.6	0.59	3	0.0060	0.0070	0.0038	0.322
22	U	1	3.0	300	5.32	0.0019	37.6	0.52	3	0.0041	0.0048	0.0031	0.294
23	U	1	3.0	50	7.25	0.0011	27.6	0.33	4	0.0052	0.0070	0.0034	0.232
24	U	1	2.0	58	5.45	0.0014	24.5	0.33	9	0.0072	0.0098	0.0037	0.255
25	U	1	2.0	570	3.55	0.0030	37.6	0.64	9	0.0050	0.0058	0.0033	0.358
26	U	1	4.25	570	6.68	0.0021	42.4	0.52	9	0.0040	0.0051	0.0029	0.400
27	U	1	3.95	535	6.41	0.0019	41.1	0.52	9	0.0038	0.0046	0.0029	0.339
28	D	1	3.0	185	6.53	0.0017	30.6	0.38	27	0.0047	0.0062	0.0029	0.319
29	D	1	3.0	185	6.65	0.0016	30.1	0.37	27	0.0048	0.0063	0.0029	0.325

[a] U = uniform width, D = diverging
[b] Includes one-half the bedform amplitude
[c] Discharge divided by (width X normal depth)
[d] Bed and wall friction factor from sidewall correction procedure, Appendix 1.
[e] Corrected for sidewall effects and made dimensionless by dividing by rRd_{50}, where R = submerged specific gravity.

Table 3.1 Summary of experimental hydraulic data

Run Number	Discharge l/s	Sediment discharge gr/min	Water Temperature Degrees Celsius	Bedform Characteristics Amplitude cm	Bedform Characteristics Wavelength cm	Speed cm/sec	$\frac{C_a}{\sqrt{g}}$	Bedform Transport gr/min[b]	Number of Profiles	Average Concentration ppm	Rouse Exponent	Suspended Sediment Load gr/min	Total Measured Sediment Discharge gr/min[c]
1	1.5	150	26	0.8	40	0.6	11.3	140					146
6	1.5	300	26	0.5	32	0.9	12.0	130	10	300	1.25	27	164
13	3.0	150	3	1.5	35	0.3	11.9	130					137
14	3.0	150	16	0.6	30	0.8	11.9	140					146
15	3.0	300	3	1.0	22	1.0	12.8	280	3	101	1.25	18	321
16	3.0	300	3	0.8	30	0.5	14.0	110	6	248	1.35	45	167
17	3.0	150	25	1.1	35	0.5	11.3	160					167
20	3.0	150	25	1.1	35	0.5	11.3	160					167
21	1.5	300	3	0.0	0.0	0.0	12.0						
22	3.0	300	3	0.0	0.0	0.0	14.4						
23	3.0	50	4	2.3	?	0.11	12.0	70					77
24	2.0	58	9	1.7	?	0.11	10.1	50					57
25	2.0	570	9	0	0	0	13.1						
26	4.25	570	9	0	0	0	14.0						
27	3.95	535	9	0	0	0	14.7						
28	3.0	185	27	0.8	30	0.6	12.7	130					185
29	3.0	185	27	0.8	30	0.6	12.6	130					185

[a] Equal to $\frac{1}{\sqrt{C_b}}$, where C_b is bed friction factor from Table 3.1.

[b] Equal to Amplitude X Speed X Shape factor X Width X Specific Gravity X (1 - Porosity)

[c] Sum of Bedform transport and Suspended sediment load.

Table 3.2 Bedform and sediment measurements

the product of point velocity and concentations, it is sufficient to characterize suspended load in the experiments. The concentration below the lowest measured point was assumed to be constant to the top of the bedform. The total load in the flume is simply the sum of the bedform load and the suspended load.

The Rouse exponent, z, was derived from regression analyses of the Rouse equation:

$$\frac{C_y}{C_a} = \left(\frac{h-y}{y}\,\frac{a}{h-a}\right)^z \qquad (3.1)$$

where C_y is the concentration of suspended sediment [ppm] at depth y, d = depth, measured from the top of the bedform to the water surface [cm], a = reference height above the bed [cm], and C_a = concentration at the reference height, a [ppm]. Equation (3.1) may be written as

$$\ln C_y = z \ln \frac{h-y}{y} + z \ln C_a \frac{a}{h-a} \qquad (3.2)$$

Linear regressions of the natural-log transformed variables were performed to derive the values of z. The z values in Table 3.2 are the averages of the indicated number of profiles for each run.

3.5.3 Velocity Profile Data

The values of mean measured velocity, u, bed shear velocity, u_*, and the Von Karman constant, κ, were derived assuming a logarithmic law applies for the velocity profiles:

$$\frac{u}{u_*} = \frac{1}{\kappa} \ln\left(\frac{30y}{k_s}\right) \qquad (3.3)$$

where u = velocity at depth y [cm/s], u_* = shear velocity [cm/s], κ = von Karman constant, y = depth above mid-dune elevation [cm], and k_s = roughness height [cm]. Equation (3.3) is valid for fully rough turbulent flows, defined by a Reynolds shear number (Re_*) greater than 50, where

$$Re_* = \frac{u_* k_s}{\nu} \qquad (3.4)$$

where ν is the kinematic viscosity of the fluid [cm^2/sec]. Table 3.3 shows the fully rough turbulent flow assumption is valid for all but two experimental runs.

Equation (3.3) may be written as

$$u = \frac{u_*}{\kappa} \ln y + \frac{u_*}{\kappa} \ln \frac{30}{k_s} \qquad (3.5)$$

The coefficients $\frac{u_*}{\kappa}$ and $\frac{u_*}{\kappa} \ln \frac{30}{k_s}$ may be found using linear regression techniques. With computed values of the coefficients, Equation (3.5) may be integrated to find the average velocity in the cross section:

Run Number	Discharge l/sec	Sediment Discharge gr/min	Normal Depth cm[a]	Velocity cm/sec[b]	Number of Profiles	Mean Measured Velocity cm/sec[c]	Bed Shear Velocity cm/sec[d]	Bed Roughness Height cm[d]	Von Karman Constant[d]	Reynolds Shear Number[e]
1	1.5	150	3.64	27.5	11	28.1	2.42	0.28	0.43	77
6	1.5	300	3.25	30.8	6	32.1	2.56	0.18	0.41	52
13	3.0	150	6.18	32.4	3	32.3	2.72	0.34	0.45	57
14	3.0	150	6.13	32.6	2	33.6	2.72	0.36	0.42	87
15	3.0	300	5.66	35.3	3	37.8	2.71	0.16	0.43	35
17	3.0	150	6.30	31.8	2	31.6	2.82	0.21	0.53	36

a Includes one-half the bedform amplitude

b Equal to Discharge divided by (Width X Normal depth)

c Mean value found by integrating measured profiles

d Corrected for sidewall influence

e Equal to bed shear stress X roughness height divided by kinematic viscosity.

Table 3.3 Velocity profile data

$$\bar{u} = \frac{1}{h}\int_{k_s}^{h}\left(\frac{u_*}{\kappa}\ln y + \frac{u_*}{\kappa}\ln\frac{30}{k_s}\right)dy$$

$$= \frac{1}{h}\left[\frac{u_*}{\kappa}(y\ln y - y) + y\frac{u_*}{\kappa}\ln\frac{30}{k_s}\right]\Bigg|_{k_s}^{h}$$

$$= \frac{u_*}{\kappa}\ln\left(11\frac{h}{k_s}\right) \qquad (3.6)$$

where h is the boundary layer thickness, taken as the normal depth from Table 3.1. The values of mean velocity in Table 3.1 are the averages of the indicated number of profiles for each run.

The shear velocity is based on the hydraulic radius pertaining to the bed, found using the sidewall correction procedure described in Appendix 1. Once the shear velocity was computed, the Von Karman constant was found by substitution in the expression for the linear regression coefficients.

3.5.4 Sediment Sluicing Data

In Table 3.4, the ratio of gate opening to normal depth is denoted as $\frac{h_g}{h_N}$, where normal depth, h_N, is defined as the depth from the water surface to the middle of the bedform for normal flow conditions in the uniform flume. Deposition is defined as the average depth of deposited sediment in the flume as a result of lowering the sluice gates as indicated. The ultimate deposition was very uniform throughout the flume. The change in tailwater elevation is denoted as $\Delta\xi_T$, and is referred to the water surface elevation with the gates completely open. The bottom distance is the distance the bed was scoured to the bottom of the flume upstream of the sluice gates, and the time to reach equilibrium for deposition or scour is as noted.

The discharge coefficient is denoted as C_d, and is computed from the orifice equation:

$$Q = C_d h_g w\sqrt{2g(\xi_R - \xi_T)} \qquad (3.7)$$

where Q = discharge [cm^3/sec], h_g = gate opening [cm], w = gate width [cm], ξ_R = water surface elevation upstream of the sluice gate [cm], and ξ_T = water surface elevation down stream of the sluice gate.

3.5.5 Sediment Transport Data

Only that portion of the shear stress acting on sediment grains is effective in producing sediment transport. The bed shear stress, corrected for the sidewalls, may be partitioned into fractions acting on the grains and the bedforms. This partitioning was performed using the Einstein-Barbarossa method for finding grain friction factors when flows may not be fully rough turbulent, and is explained in Appendix 1. The sediment transport values listed in Table 3.5 are the actual measured input rates from the sediment feeder.

Run Number	Discharge l/s	Sediment Discharge gr/min	Normal Slope	Calculated velocity cm/s[a]	Bed Friction Factor[b]	Dimensionless Bed Shear Stress	Grain Friction Factor[c]	Dimensionless Grain Shear Stress	Dimensionless Sediment Transport
1	1.5	150	0.0020	27.5	0.0078	0.256	0.0042	0.138	0.384
6	1.5	300	0.0025	30.8	0.0070	0.287	0.0042	0.174	0.769
13	3.0	150	0.0017	32.4	0.0071	0.322	0.0038	0.172	0.384
14	3.0	150	0.0017	32.6	0.0071	0.327	0.0037	0.172	0.384
15	3.0	300	0.0019	35.3	0.0061	0.332	0.0037	0.200	0.769
16	3.0	300	0.0019	37.0	0.0051	0.302	0.0036	0.216	0.769
17	3.0	150	0.0017	31.8	0.0079	0.345	0.0038	0.166	0.384
20	3.0	150	0.0017	31.8	0.0079	0.345	0.0038	0.166	0.384
21	1.5	300	0.0030	32.6	0.0070	0.322	0.0043	0.199	0.769
22	3.0	300	0.0019	37.6	0.0048	0.294	0.0036	0.221	0.769
23	3.0	50	0.0011	27.6	0.0070	0.232	0.0037	0.127	0.128
24	2.0	58	0.0014	24.5	0.0098	0.255	0.0041	0.108	0.149
25	2.0	570	0.0030	37.6	0.0058	0.358	0.0040	0.244	1.461
26	4.25	570	0.0021	42.4	0.0051	0.400	0.0035	0.271	1.461
27	3.95	535	0.0019	41.1	0.0046	0.339	0.0034	0.252	1.371
28	3.0	185	0.0017	30.6	0.0062	0.319	0.0037	0.185	0.474
29	3.0	185	0.0016	30.1	0.0063	0.325	0.0037	0.178	0.474

[a] From Table 3.1, equal to discharge divided by (width X normal depth)

[b] From Table 3.1.

[c] Found using the Einstein-Barbarossa procedure for the transition region between smooth and turbulent rough flows.

Table 3.5 Sediment transport data

Run Number	Channel[a]	No. of gates open	Discharge l/s	Sediment discharge gr/min	Normal depth cm[b]	Gate opening divided by depth	Discharge Coefficient	Deposition cm	Change in Tailwater Elevation cm	Bottom Scour Distance[c] cm	Time to Reach Equilibrium, hrs Deposit	Scour
1A	U	1	1.5	150	3.64	2.01	0.49	0	0	0		
2						1.55	0.57	0.31	0.1	0	2.5	3.9 From Run #5
3						1.10	0.49	0.6	-0.1	4		2.1 From Run #5
4						0.59	0.53	2.6	-0.4	5.5		1.8 From Run #5
5						0.19	0.66	21.3	-2.3	7.5	20	
6A	U	1	1.5	300	3.25	2.29	0.48	0.3	0	0		7.5 From Run #12
7						2.08	0.48	0.1	0	0		6 From Run #12
8						1.83	0.54	0.6	0.1	0		
9						1.34	0.49	1.0	-0.1	3.5		3.5 From Run #12
10						0.88	0.55	1.8	-0.1	6.8		2 From Run #12
11						0.63	0.63	1.8	-1.0	7		
12						0.38	0.65	6.3	-1.1	7	3	
13	U	1	3.0	150	6.18	0.32	0.64	10.8	-2.2	9		
14					6.13	1.29	0.60	1.5	0	2		
15	U	1	3.0	300	5.66	1.28	0.49	0.6	0	0		
16					5.4	0.31	0.67	15.2	-2.1	10	5.3 From Run #15	
17	D	1	3.0	150	6.3	0.89	0.58	1.4	-0.5	5		5.5 From Run #19
18						0.54	0.66	3.6	-0.5	6		3 From Run #19
19						0.27	0.71	13.3	-0.5	8	16.5 From Run #17	
20	D	3	3.0	150	6.3	0.27	0.77	1.3	-0.3	4		
28	D	1	3.0	185	6.53	0.25	0.75	12	0	10	14.3	

[a] U = uniform width, D = diverging

[b] Includes one half the bedform amplitude

[c] Distance that the bed is scoured to the flume bottom

Table 3.4 Summary of sediment sluicing data

3.5.6 Results Specific to the Uniform Width Flume

3.5.6.1 Centerline velocity profiles.

Figure 3.6 depicts three velocity profiles for Run 5. If the data points followed the logarithmic law perfectly, they would plot as a straight line. Similar plots are shown in Appendix 2 along with the velocity data for all the experiments.

3.5.6.2 Additional velocity profiles.

Figure 3.7 shows velocity profiles taken at the centerline and at locations corresponding to 25 per cent and 75 per cent of the channel width for Run 17. These vertical profiles, typical of those in all experiments, show the need for the sidewall correction procedure described in Appendix 1.

3.5.7 Results Specific to Expanding Region

3.5.7.1 Plan views of equilibrium bed in expanding region.

Figure 3.8 is a plan view of the expanding section for run 19 under equilibrium conditions. One gate of three was open to 1.7 cm for this run. Cross sections are shown for locations near the entrance to the expanding section and the lip. The location of the foreset slope and shape of the delta are also shown. Similar plots are found in Appendix 2.

3.5.7.2 Longitudinal bed profiles in expanding region.

Figure 3.9 shows a dimensionless longitudinal bed profile in the expanding section for run 19. A definition sketch accompanies the plot. Note that the flow produced an adverse bed slope. Similar plots are shown in Appendix 2.

3.5.7.3 Transverse velocity profiles.

Figure 3.10 shows a velocity profile taken across the flume transverse to the flow direction at 0.5 times the depth 30 cm upstream from the sluice gates for equilibrium conditions of run 17. Similar plots are found in Appendix 2.

3.6 Discussion of Results

3.6.1 Nature of Response to Sluicing

3.6.1.1 Aggradation.

Upon lowering the sluice gate a significant amount, the water surface in front of the dam quickly rises to a new equilibrium elevation sufficient to pass the flow through the more restricted sluice gate opening. The backwater influence quickly extends to the flume entrance. Any further adjustment in water level is in response to changes in bed levels. Sediment transport ceases throughout the flume as bedforms are "frozen" in place and sediment in suspension drops out. Sediment accumulates at the upstream end of the flume. Due to the increased depth and decreased velocity, the sediment deposits until the flow depth decreases sufficiently to produce adequate velocity for transport. A delta thus forms at the flume entrance and moves downstream. The sediment is transported across the lip of the advancing delta and falls onto the foreset slope under the influence of gravity. The foreset slope attains the submerged angle of repose, and the delta moves downstream into the flume as the sediment continues to be transported across the lip to the foreset slope. The channel slope upstream of the delta appears to be equal to the slope before the sluice gate setting was changed, even in the diverging region of the flume upstream from the dam.

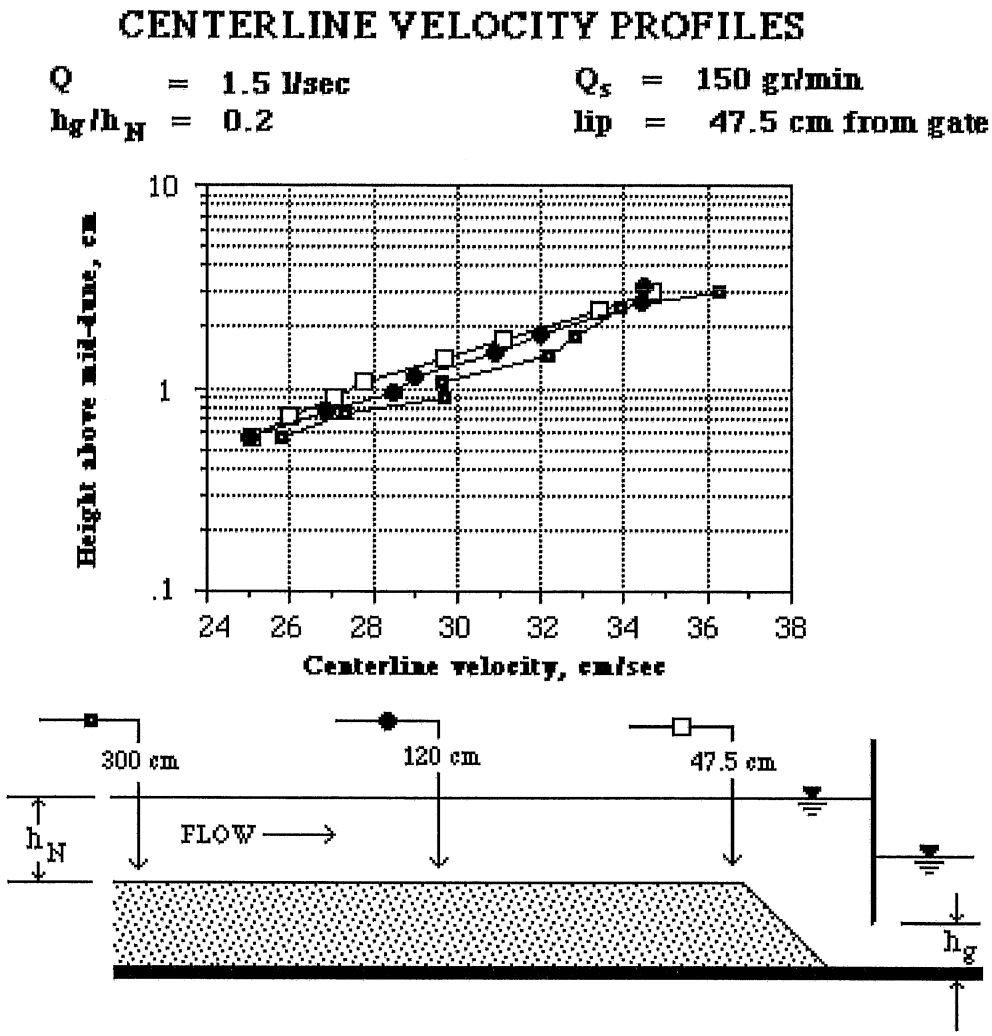

Figure 3.6 Centerline velocity profiles for Run 5

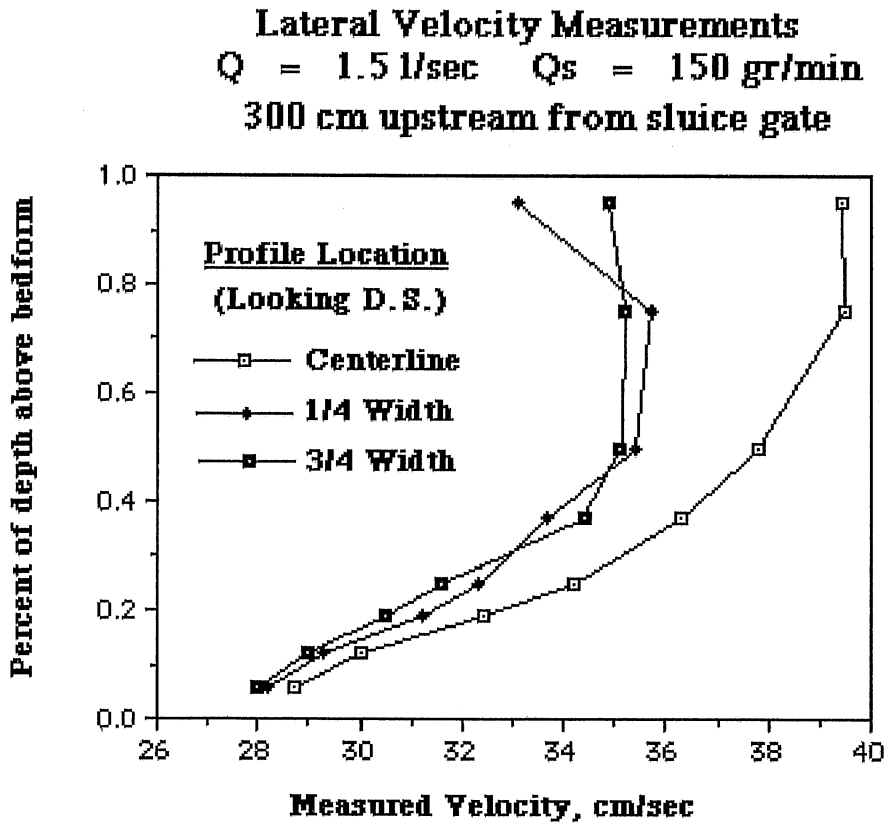

Figure 3.7 Lateral velocity profiles for Run 17

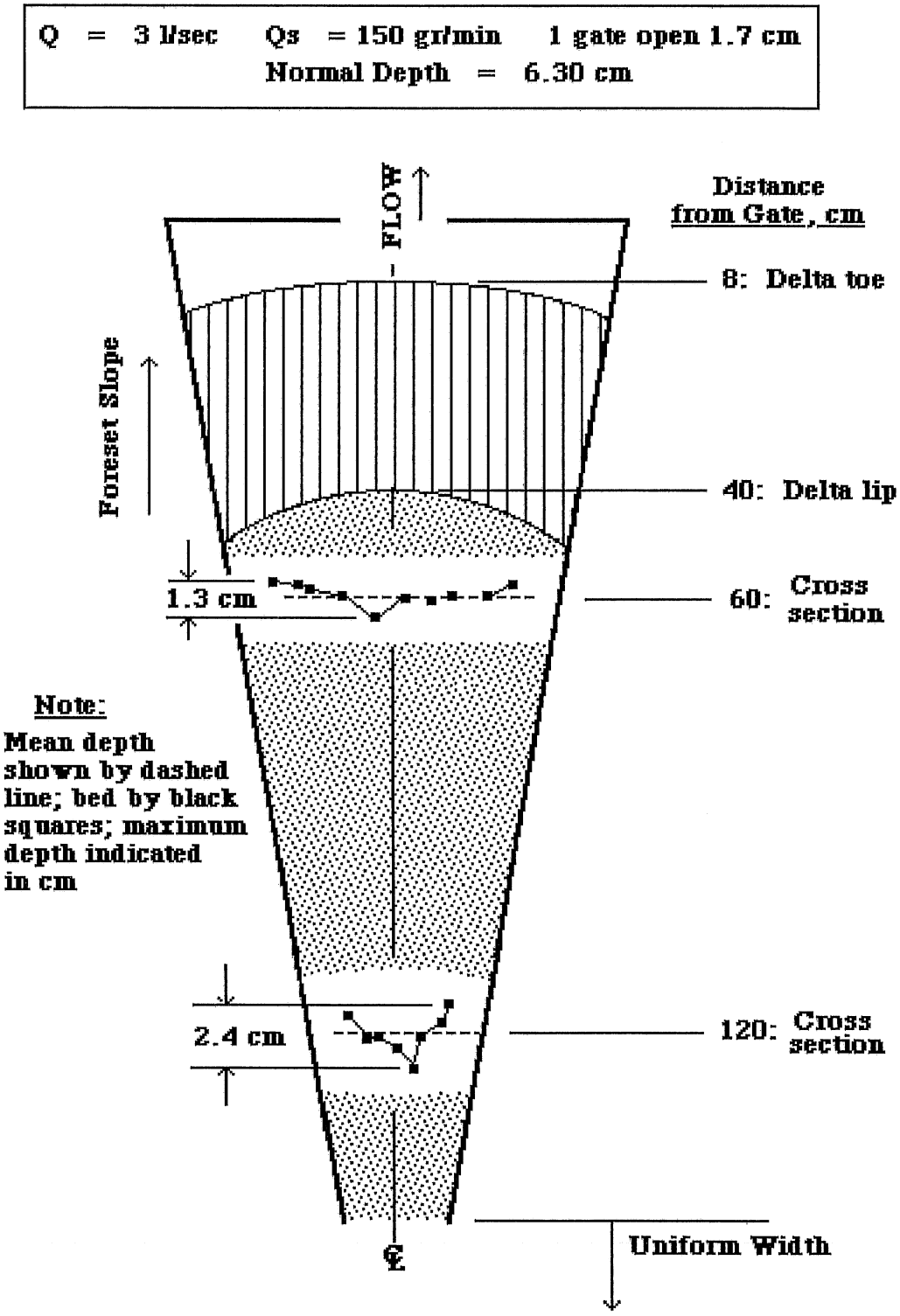

Figure 3.8 Plan view of expanding region upstream of dam for Run 19

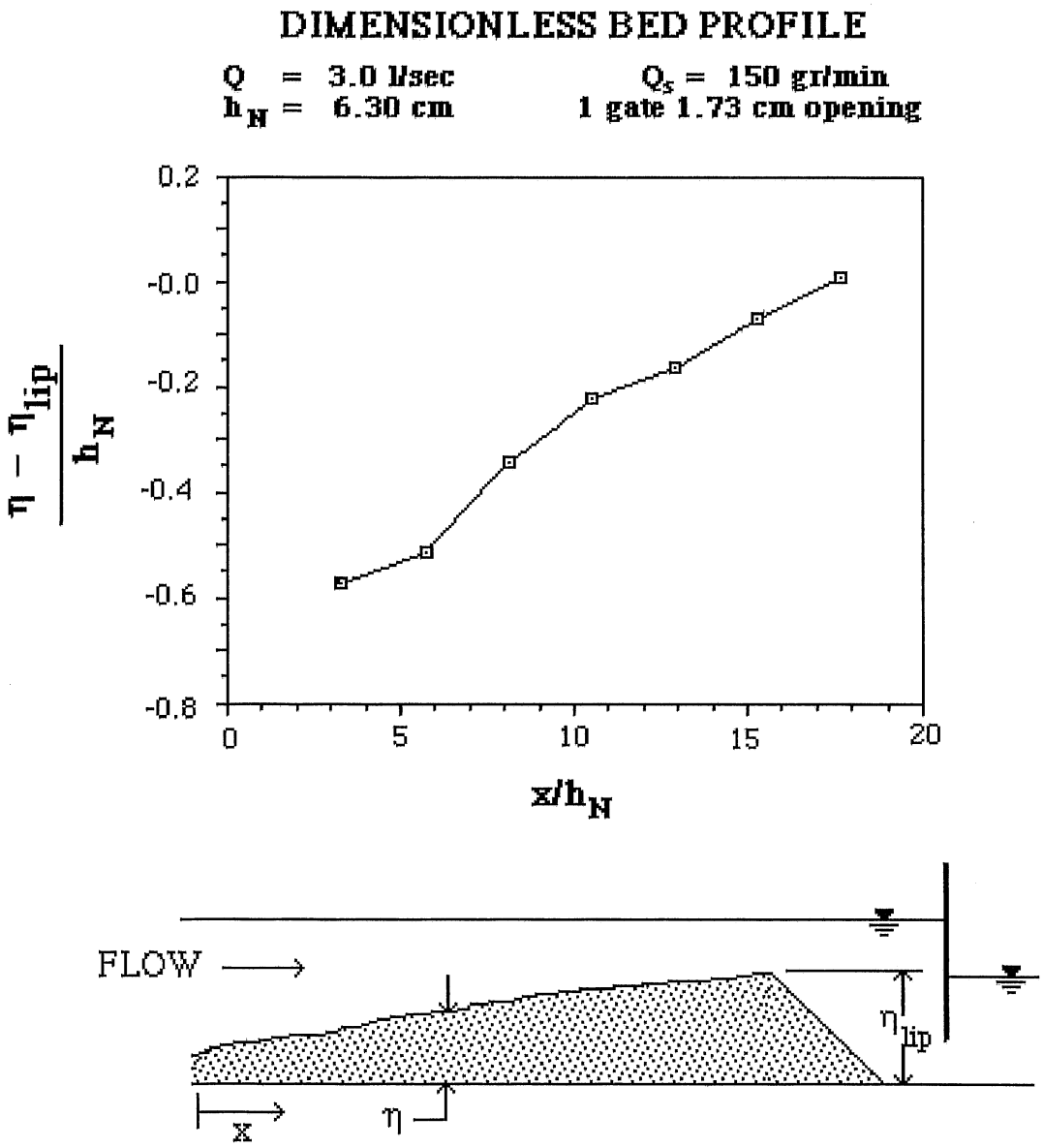

Figure 3.9 Dimensionless longitudinal bed profile in expanding region upstream of dam for Run 19

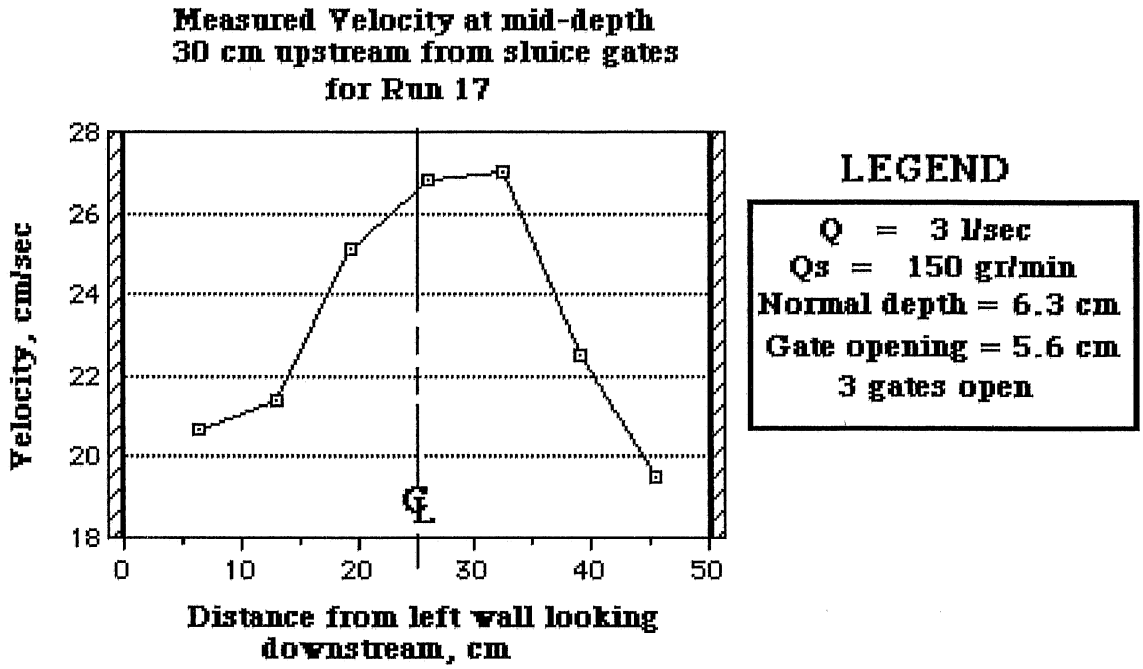

Figure 3.10 Mean velocity at one-half depth at a location 30 cm upstream from sluice gates in diverging flume for Run 17

In the experiments with an expanding region upstream from the dam, the delta enters the flared region, and the sediment spilling down the foreset slope spreads laterally to fill the width of the flume. The delta then continues downstream. The delta eventually stops progressing downstream as it approaches the sluice gates, and the incoming sediment is transported down the foreset slope and passes under the sluice gates.

After new equilibrium conditions have been established, the flow field in the flume appears exactly as before changing the sluice gate setting except that the bed has risen as much as the water surface and a delta appears upstream of the sluice gates. The bedforms retain the same amplitude, wavelength, and wave speed.

This description agrees with Garde and Ranga Raju's 1985 thought experiment in that the bed rises as much as the water surface and all sediment passes under the sluice gate (over the dam in their case). The process also agrees with Chee and Sweetman (1971), especially as they describe a mound of sediment forming at the inlet to the reservoir. The observed formation of two distinct reaches, one upstream and the other downstream of the delta, agree exactly with the observations of Bhamidipaty and Shen (1971), including their description of the foreset slope attaining the submerged angle of repose. Observations seem to confirm Sugio's statement (1972) that the aggrading

profile can be considered to be almost in equilibrium as the sediment front advances. That the equilibrium bed slope after lowering the sluice gate is the same as before agrees with the observations of the scale model of Chitale, Galgali, and Appukuttan (1975).

The flume experiments apparently represent the portion of a reservoir immediately upstream from the dam in its final stage of sedimentation. Backwater calculations, in fact, show that the influence of lowering the sluice gates would extend several flume lengths upstream. Hence, the flume does not include the zone far upstream initially affected by backwater. This explains why a mound of sediment forms at the entrance to the flume before moving downstream. So in comparing the flume experiments to a prototype situation, the flume entrance must be considered to be relatively close to the dam, say 1 kilometer in a backwater reach that may extend10 kilometers or more upstream.

The experimental observations of this study do not agree with observations in many large reservoirs that the topset slope is between one-half and two-thirds the original bed slope. The reservoir studies by Borland (1971) and others, however, include reservoirs of increasing width in the downstream direction. Recall that Woolhiser and Lenz (1965) account for decreases in slope under equilibrium conditions by implicitly recognizing that reservoir width usually increases in the downstream direction. If, for example, using their equations, equilibrium holds and the stream width does not change, then the new slope is found to be equal to the previous one. More discussion on this point follows later.

The foreset slope is apparently steeper in the flume experiments than in the field. This is probably due to fine sediment depositing at the toe of field deltas, which would tend to decrease the foreset slope. The data of Strand and Pemberton (1982) surely reflect such cases, with values for the foreset slope of up to 100 times that of the topset slope.

3.6.1.2 Degradation.

Upon raising the sluice gate after a delta had reached equilibrium, the headwater surface elevation drops rapidly in response to the increase in flow area through the sluice gate. A negative surface wave proceeds upstream and is followed more slowly by upstream progressing degradation of the channel bed. Sediment transport rate is increased throughout the flume, and plane-bed conditions prevail for some time. Eventually bedforms appear at the upstream end of the flume and proceed downstream, and a new equilibrium profile is established. The bed recovers the same slope as before, and the height of the delta is decreased and is located nearer to the sluice gate than before. Uniform scour is observed across the flume width, even in the expanding region.

There are no other experimental or field data with which to compare these experimental observations.

3.6.2 Nature of Flow Upstream of Delta

Observations of the flume experiments agree with other experimental and field observations that flow conditions in a constant-width channel appear to be uniform upstream of the lip of the delta for equilibrium conditions, i.e. with the delta at its final position near the sluice gate. This is substantiated by the fact that measured bed slopes were equal to the bed slope before deposition. If uniform conditions prevail, velocity profiles should be similar upstream of the delta lip.

Figure 3.6 shows velocity profiles for three locations in the flume for run 5. The sluice gate opening was equal to 0.2 times the normal flow depth, and the bed had risen

21.3 cm from its open channel elevation. The three velocity profiles are very similar, showing that, indeed, uniform flow conditions prevail, even at the lip of the delta.

3.6.3 Sediment Continuity and Transport

3.6.3.1 Sediment continuity.

The sum of the bedform transport and suspended load transport should equal the measured sediment input to the flume. Suspended load was insignificant for the runs with sediment feed rates of 150 gr/min, while calculations of bedform load using the porosity value of 0.53 vary from 130 to 160 grams per minute, i.e., from 13 per cent low to 7 per cent high.

Results for the runs with feed rates of 300 grams per minute are less satisfactory (Table 3.2). The bedform transport in most of these runs was measured as a smaller percentage of the total transport than in the 150 gr/min feed cases. And although the suspended load was higher with the higher feed rate, the suspended sediment measurements show consistently low results, such that the sum of the suspended load and the bedload is significantly less than the input load. The average concentration was very low, indicating that the experiments may have been out of the range of meaningful results using the electro-optical concentration meter.

3.6.3.2 Sediment transport relationship.

The dimensionless sediment transport and grain shear stress values from Table 3.5 are plotted in Figure 3.11 along with some well-known sediment transport relationships. The Meyer-Peter Müller formula (1948) was derived from measurements of sand and gravel transport over a relatively narrow range of shear stresses and is written:

$$q_s^* = 8(\tau_g^* - 0.047)^{1.5} \qquad (3.8),$$

where q_s^* = dimensionless sediment transport per unit width and τ_g^* = dimensionless grain shear stress.

The Engelund-Hansen relationship was developed using data from four sets of experiments in a large flume 2.44 meter wide and 45.7 feet long (Vanoni, 1975). The sediments had median fall diameters of 0.19 to 0.93 millimeters, and were well-sorted to poorly sorted. The equation is not recommended for median grain sizes of less than 0.15 millimeters or for geometric standard deviations greater than two. It reads:

$$q_s^* = \frac{0.05}{C_b}\tau_b^{*\,1.5} \qquad (3.9),$$

where τ_b^* is the bed shear stress after being corrected for sidewall influences. Engelund and Hansen recognized the role of bedforms in sediment transport and developed the relationship between bed shear stress and grain shear stress shown in Figure 3.12. Their data show that bed shear stress can actually decrease with increasing discharge as lower regime bedforms (ripples and dunes) are washed out. In practice equation 3.9 is used with Figure 3.12 to estimate sediment transport. The "Engelund-Hansen" type relationship plotted for this thesis is based on a best-fit line through the flume data pairs of bed and grain shear stress, also shown in Figure 3.12.

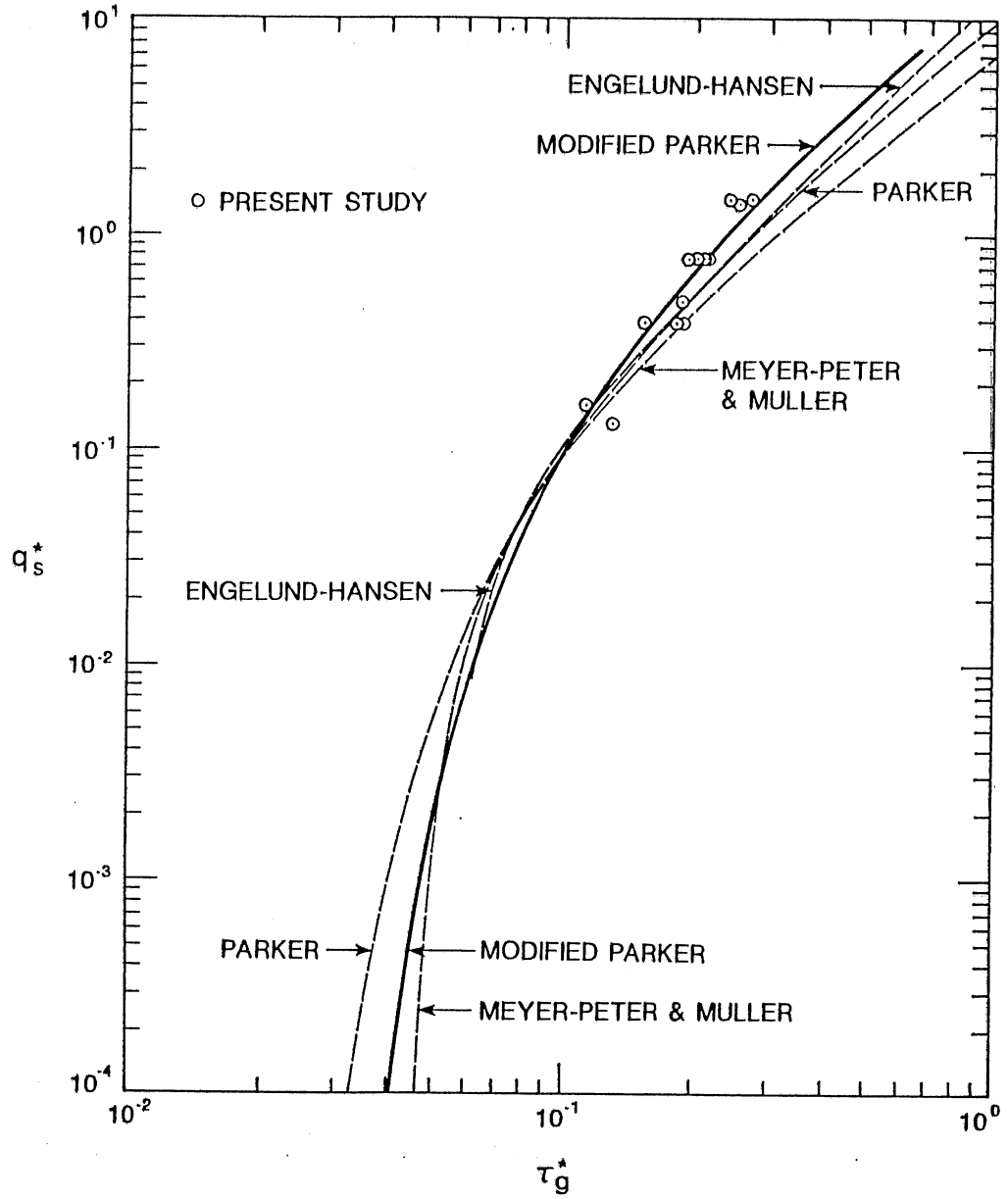

Figure 3.11 Dimensionless sediment transport per unit width versus dimensionless grain shear stress

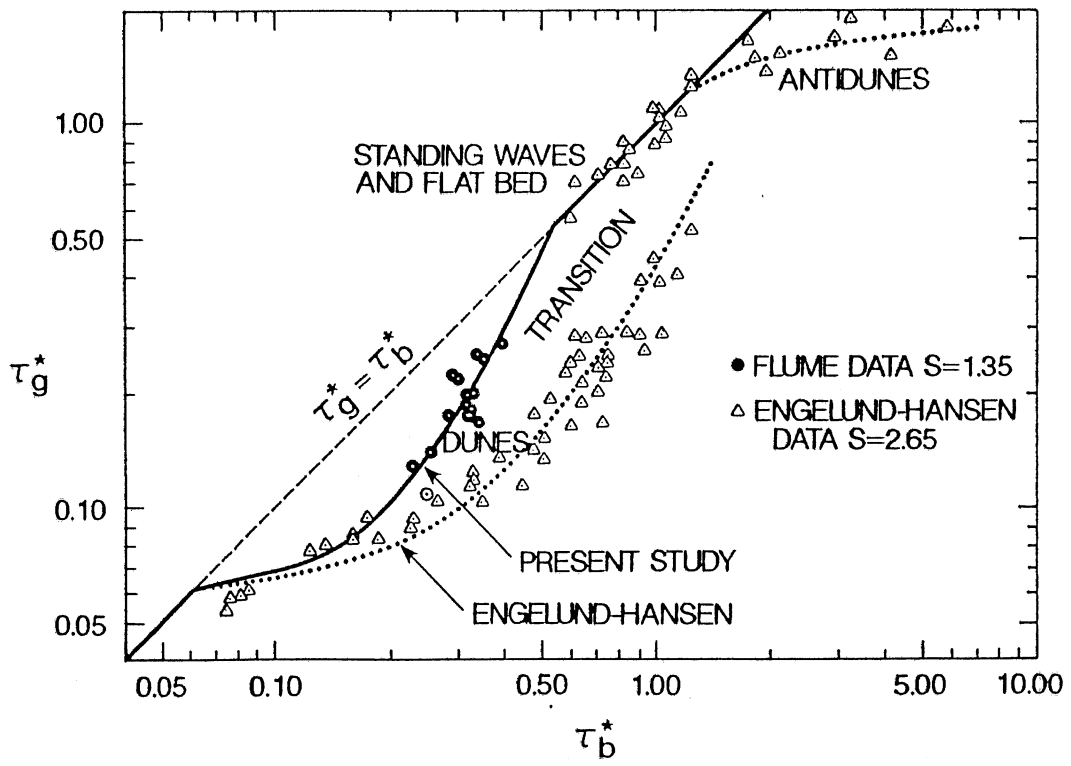

Figure 3.12 Dimensionless grain shear stress versus dimensionless bed shear stress

The best-fit line is described by

$$\tau_g^* = \tau_b^* \qquad \text{if } \tau_b^* \leq 0.0626,$$

$$\tau_g^* = 0.06 + 2.14\tau_b^{*2.43} \qquad \text{for } 0.0626 \leq \tau_b^* \leq 0.541, \text{ and}$$

$$\tau_g^* = \tau_b^* \qquad \text{if } \tau_b^* > 0.541 \qquad (3.10)$$

This equation reflects the slight trend in the experimental data towards an upper-regime flat -bed flow as shown in Figure 3.12.

The Parker relationship is

$$q_s^* = 11.2\,\tau_g^{*1.5}\left(1 - 0.853\frac{\tau_r^*}{\tau_g^*}\right)^{4.5} \qquad (3.11)$$

where τ_r^* is a dimensionless reference shear stress,taken as 0.03 for uniform sediments (Parker, 1976). Equation (3.11) is based on 278 data sets of gravel transport in hydraulically rough channels with aspect ratios greater than 5.

For use in the computer simulation of flume sediment transport, a relationship similar to Parker's was fitted by eye to the experimental data of Figure 3.11:

$$q_s^* = 18\,\tau_g^{*1.5}\left(1 - 0.853\frac{\tau_r^*}{\tau_g^*}\right)^{4.5} \qquad (3.12),$$

where τ_r^* is taken as 0.04.

3.6.4 Position of Delta

At final equilibrium, the delta front was located just upstream of the sluice gates. Typically the bottom of the front was separated from the gate by a short reach in which the flume bottom was exposed. The distance the flume bottom was exposed upstream of the sluice gates is plotted in Figure 3.13, and is made dimensionless using normal upstream depth. The ordinate in the figure, the gate Froude number, relates velocity under the sluice gate to gate opening and is a measure of scouring strength. There is significant scatter in Figure 3.13, but the results show that scouring distance is proportional to gate Froude number and inversely proportional to gate width. It appears that the minimum gate Froude number to achieve total scour is about 0.4.

The experimental results confirm White and Bettes' 1984 numerical results that sluice gates are effective in completely eroding the bed for only a short distance upstream. The attendant increase in reservoir storage capacity is very small.

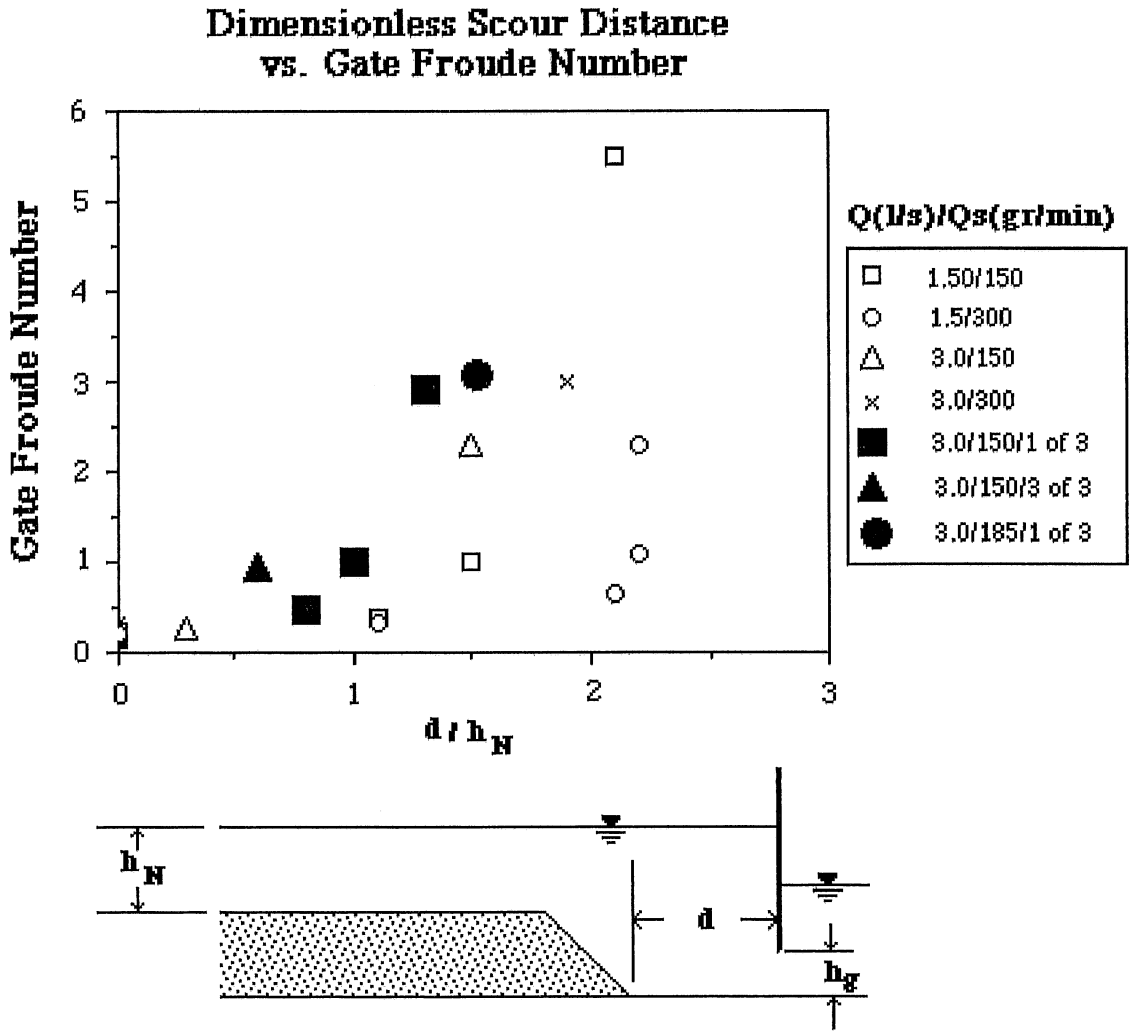

Figure 3.13 Dimensionless distance upstream of sluice gate(s) for which the flume bottom was exposed

3.6.5 Flume Response to Sluicing

Previous experiments suggest the bed and water surface change an equal amount in response to a change in sluice gate setting. Results in these simple experiments confirm that notion. If closing the sluice gate increases the upstream water level by 2 cm, the equilibrium bed profile will be 2 cm higher than before.

In summary: for a narrow, gorge-like reservoir with uniform non-cohesive sediments, actions which raise or lower the water surface near the dam will ultimately result in raising or lowering the bed an equal amount.

If the reservoir water surface elevation at the dam can be estimated from the gate opening, the change in bed elevation can also be estimated. The water surface elevation is related to the gate opening by the orifice equation, Equation (3.7). Solving (3.7) for ξ_R yields (for unit width discharge)

$$\xi_R = \xi_T + \frac{q^2}{2gC_d^2 h_g^2} \qquad (3.13).$$

Defining η_R as upstream bed elevation and using h_N as open channel normal depth,

$$\eta_R = \xi_R - h_N \qquad (3.14),$$

and from (3.13),

$$\eta_R = \xi_T + \frac{q^2}{2gC_d^2 h_g^2} - h_N \qquad (3.15).$$

Changing the gate opening may change the discharge coefficient and tailwater elevation in addition to the upstream bed elevation. Denoting changes by Δ,

$$\Delta\eta_R = \Delta\xi_T + \frac{q^2}{2g}\Delta\frac{1}{C_d^2 h_g^2} \qquad (3.16).$$

Equation (3.16) may be made dimensionless by dividing by the normal depth:

$$\frac{\Delta\eta_R}{h_N} = \frac{\Delta\xi_T}{h_N} + \frac{q^2}{2gh_N^3}\Delta\frac{1}{C_d^2}\frac{1}{(\frac{h_g}{h_N})^2}$$

or

$$\frac{\Delta\xi_R}{h_N} = \frac{\Delta\xi_T}{h_N} + \frac{1}{2}F_r^2\Delta\frac{1}{C_d^2}\frac{1}{(\frac{h_g}{h_N})^2} \qquad (3.17).$$

Equation (3.17) may be used to predict the bed response to sluicing in either a narrow or diverging channel with vertical sidewalls. The input parameters are on the right-hand side of the equation, and include changes in the tailwater elevation, discharge coefficient, Froude number, and sluice gate opening. These data are readily available in the laboratory or the field. The equation is tested with the observed results of Table 3.4 shown in Figure 3.14. Here the observed deposition, made dimensionless with normal depth, is plotted against the predicted deposition using Equation (3.17). Significant scatter for smaller changes in bed elevation is due partly to the difficulty in measuring small changes in the elevation of a dune-covered bed. Agreement is much better for large changes in bed elevation as shown in the figure.

The above results apply for straight-walled reservoirs with uniform non-cohesive sediment that are sufficiently narrow to exhibit fairly uniform deposition and scour across the entire cross section.

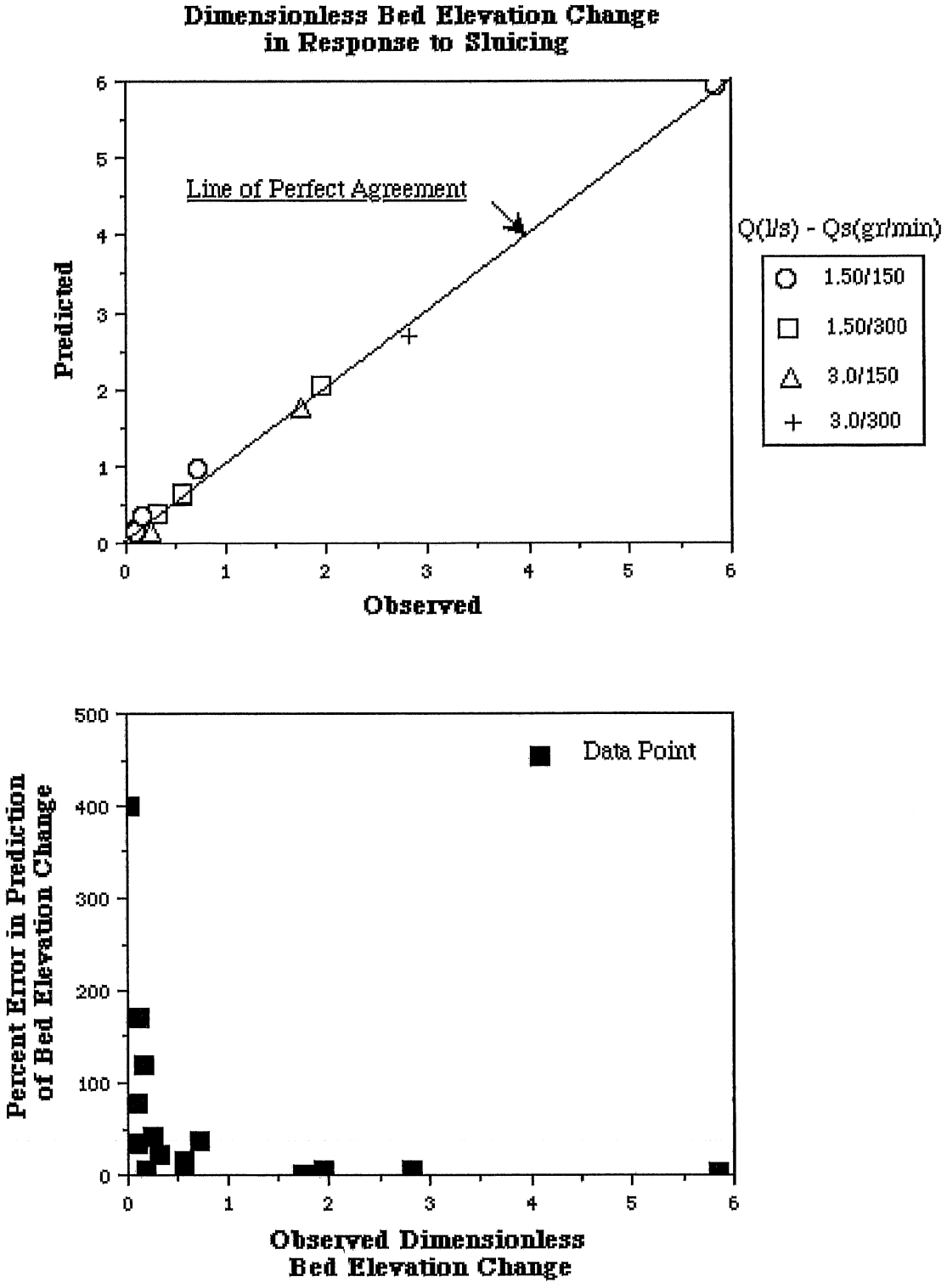

Figure 3.14 Observed vs. predicted change in bed elevation

CHAPTER 4 NUMERICAL MODEL OF RESERVOIR AGGRADATION AND DEGRADATION

The purpose of this chapter is to describe the development of a numerical model for reservoir aggradation and degradation.

4.1 Objectives of Numerical Model

The numerical model for aggradation and degradation in reservoirs should:

1. predict the occurrence of a delta formation
2. track the movement and growth of the delta in the reservoir
3. model the degradation process in a mathematically stable manner
4. reproduce observed laboratory results
5. be applicable to field-scale problems
6. provide general insight into reservoir sedimentation behavior

4.2 Governing Equations and Limitations

All notation has been introduced in previous chapters.

4.2.1 Governing Equations

4.2.1.1 St. Venant equations.

The quasi-steady form of the St. Venant equations are used to describe momentum and continuity for water:

$$\frac{\partial(u\,h\,b)}{\partial t} + \frac{\partial(u^2\,hb\theta)}{\partial x} = -g\,b\,h\frac{\partial \xi}{\partial x} - p\,C_f u^2 \qquad (4.1);$$

and

$$\frac{\partial(h\,b)}{\partial t} + \frac{\partial(u\,h\,b)}{\partial x} = 0 \qquad (4.2).$$

Equations (4.1) and (4.2) are one-dimensional but allow for variations in channel width. A rectangular cross section is assumed.

4.2.1.2 Sediment continuity.

The unsteady sediment continuity equation is

$$\frac{\partial(\eta\,b)}{\partial t} + \frac{1}{1-\lambda_p}\frac{\partial(q_s\,b)}{\partial x} = 0 \qquad (4.3).$$

Once again one-dimensionality is assumed, and sediment is uniformly deposited or scoured across each modeled reach.

4.2.1.3 Sediment transport.

Sediment transport is estimated using the Parker relationship introduced in Chapter 3:

$$q_s^* = c_2 \tau_g^{*1.5} \left(1 - 0.853 \frac{\tau_r^*}{\tau_g^*}\right)^{4.5} \qquad (4.4),$$

where c_2 is a coefficient and τ_r^* is a near-critical reference bed shear stress. For the experiments in this investigation, $c_2 = 18$ and $\tau_r^* = 0.04$. For field cases, c_2 and τ_r^* may vary, but will be taken as 11.2 and 0.03 as in Parker's original analysis. Equation (4.4) is for a uniform, non-cohesive sediment.

4.2.1.4 Friction relationship.

Relationships discussed in Chapter 3 are used in the model to relate friction factors to shear stress and energy slope. For the experimental runs of this investigation, Equations (A1.11) and (A1.12) from Appendix A1 are used:

$$\frac{1}{\sqrt{C_g}} = 2.5 \ln\left(12.3 \frac{r_g}{k_s} X\right) \qquad (4.5),$$

for fully rough turbulent flow, and

$$\frac{1}{\sqrt{C_g}} = 2.5 \ln\left(3.67 \frac{r_g u_{*g}}{\nu}\right) \qquad (4.6)$$

for turbulent smooth flow. The parameters X and r_g are defined in Appendix A1.

For wide channels the Engelund-Hansen relationship is used (Equation (A1.14)):

$$\frac{1}{\sqrt{C_g}} = 2.5 \ln\left(11 \frac{r_g}{2 d_{50}}\right) \qquad (4.7).$$

These friction factors are related to grain shear stress by Equation (A1.16):

$$\tau_g = \rho C_g u^2 \qquad (4.8),$$

providing the necessary link to the sediment transport equation.

The friction factor pertaining to the bed, C_f, in Equation (4.1) is composed of the grain friction factor and the bedform friction factor. For the flume experiments, a modified Engelund-Hansen relationship provides this link as described in Chapter 3 using shear stresses:

$$\tau_g^* = \tau_b^* \qquad \text{if } \tau_b^* \le 0.0626,$$

$$\tau_g^* = 0.06 + 2.14 \tau_b^{*2.43} \qquad \text{for } 0.0626 \le \tau_b^* \le 0.541, \text{ and}$$

$$\tau_g^* \qquad \text{if } \tau_b^* > 0.541 \qquad (4.9).$$

The original Engelund-Hansen relationship (Figure 3.12) is used for field cases. Their analysis shows a discontinuity in the relationship between bed and grain shear stress at the transition to upper regime flow. For the purposes of this study this discontinuity is not modeled, and the grain and bed shear stress are related as

$$C_b u^{*2} = C_g u^{*2} \text{ for } C_g u^{*2} < 0.0615 \text{ or } C_g u^{*2} \geq 2.435, \text{ and}$$

$$C_b u^{*2} = 1.581\sqrt{C_g u^{*2} - 0.06} \text{ for } 0.0615 \leq C_g u^{*2} < 2.435 \qquad (4.10),$$

where $u^{*2} = \dfrac{u^2}{\rho g R d_{50}}$.

4.2.2 Modeling Limitations

The numerical model is developed as a research tool to complement the experimental investigations of reservoir aggradation and degradation. It is subject to the same limitations as are the experimental results, namely,

1. Steady inflow and outflow of water and steady inflow of sediment at all times. This means that unsteady input phenomena such as storm or seasonal hydrographs are not modeled, nor are their associated unsteady sediment inflows. It also means that the unsteady flow response to reservoir sluicing is not considered.
2. Froude numbers must be less than about 0.7 . This is a result of using the water and sediment equations in an uncoupled fashion, solving for each independently for each time step.
3. From the restriction that Froude number should be less than about 0.7, it follows that subcritical flow must be maintained at all times. All calculations for backwater profiles therefore begin at a downstream boundary and proceed upstream, as is appropriate for subcritical flow conditions.
4. Uniform, non-cohesive sediment is used. The model does not account for sorting, armoring, or communition of grains.
5. Channel widths are allowed to vary with distance but not with time.

4.3 Model Development

4.3.1. Solution Techniques

For each modeled reach there are 5 unknowns: water depth and velocity, friction slope, sediment transport, and bed elevation. Once values for these unknowns are found, computations proceed forward one time step.

4.3.1.1 Depth, velocity and friction slope.

The St. Venant equations are used to solve for depth, velocity, and friction slope for each reach. Equation (4.1) is re-written as

$$u\frac{\partial (u\,hb)}{\partial x} + u\,b\,h\frac{\partial u}{\partial x} = -g\,b\,h\frac{\partial \xi}{\partial x} - p\,C_f u^2 \qquad (4.11),$$

where the momentum flux correction factor, θ, is assumed to be 1.0.

From continuity, the first term in equation (4.11) is zero, so after dividing by gbh,

$$\frac{u}{g}\frac{\partial u}{\partial x} = \frac{\partial \xi}{\partial x} - \frac{p\,C_f u^2}{gbh} \qquad (4.12).$$

From the relations $\xi = h + \eta$, $p = b + 2h$, and $C_f u^2 = grS_f$,

$$\frac{\partial}{\partial x}\left(\frac{u^2}{2g} + h + \eta\right) = -S_f$$

or

$$\frac{\partial H}{\partial x} = -S_f \qquad (4.13)$$

where

$$H = \frac{u^2}{2g} + h + \eta \qquad (4.14),$$

and H is the total energy head at a section.

Equation (4.14) is the standard step backwater equation, which for subcritical flow is solved in a backward difference numerical scheme:

$$\frac{H_i - H_{i+1}}{\Delta x} = -\frac{1}{2}(S_{f,i} + S_{f,i+1})$$

or

$$D(h) = 0 = H_{i+1} - H_i - \frac{\Delta x}{2}(S_{f,i} + S_{f,i+1}) \qquad (4.15),$$

where node i is downstream and node i + 1 is upstream.

For known values of H and S_f at node i, (4.15) is written

$$D(h) = 0 = \frac{q_{w\,i+1}}{2gh_{i+1}^2} + h_{i+1} + \eta_{i+1} - H_i - \frac{\Delta x}{2}(S_{f,i} + S_{f,i+1}) \qquad (4.16),$$

where h_{i+1} and $S_{f,i+1}$ are the only unknowns.

According to the Newton-Raphson iteration scheme, (4.16) is solved by successive approximation, where the next guess for the depth, h_{i+1}, is equal to $-\frac{D(h)}{D'(h)}$, where

$$D'(h) = -Fr_{i+1}^2 + 1 + \frac{3}{2}\left(\frac{\Delta x}{h_{i+1}}S_{f,i+1}\right) \qquad (4.17).$$

The friction slope, S_f, is found from $S_f = \frac{C_f u^2}{gr}$ where C_f is from the sidewall correction procedure in Appendix 1.

The above equations return values of h, u, and S_f at a node. The calculations proceed upstream until the calculated depth is within 1 per cent of normal, or until a user-specified distance, such as the length of the flume, is reached. This location represents the upstream boundary of the modeled reach and is where the constant sediment supply is input. If the user-specified reach is shorter than the actual backwater profile, the natural process of the backwater zone extending upstream in response to aggradation cannot be simulated.

4.3.1.2 Sediment transport and bed elevation

Sediment movement is predicted using (4.4) with appropriate coefficients. Bed elevations are then calculated using the sediment continuity equation, written here in backward finite difference form:

$$\eta_{i,j+1} = \eta_{i,j} + \frac{\Delta t}{(1-\lambda_p)(\Delta x)} \frac{1}{b_i} (q_{s,i+1} b_{i+1} - q_{s,i} b_i) \qquad (4.18).$$

The backward difference scheme is especially appropriate for modeling deltaic movement, where bed elevations downstream are dependent upon transport from upstream.

4.3.1.3. Selection of spatial and temporal step lengths.

The accuracy of a backward-difference numerical scheme is of order Δx, the distance increment (Street, 1973). The distance increment should be chosen to be appropriate for the scale of the problem and process being modeled. An upper limit for Δx may be estimated by first choosing a Δt and then solving for the bedform celerity from (2.19):

$$\frac{(1-\lambda_p)\Delta x}{\Delta t} = C_n = 2.33 \left[a_1 (b_1 - c_1) u^{b_1} h^{c_1 - b_1} \right]^{0.96} \qquad (2.19)$$

where q_s is expressed as $q_s = a_1 q^{b_1} (\xi - \eta)^{c_1 - 1}$. For example, if Parker's equation for field conditions is used, then for large values of τ_g^*, a = channel width, b = 3, and c = 0.

The values of Δx and Δt can then be tested in the model to see if any numerical instabilities develop.

4.3.2 Aggradation

4.3.2.1 Summary of aggradation process.

As described in detail in Chapter 3, upon lowering the sluice gate into the flow in the experimental flume, the water surface rises upstream and a mound of sediment deposits downstream of the flume entrance. A delta forms and moves forward toward the sluice gates. The topset slope is maintained at a near-normal value in the uniform-width portion of the flume and conserves the observed adverse slope in the diverging portion of the flume. Field data indicate the topset slope is between one-half and two-thirds the normal slope.

4.3.2.2 Modeling approach

It is a violation of the one-dimensional equations of motion to attempt to model flow over a delta lip where the immediate downstream slope approaches the submerged angle of repose (about 33°). Flow separation and recirculation are observed to occur in this region. Pressure is not uniformly hydrostatic, and flow is certainly not well described by a one-dimensional approach. As an alternative, the evolution of a steepening bed is monitored in the computer program. When the slope exceeds a certain criterion, a vertical face is mathematically fitted at the node of maximum slope. The vertical front, a shock, is then moved forward into the reservoir based on the continuity equation for sediment. From experimental observations, a delta forms when the sediment transport decreases to zero at some point upstream of the dam. In this investigation, a shock is fitted to the incipient delta when the computed bed slope in the aggrading region exceeds five times the normal slope. As actual bed slopes rarely exceed 1 or 2 per cent, the model tracks a developing delta until the bed slope is a maximum of 10 per cent. This is still considered to be within the range of valid one-dimensional modeling. Most streams have slopes that are one or more orders of magnitude flatter, so there is no question as to the validity of one-dimensional modeling slopes five times the normal value.

Once the slope in a modeling reach reaches a five times the normal value, the bed elevations at locations 16 and 6 nodes upstream are used to extrapolate downstream to establish the elevation of the top of the vertical delta face. Nodes relatively far upstream are used as a basis for extrapolating to the top of the shock to avoid spurious extrapolations from nodes near the delta location, where the bed progressively steepens. In a similar fashion, the bed elevations at locations 5 and 6 nodes downstream are used to extrapolate upstream to establish the elevation of the bottom of the vertical delta face (see Figure 4.1). Nodes closer to the delta location are used for upstream extrapolation because the bed profile downstream from the delta is relatively unchanged from initial conditions. From this time step forward, sediment transport downstream of the vertical delta face (shock) is taken to be zero.

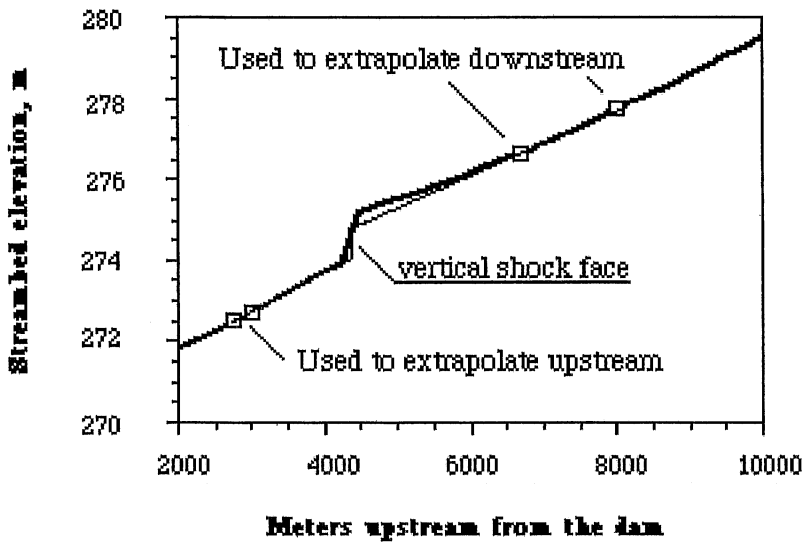

Figure 4.1 Establishing the height of the vertical shock face

Since sediment transport downstream of the shock is indeed zero, the bed and water surface elevations remain unchanged for future time steps. Backwater calculations can therefore subsequently begin one node downstream of the shock and proceed upstream. Once the delta has been located, the computational grid may be made less dense, resulting in fewer computational nodes.

Subsequent sediment calculations begin at the upstream boundary as usual, but terminate at the last node upstream of the shock. Excess sediment passing the last node (refer to Figure 4.2) is first used to raise the top of the shock according to a linear extrapolation from the two closest nodes upstream. Any excess sediment is considered effective in moving the shock forward. The elevation of the bottom of the shock is determined by linear extrapolation from the two closest nodes downstream. An iterative procedure is used to determine the distance the shock moves forward.

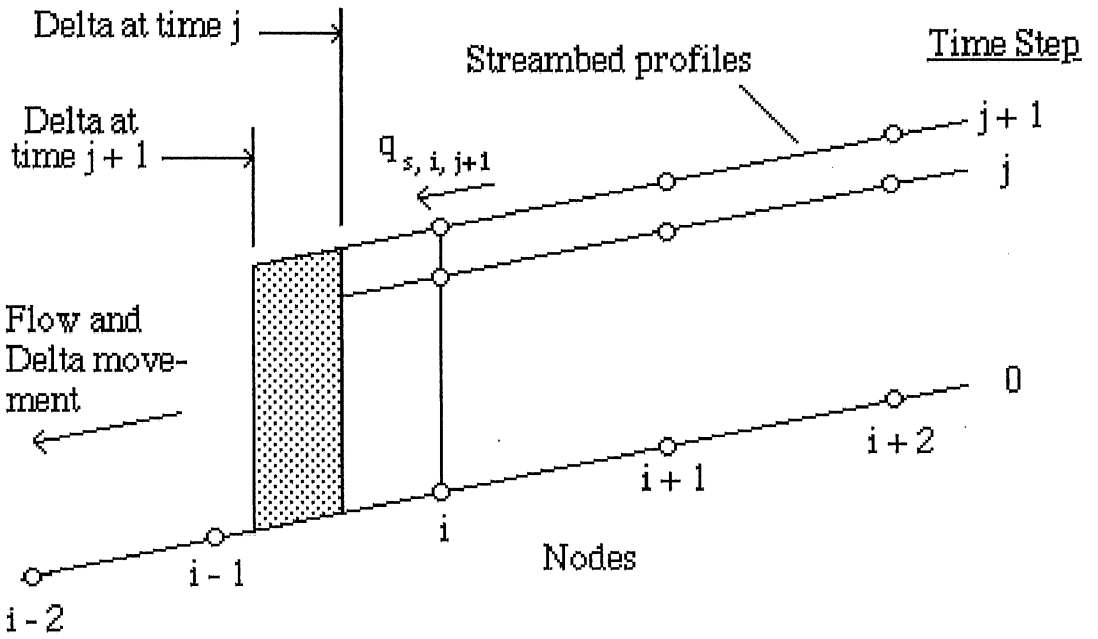

Figure 4.2 Method of moving the shock face forward

If a simulated reservoir is described with less than sixteen nodes, the model will not locate a shock, even though one may be justified by the slope criterion. Neither would a shock be fitted if a delta were to form within the first sixteen nodes from the upstream computational boundary of the model. In this case a shock would be fitted to the bed when the evolving delta passes the sixteenth node in the downstream direction.

In accordance with the concept of a shock, the delta is simulated with a vertical face. This approximation is considered adequate since the longitudinal dimension of the

delta foreset slope is negligible when compared to the longitudinal dimension of the reservoir.

4.3.3 Degradation

4.3.3.1 Summary of degradation process.

Upon raising the sluice gate in the laboratory flume, the water level upstream immediately begins to drop. Sediment transport increases in the vicinity of the sluice gate, and is soon increased throughout the flume as the water surface drops in the upstream direction. Water and sediment transport characteristics immediately downstream of the delta are very unsteady and multi-dimensional.

4.3.3.2 Modeling approach.

Since in the sluicing case there is general movement throughout the reservoir, there can be no computational shortcuts in the degradation case, unlike the aggradational case, where conditions remain unchanged downstream of the delta. Since flow patterns downstream of the eroding delta are very complicated, sluicing computations for every time step begin at the delta lip, which is typically no more than a few normal depths upstream of the dam.

Since the model is not set up for supercritical flow conditions, and since the Froude number is constrained to be less than about 0.7, the water surface can be dropped only relatively slowly. Two computational approaches have been developed for modeling the drop ing the water surface at the downstream boundary which simulate the reservoir draining process. Both allow an eventual total lowering of the water surface equal to the user-input value, which may be several times the normal flow depth in the case of deep reservoir deposits. The first technique, applicable for field cases, allows an initial lowering of the water surface to within one percent of the critical depth above the delta lip. The depth of scour is computed for the location using the sediment continuity and transport equations, and the water surface is next lowered an amount equal to the scour. In this way the water surface is dropped as quickly as possible while maintaining near-critical flows at the delta lip. This process continues until the water surface has been lowered the total amount input by the user. The second technique, applicable for smaller scales such as those of laboratory flumes, further slows the sluicing process. Sluicing at the laboratory scale proceeds very quickly due to the lightweight sediment used and the small geometry of the flume, often producing supercritical flow and extremely unsteady flow conditions. Initial numerical experiments are performed to determine how often the water surface may be dropped a discrete value while maintaining numerical stability in the model. Once this time step value and intervening time has been determined, it is used to lower the water surface at the dam in the model. Sluicing proceeds in almost a semi-equilibrium process, simulated by lowering the water surface a discrete amount with a specified time interval between.

4.3.4 Model Flowchart and Input Requirements

4.3.4.1 Model flowchart.

A model flowchart is shown in Figure 4.3. The input data segment reads the data necessary to initiate a new run or continue a previous run. The initialization segment computes the normal depth and sediment input rate for open channel conditions and computes the initial backwater profile showing the effect of either raising or lowering the downstream water surface. The main program segment is a computational loop. A backwater profile is computed, after which sediment transport and bed elevation changes are calculated for each node. For the case of aggradation, the bed profile is checked to see if the slope criterion for shock fitting is met. If it is, the shock is fitted to the bed if

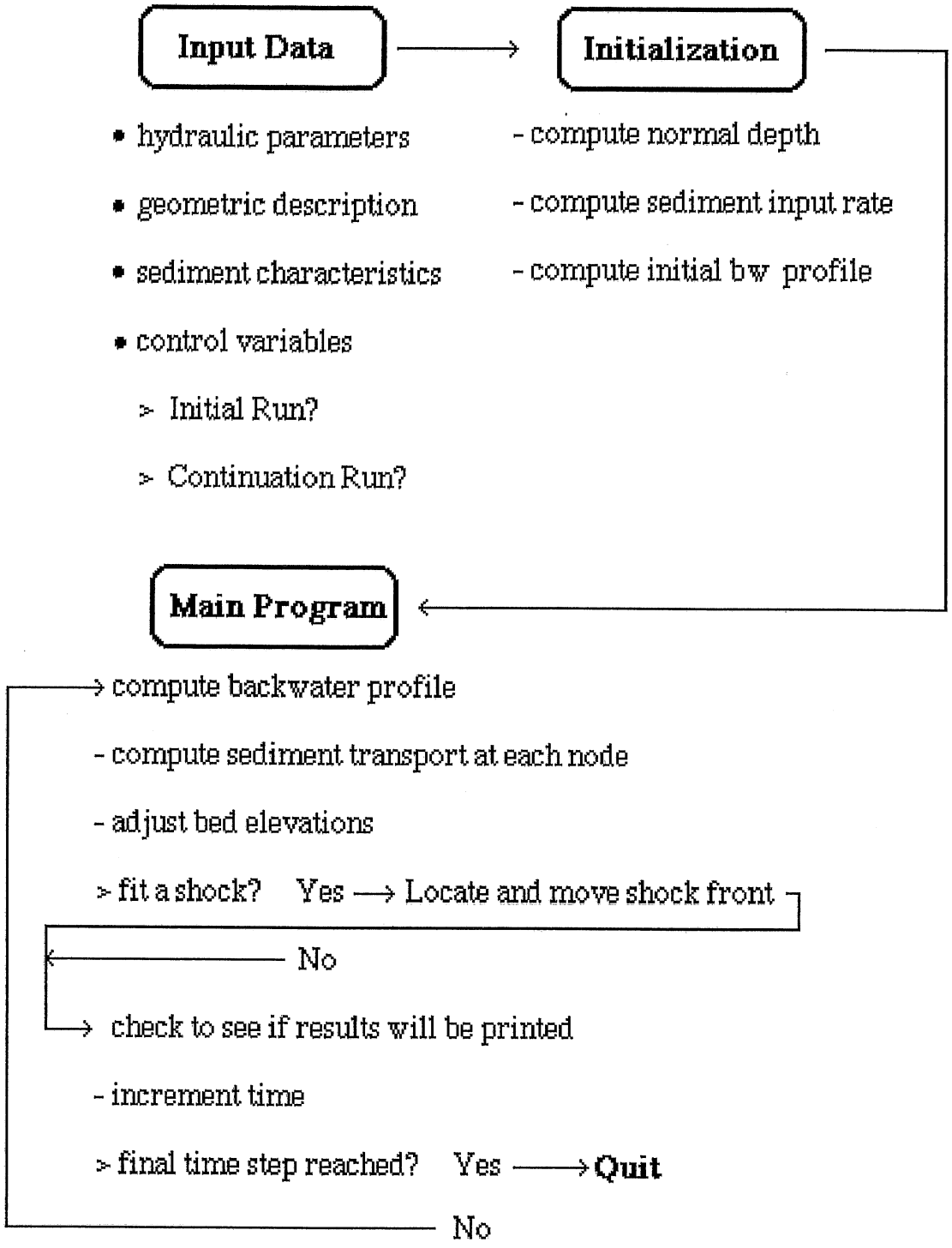

Figure 4.3 Flowchart for numerical model of reservoir aggradation and degradation

the user has selected the shock-fitting option. A check is made to see if results should be printed, and the time step is incremented. The process is repeated for the user-specified number of time steps. If a shock has been fitted to the bed, it is moved forward according to the procedure described previously.

4.3.4.2 Input requirements

The computer code is listed in Appendix 3. Input requirements can be classified in four categories: hydraulic parameters, geometric input, sediment properties, and control variables.

Hydraulic parameters are total discharge, initial normal slope, water temperature, initial depth at the downstream boundary in the case of a diverging channel, and the amount the water surface will be raised or lowered at the downstream boundary.

Geometric input includes the uniform channel width, the rate at which the channel widens and the distance at which the widening begins (if applicable) , the initial bed elevations at the downstream boundary and in the diverging region (if applicable), and values pertaining to cases for which a shock is already in place at the beginning of the run: the shock location, the elevations at the top and bottom of the shock, and the shock width. Finally, distance associated with the dam location (i.e. river kilometer) is required.

Control variables are for choosing model computational and printing options. The user must specify if the run is for a flume or a field case, whether or not a shock will be fit in the case of aggradation, and whether the run is a continuing run or a new study. If it is a continuing run, the user must enter the locations, widths, and bed elevations for each computational node. If a new run is initiated, the program computes the initial bed profile using the initial slope and distance increments. Additional control variables affect how long the computed backwater zone will be and how computations proceed if a shock is fitted to the bed during the run. The user must specify if the initial backwater zone will be extended by a multiple of the initial length to accommodate upstream migration of the backwater zone, or if the zone will be allowed to elongate only when necessary (when the depth at the upstream boundary is no longer within one per cent of normal). If the latter condition is specified, the ultimate backwater reach length is entered. If a shock is to be fitted to the bed, the user must specify by what multiple the distance and time steps will be increased after shock fitting has occurred. The uniform distance and time steps for the run are required, as are the starting time and total time of the run. Finally, the time between printing results is specified. Results include the distance and width assigned to each node, and the elevation of the bed and water surface and the depth and sediment transport for each node.

4.3.5 Model Listing

The computer code is listed in Appendix 3. Included is a definition of program variables and procedure names and descriptions. The code was developed as a research tool and is not particularly user-friendly. It was initially written in TurboPascal and run on a Macintosh SE computer, then moved to a CYBER 855 mainframe and compiled in Pascal-6000.

4.4 Numerical Modeling of Laboratory Runs

The computer model was used to predict normal depths for all the runs listed in Table 3.1 and to predict in detail the aggradation of Run 28 and the degradation of Run 29.

4.4.1 Normal Depth Predictions

Normal depths for open-channel conditions were computed using the Einstein-Barbarossa method and the sidewall correction procedure described in Appendix A1. Observed and computed depths are listed in Table 4.1. Observed normal depths include one-half the observed bedform amplitude. The computed estimates range from 10 per cent low to 6.6 high, and average 2.1 per cent low. The agreement is excellent, especially considering the variability in bedforms and the difficulty in accurately determining bedform amplitude.

4.4.2 Aggradation: flume case

4.4.2.1 Model setup

Run 28, carried out in the experimental flume fitted with an expanding region upstream of the sluice gates, was selected for detailed modeling of aggradation. Bed and water surface profiles were measured every hour after the middle of three sluice gates was set to within 0.0163 meters of the flume bottom. The adjoining sluice gates were closed. After the initial delta formed at the upstream entrance to the flume, 14.3 hours were required for the delta to reach its final position about 0.40 m upstream of the sluice gate. Another 4 or 5 hours were required for the bed to reach its equilibrium state throughout the entire flume.

A time step of 30 seconds and a distance step of 0.6 m were used for the initial portion of the run when the delta was moving through the uniform-width portion of the flume. These values were based on the observed sediment wave celerity in the flume, assuring that the sediment would not travel through an entire model reach in a single time step.

The computer model was first run with the observed open channel equilibrium bed as input. The model was run for two simulated hours without increasing the downstream water surface in order to allow the computed bed and water surface to reach equilibrium. The computed equilibrium bed was then used as the initial condition for the actual simulation. The position of the observed 0.10 meter-high delta two hours after the experiment began was used in the model as a shock and then run until the model predicted that the shock had reached the beginning of the diverging portion of the flume. The distance and time steps were then reduced to 5 seconds and 0.1 meters respectively to model more accurately model the flow in the diverging portion of the flume. The model required 42 computational seconds to track the delta to the beginning of the diverging portion of the flume and 386 computational seconds to reach final equilibrium.

4.4.2.2 Results and discussion.

The computer model estimated the normal depth to be 0.0587 meters compared to an observed value of 0.0653 meters, and estimated the accompanying steady inflow rate of sediment as 227 grams per minute compared to the observed value of 186 grams per minute. The calculated sediment input rate is only 22 per cent higher than observed, which is exceptionally close considering the scatter in the sediment transport data of Figure 3.11. A comparison of the initial observed and computed bed and water surface profiles is shown in Figure 4.4. Agreement is very good. Figures 4.5, 4.6, and 4.7 show bed profile comparisons 1 hour and 7 hours later and for the final equilibrium

Run Number	Normal Depth, cm Observed	Computed	Percent Error
1	3.64	3.64	0.00
6	3.25	3.31	+ 1.9
13	6.18	5.98	- 3.2
14	6.13	5.90	- 3.8
15	5.66	5.61	- 0.9
16	5.40	5.67	+ 5.0
17	6.30	5.87	- 6.8
20	6.30	5.87	- 6.8
21	3.07	3.08	+ 0.3
22	5.32	5.67	+ 6.6
23	7.25	7.27	+ 0.3
24	5.45	5.05	- 7.3
25	3.55	3.58	+ 0.9
26	6.68	6.60	- 1.2
27	6.41	6.64	+ 3.6
28	6.53	5.87	- 10.1
29	6.65	6.03	-9.3
		Average:	-2.1

Table 4.1 Observed and computed normal depths for experimental runs

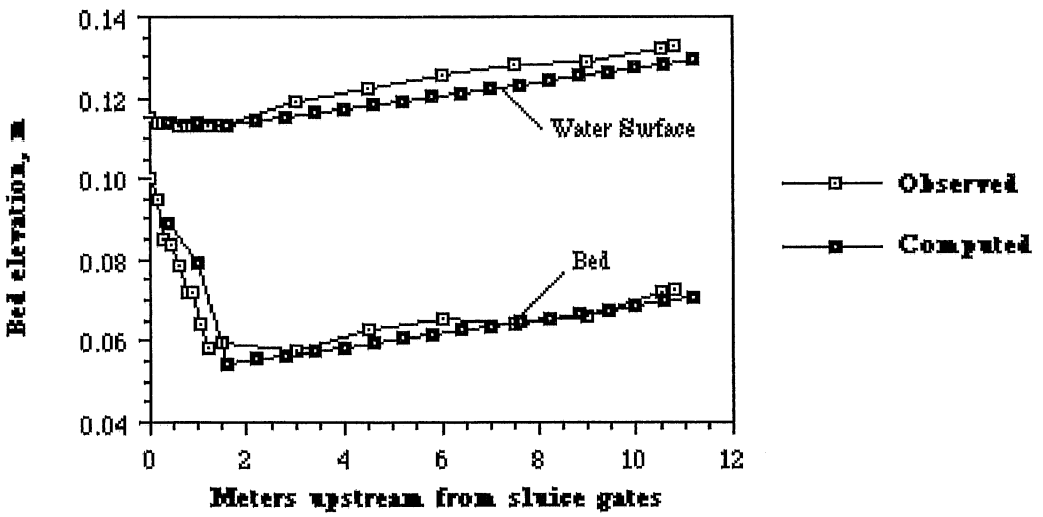

Figure 4.4 Observed and computed initial conditions for Run 28

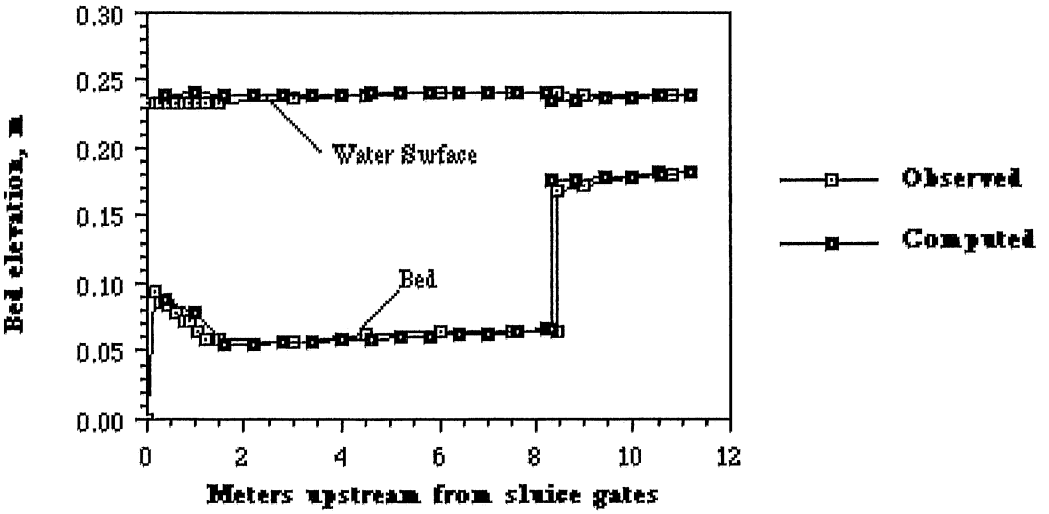

Figure 4.5 Observed and computed bed profiles 1 hour later for Run 28

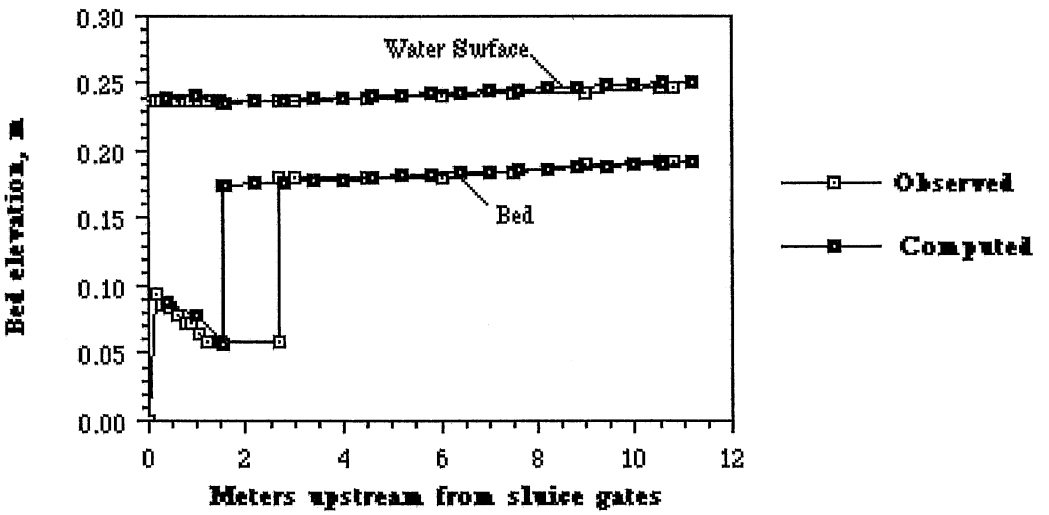

Figure 4.6 Observed and computed bed profiles 7 hours later for Run 28

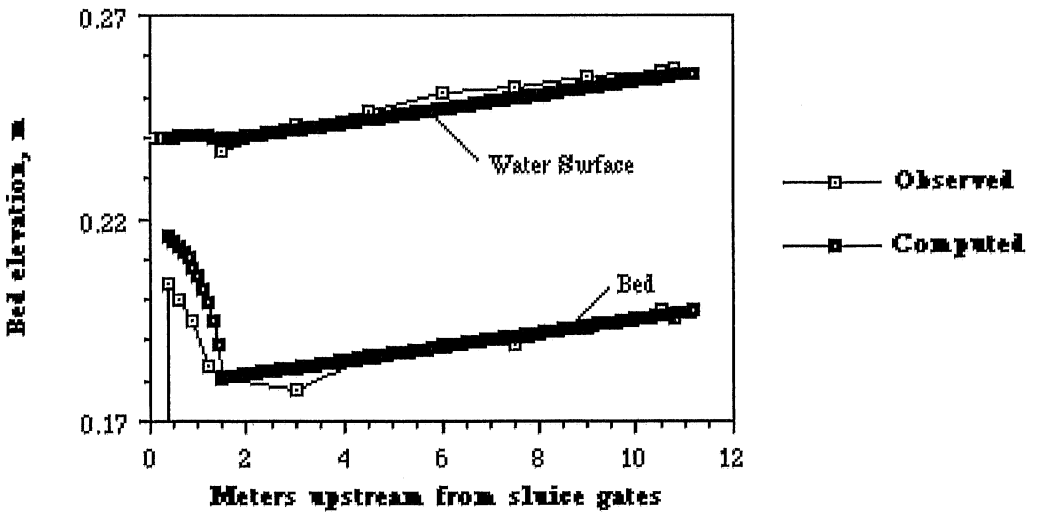

Figure 4.7 Observed and computed final equilibrium profiles for Run 28

condition. Table 4.2 lists observed and predicted locations of the delta and delta propagation speeds. The computer model overestimates delta propagation speed by 27 per cent as can be seen in the Figures and Table. The rate at which the shock moves forward in the program is directly proportional to the sediment delivered to the front, which for this case is very nearly equal to the computed input value, which is 22 per cent higher than observed. Correspondingly better or worse results would be expected depending upon the prediction of sediment transport rates.

The plot of final equilibrium conditions in Figure 4.7 shows that the computer model over-predicted the bed elevation in the diverging portion of the flume by about one-third. This may indicate that experimental conditions were not quite at equilibrium when the experiment was stopped.

Both the observed and calculated profiles and depths are very near the equilibrium values as the delta moves downstream. This confirms other experimental observations that flow upstream of a delta is nearly uniform during the downstream delta progression. The near-uniform condition is due to the short experimental facility, where the sediment input source is relatively close to the simulated dam, and the backwater zone cannot extend farther upstream than the flume entrance. The same run was simulated on the computer without the constraint of the flume length, and showed an actual backwater zone of 120 meters compared to the 12 meter-long flume. The short flume also accounts for the near-normal bed slopes as the delta moves forward. Figure 4.8 compares the sediment transport rates for the simulated flume run and for a run where the backwater zone is 120 meters long. The input rate to the flume is $2.8 \cdot 10^{-6}$ m^3/sec for each case. For the 12-meter-long flume the sediment transport rate is $2.5 \cdot 10^{-6}$ m^3/sec when the delta has moved about 9 meters, a reduction of only 12 percent. If the delta had moved the 100 meters or so it would if the backwater zone were 120 meters long, the sediment transport rate over the lip would be $1.2 \cdot 10^{-6}$, or about 50 per cent of the input rate. The bed profiles corresponding to these sediment transport rates are shown in Figure 4.9. The slope of the bed in the short flume as the delta moves downstream is almost 0.0017,

Time (gate lowered at 4:45 p.m.)	Position of Delta, meters upstream from sluice gate		Delta Propagation Speed, meters per hour	
	Observed	Computed	Observed	Computed
6:45 p.m.	9.56[1]	9.56[1]	-	-
7:55 p.m.	8.43	8.33	1.0	1.2
8:45 p.m.	7.61	7.11	1.0	1.2
9:40 p.m.	6.63	5.93	1.1	1.2
10:45 p.m.	5.66	4.80	0.9	1.1
11:45 p.m.	4.68	3.69	1.0	1.1
12:45 a.m.	3.63	2.60	1.1	1.1
1:48 a.m.	2.66	1.54	0.9	1.1
2:45 a.m.	1.83	0.90	0.9	0.6
3:45 a.m.	1.50[2]	0.50	0.3	0.4
4:45 a.m.	1.13	0.40[3]	0.4	0.4
5:55 a.m.	0.75	0.40	0.4	-
6:45 a.m.	0.40[1]	0.40	0.4	-
		Mean speed for entire run:	0.9	1.2

the equilibrium value, while the slope of the bed in the longer backwater zone case is 0.0013, or about 76 per cent of the equilibrium value.

---

1 Initial conditions

2 Flume begins to diverge 1.50 meters upstream from sluice gate

3 Equilibrium distance from sluice gate

Table 4.2 Observed and computed delta locations and propagation speeds for Run 28

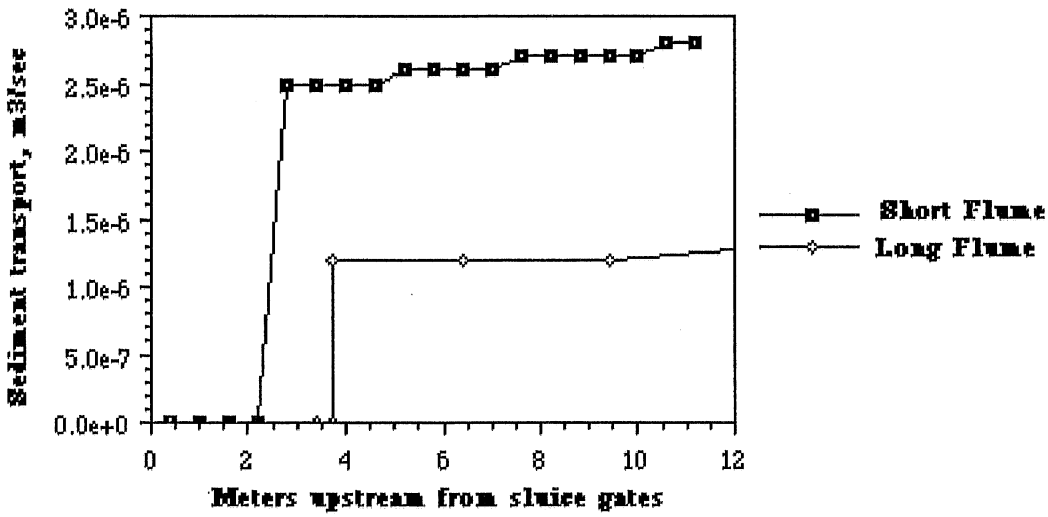

Figure 4.8 Computed sediment transport rates for 12-meter-long and 120-meter-long backwater reaches

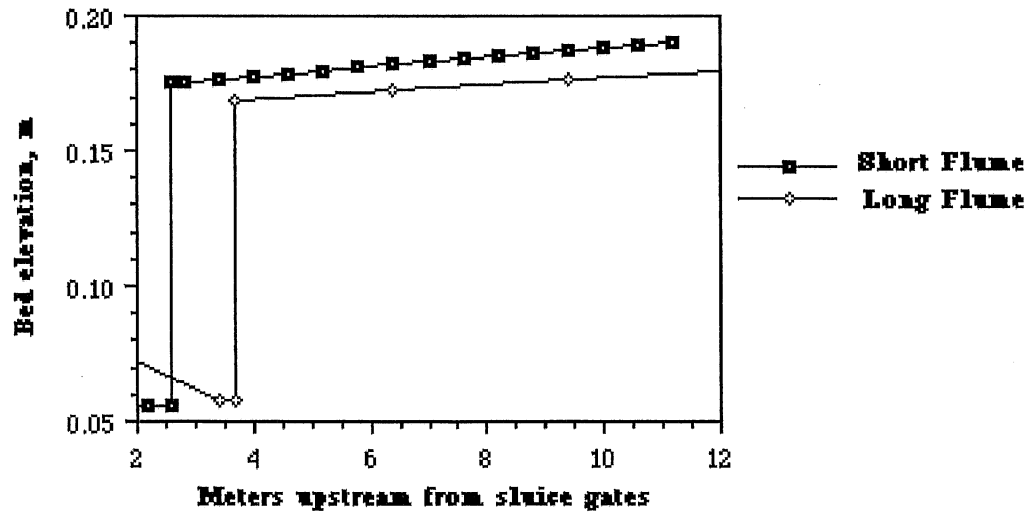

Figure 4.9 Computed bed profiles when the delta is about 3 meters upstream of the sluice gates for the 12-meter-long and120-meter-long backwater reaches

4.4.3. Sediment Sluicing: flume case

4.4.3.1 Model setup

Run 29, also performed in the diverging flume, was selected for the detailed modeling of sediment sluicing. The run was performed independently of Run 28, the aggradation case, but has very similar hydraulic conditions. The experimental run began with an equilibrium delta located 0.4 meters upstream of the sluice gates. Only the center

sluice gate was operated. Input sediment feed rate was 185 grams per minute. The sluice gate was opened enough to lower the water surface at the delta 3 millimeters. every 20 minutes. This procedure was repeated for 8 hours, resulting in a total drawdown of 0.075 meters, or 1.12 times the observed normal depth of 0.0665 meters. Bed and water surface profiles were measured every 100 minutes during the run. After the final gate adjustment, about 30 minutes were required to establish equilibrium conditions throughout the flume. Equilibrium slope was 0.0016.

A distance step of 0.10 meters and a time step of 4 seconds was selected for the computer run based on preliminary runs with different distance and time steps. The smaller distance and time steps are necessary to maintain computational stability during the simulated sluicing, which produces higher-than-normal sediment transport rates. The observed bed profile before sluicing began was input as an initial condition to the computer and run until the model estimated that equilibrium had been achieved. The water surface elevation at the delta lip, (downstream boundary) was then decreased 3 millimeters every 20 minutes for 8 hours, and then run to equilibrium.

4.4.3.2 Results and discussion

The computer model predicts a normal depth of 0.0603 meters, a normal slope of 0.0016, and a sediment input rate of 194 grams per minute. The computed sediment input rate is unusually close to the observed. The observed and computed initial equilibrium bed and water surface profiles are shown in Figure 4.10, and observed and computed profiles for intermediate and final stages of the run are shown in Figures 4.11, 4.12, and 4.13. A total of 683 seconds of computer time were required to complete the run. The observed and computed initial conditions are in very

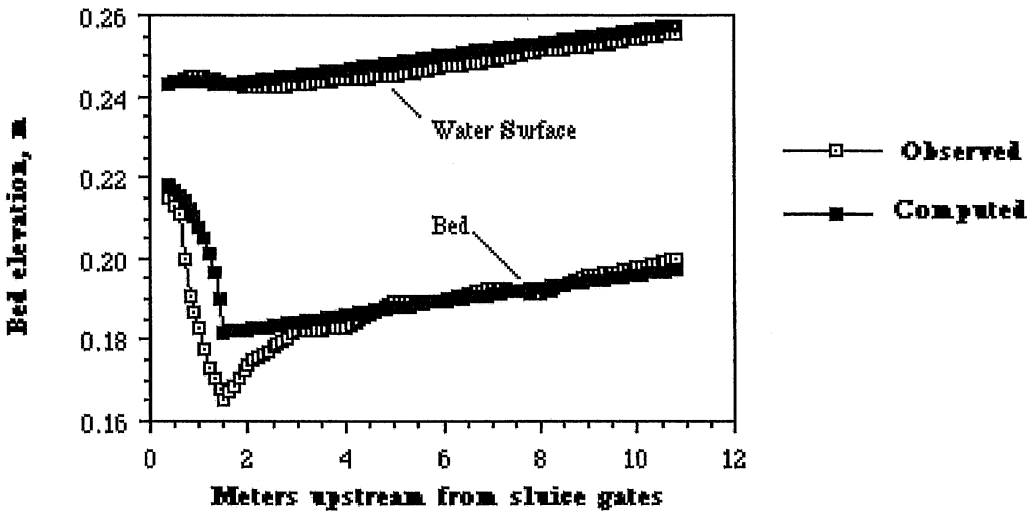

Figure 4.10 Observed and computed initial conditions for Run 29

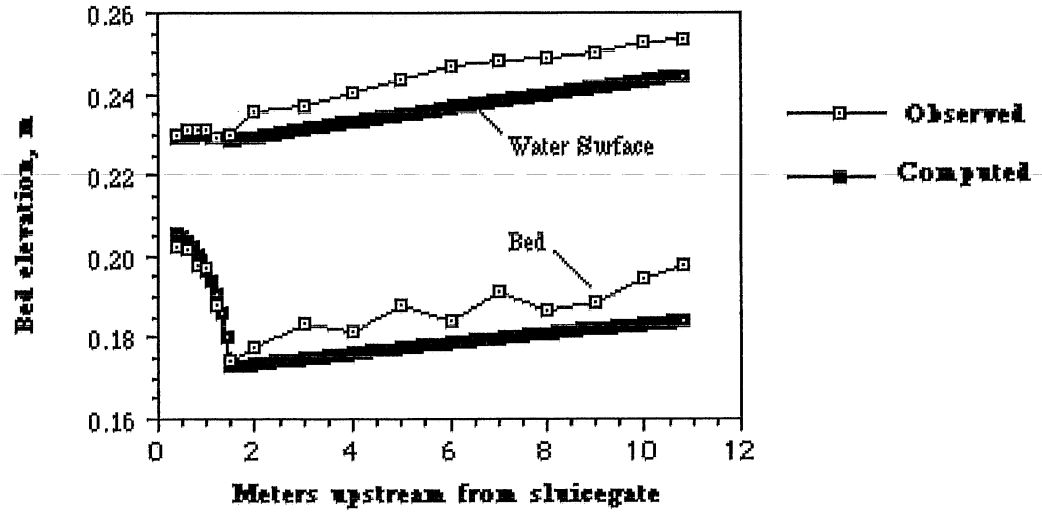

Figure 4.11 Observed and computed profiles 1 hour and 40 minutes later for Run 29

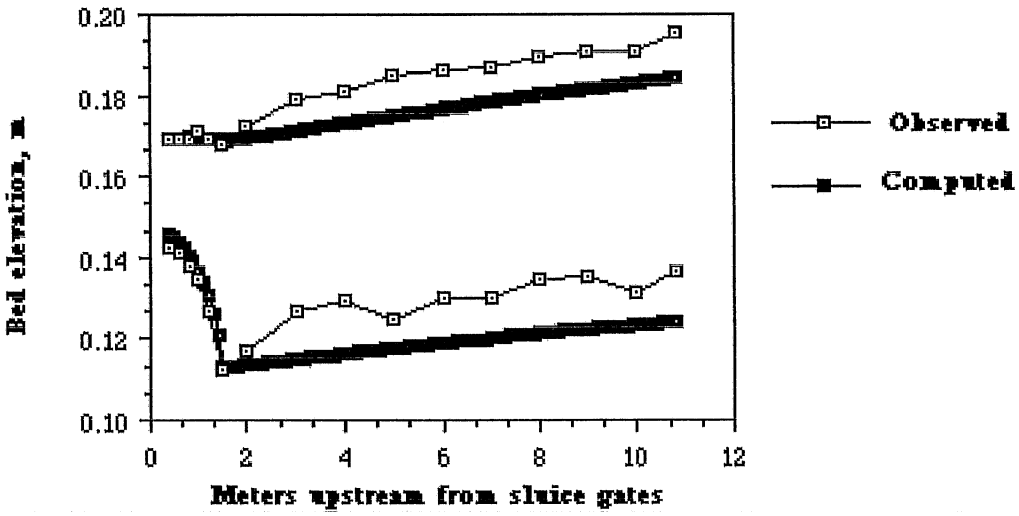

Figure 4.12 Observed and computed profiles 8 hours later for Run 29

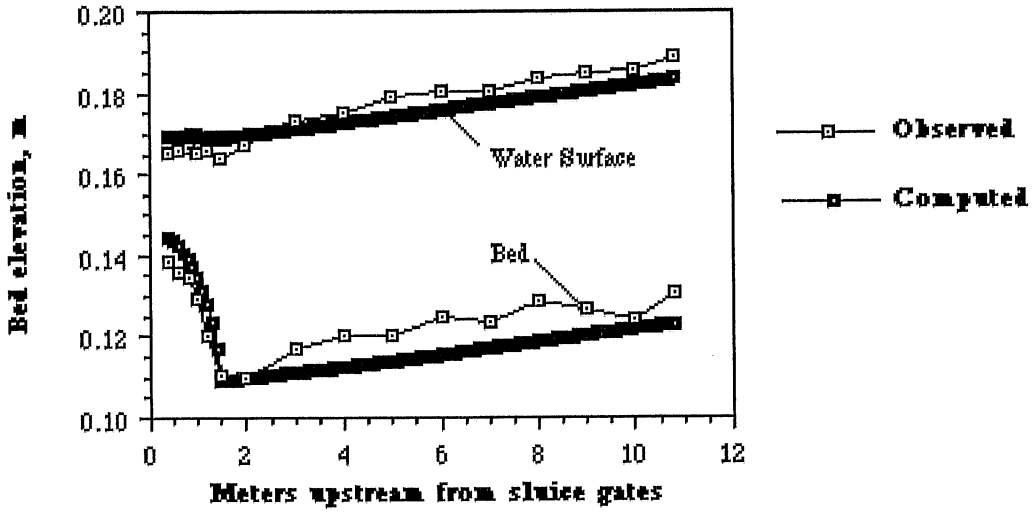

Figure 4.13 Observed and computed final equilibrium profiles for Run 29

close agreement, while the intermediate computed profiles are about 0.01 meter lower than observed,and the final computed equilibrium profile is about 0.005 meters below the observed. This pattern suggests most of the computational discrepancy occurred during the first 100 minutes of simulation, because the discrepancy does not grow with time. Close inspection of the observed bed profiles shows that during the first 100 minutes of the actual run, the bed actually aggraded in the diverging portion of the flume and degraded only slightly in the uniform width portion. It is

The relatively slow drawdown rate used in Run 29 ensured that subcritical flow conditions existed at all times in the flume, and provided a drawdown rate commensurate with a field scale problem. For example, if a scaling ratio of 1:100 is used, then the experimental procedure corresponds to drawing the water surface down 0.030 meters every 3 hours, or about 3 meters per day, a value not unreasonable to expect in a field case.

4.5 Numerical Modeling of Field Case

There were no detailed field data readily available with which to test the numerical model, so a river-reservoir for which limited information was available was selected to illustrate the application of the code to a field-scale problem. Results are of qualitative significance.

4.5.1 Description of Site

In 1911 the city of Granite Falls, Minnesota, built a 5.5-meter high concrete gravity dam on the Minnesota River adjacent to the city. The dam replaced a similar one built in 1872 that was used for flour milling operations (Gake, Garver, Gulliver, and Renaud, 1981). The drought of the early 1930's dried up the reservoir and people walked on the sediment that had completely filled the impoundment (oral communication with Alan Rindels, 1989). The reservoir filled with sediment, therefore, in a period of from 20 to 58 years. The present-day reservoir is said to have about a 5.6 kilometer-long backwater zone with a mean depth of 1.8 meters.

4.5.2 Hydrology and Sediment Characteristics

The mean annual water discharge at the site is 20 m^3/sec, and the river slope is about 0.0009 (Gake, Garver, Gulliver, and Renaud, 1981, and Barr Engineering, 1986). The channel width corresponding to the mean annual discharge is about 80 meters (U.S.G.S. Granite Falls quadrangle map, 1965). Channel depths average between 0.3 and 1.2 meters (Schneider, 1966). The bed material consists of fairly uniform sand with a median diameter of 0.45 millimeters and a specific gravity of 2.65 (Johannesson, 1988). The porosity of the material was assumed to be 0.30. The water temperature was assumed to be 10 degrees Celsius, representing a mean annual temperature.

4.5.3 Modeling Approach

Consistent with the constraints of the computer model, water and sediment discharge are modeled as being constant for the simulation period. Since most interest is in determining how long the reservoir takes to fill with sediment, it is important to preserve sediment continuity during the simulation period. This is accomplished using the concept of dominant discharge. Dominant discharge is defined as that discharge, which if maintained constant throughout the year, would transport the annual sediment load past a site. The dominant discharge for the Minnesota River at Granite Falls is based on calculations of discharge and sediment rating curves. The discharge rating curve was calculated using the Engelund-Hansen equation (Equation 3.9), while sediment transport was calculated using the Parker equation for field conditions (Equation 3.11). The actual value of dominant discharge was estimated to be 28.3 m^3/sec and was found using the sediment rating curve and a flow duration curve for the site computed by Gake, Garver, Gulliver, and Renaud (1981).

4.5.4 Aggradation Analysis: field case

4.5.4.1 Model setup.

A distance step of 250 meters in the computer model produced satisfactory backwater profiles for the site, and a time step of 2.5 days maintained computational stability. Three different runs were made for the aggradation case. In the first, the length of the initial backwater zone computed by the model was kept constant for the entire simulation. This prevents the migration of the backwater zone upstream, and like the flume case in the laboratory, provides a lower limit on the time required to fill the reservoir. Runs were made with and without the shock-fitting option. A second and third run were made in which the initial length of the backwater zone was multiplied by 5 and 10, respectively. Computations then proceeded as in the first case, but with the longer computational domains, as indicated. Since it is unknown how long the eventual profile might be, the multiplier values were used to provide an approximate upper limit to the upstream migration of the backwater zone.

4.5.4.2 Results and discussion.

The computer model predicts a normal depth of 0.5 meters, within the range of depths quoted by Schneider (1966). A comparison of delta progression with and without a shock fitted to the delta is shown in Figure 4.14 for the case of a non-extended backwater zone. The shock-fitting routine tracks the delta well, and even though the slope of the delta appears steep, it is only 1.6 per cent, and is therefore valid to be modeled by the one-dimensional equations of motion. The value of 1.6 per cent, however, is not necessarily physically realistic, since field observations (Chapter 2) and

flume observations in this study suggest that the delta moves forward in a narrow reservoir with a foreset slope of about 33°, or about 60 per cent.

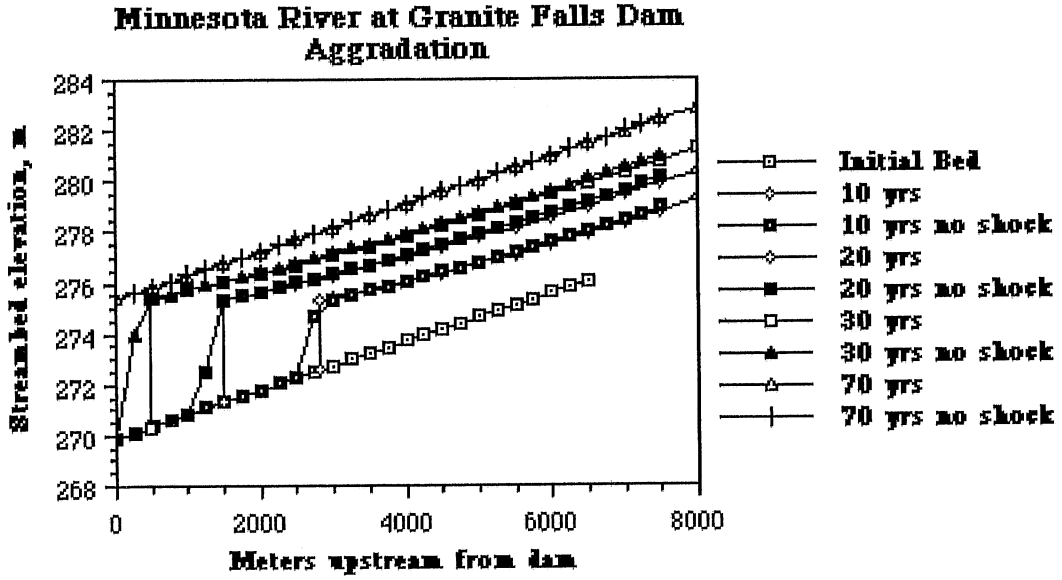

Figure 4.14 Computed bed profiles for field case with and without the shock-fitting option

The establishment of the delta and its progression as simulated by the shock front are shown in Figure 4.15 for the case where the backwater zone is extended 5 times farther upstream than initially predicted. A total of 165 computer seconds was required for the solution. Note the orderly progression of the delta, and the fact that it slows down as it moves farther into the reservoir. It is estimated to take about 48 years to fill the reservoir for this modeling case, although the bed continues to modify its slope for 20 years after reaching the dam. The bed slope upstream of the delta as it moves forward is about 0.00055, or 60 percent of the initial bed slope. This is between the values of one-half and two-thirds quoted by Borland (1971) for observed field cases. Different results (likely a lower slope) would be expected if the modeled reservoir had a widening section.

Table 4.3 lists the filling times and locations of the initial delta for the three runs with different lengths of backwater zones. All are well within the actual estimated range of from 20 to 58 years. Note that the calculated backwater zone evidently does not migrate farther than five times the original because the results for the two cases with longer backwater zones are the same.

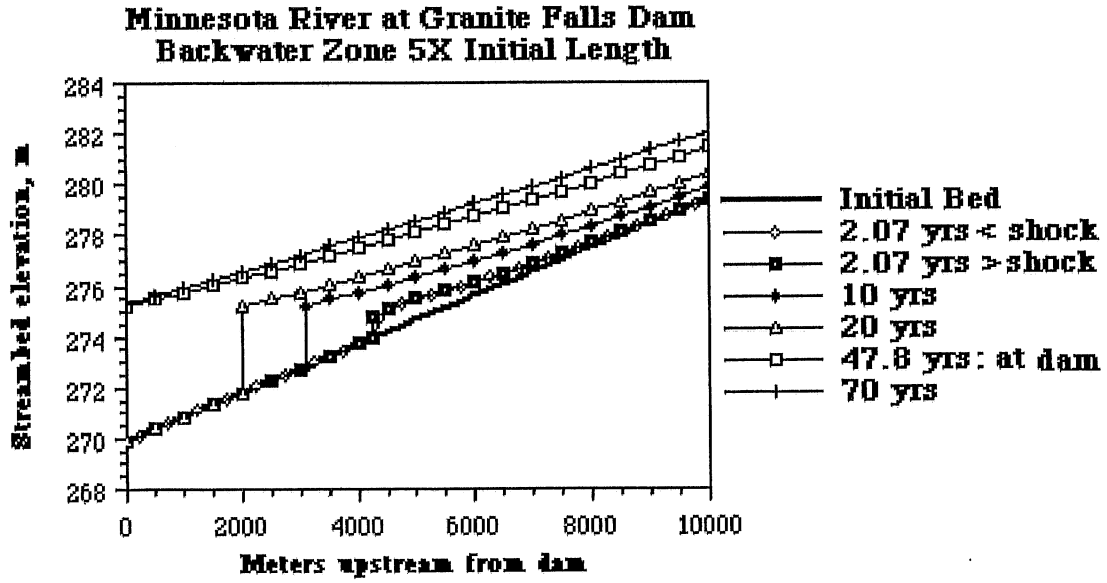

Figure 4.15 Computed bed profiles for field case with length of backwater zone 5 times initial length

Length of Computational Domain, kilometers	Delta forms when bed slope is five times the original		Time required to fill reservoir with sediment, years
	kilometers upstream from dam	years from closure	
6.5	3.3	5.6	35
32.5	4.3	2.1	48
65	4.3	2.1	48

Table 4.3 Computed initial locations of deltas and times required to fill the reservoir for the field case

Despite the computed results being within the estimated range of filling times, there are several reasons why the results are probably not exact. The simulated model used uniform sand for the sediment and did not account for fine materials in suspension. These fines, present in the Minnesota River, if not passed over the dam, deposit in the reservoir and contribute to the loss in storage volume. Conversely, all of the simulated sediment is trapped in the reservoir, implying a trap efficiency of 100 per cent. Such may not be the case in the field. Finally, detailed information was not available on the channel bed topography upstream, so the length of the actual backwater zone is unknown. Nevertheless, the computed bed profiles do appear to be consistent with the information available for the site and do conform to the information about topset beds discussed in Chapter 2.

4.5.5 Degradation Analysis: field case

4.5.5.1 Model setup.

The simulation of sediment sluicing at the site was begun with a condition of complete sedimentation in the reservoir where normal depths and slope prevail throughout. This corresponds to a case where the bed above the Granite Falls dam is raised uniformly to the height of the dam, 5.5 meters. It is similar to the condition predicted for the aggradation case after 70 years of simulation, except that even after that amount of time the calculated slope was not at equilibrium throughout the reservoir.

The water surface at the dam was allowed to drop as quickly as possible, maintaining depths just above critical at the dam until the total drawdown of 5.5 meters was achieved. The water surface elevation thereafter was held constant and the bed was allowed to freely adjust upstream.

Sluicing was simulated in two steps. The first modeling segment consisted of a 150-day simulation with a distance step of 50 meters and a time step of 30 minutes. These short step values were selected to accommodate the higher transport rates expected during the initial stages of drawdown. For the second modeling segment, a distance step of 250 meters and a time step of 12 hours was used. The distance step is the same as used in the aggradation case, but the time step is 5 times shorter, once again to accommodate the higher-than-normal sediment transport rates. For both modeling segments the backwater zone was allowed to be extended as necessary upstream as the bed at the upstream limit was eroded.

4.5.5.2 Results.

Results for the two modeling segments are shown separately in Figures 4.16 and 4.17. A combined total of 333 computer seconds was required for the solution. All the computed bed profiles show the expected concavity during the sluicing period of 10.67 years. According to Figure 4.16, 5.5 meters of bed erosion took place in the first 120 days of the operation, but even after 10.67 years, the bed had not achieved its estimated initial state before the dam was closed.

These results are qualitative. The actual case would likely be somewhat different, especially if cohesive sediments are present in the bed. These sediments can impede and even stop the erosion process. The pattern of erosion is as expected, that is, progressing in the upstream direction from the dam, and not unrealistic.

4.6 Applying the Numerical Model to Field Cases

The numerical model developed for this investigation is based on the observation of aggradation and degradation in laboratory flume experiments. Results for the field case are consistent and logical. The purpose of this discussion is to demonstrate the applicability of the model to real field cases by considering scaling and three-dimensional effects.

4.6.1 Scaling Laboratory Results to Prototype Projects

In order for the experimental results to be applicable to prototype projects, dynamic similarity for flow and an appropriate measure of similarity for sediment transport must be achieved.

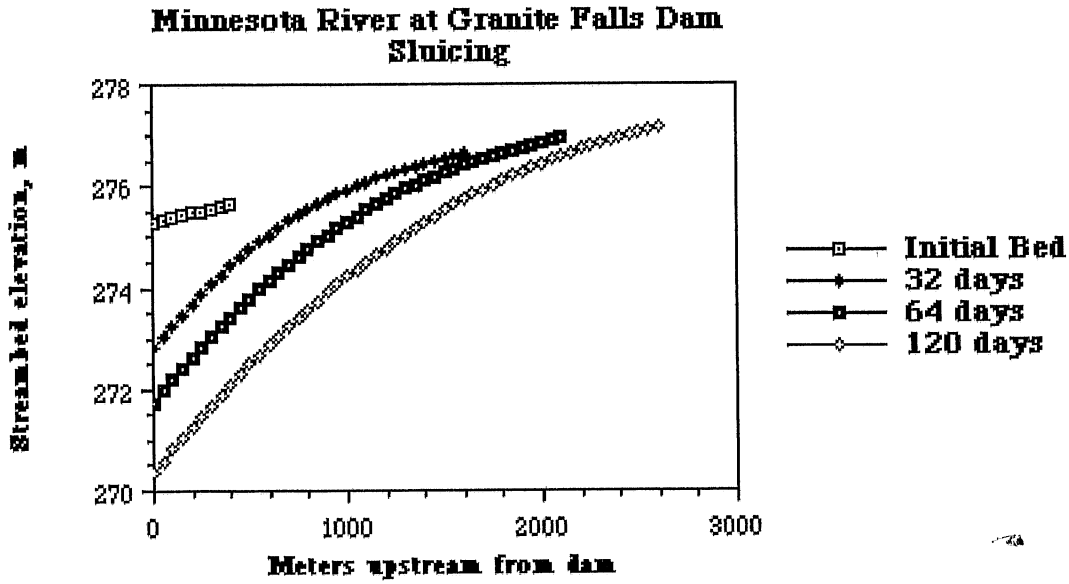

Figure 4.16 Computed bed profiles for the first 150 days of sediment sluicing

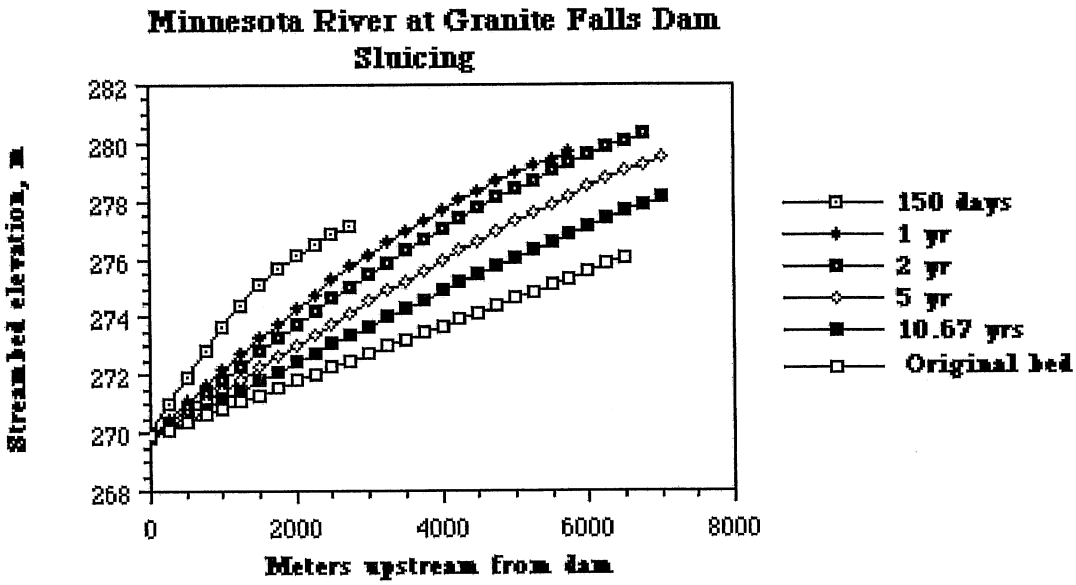

Figure 4.17 Computed bed profiles for the remainder of the sediment sluicing simulation period

4.6.1.1 Dynamic similarity.

Dynamic similarity for flow is satisfied if the Froude number (Fr) of the model and prototype are equal:

$$Fr_m = Fr_p \qquad (4.19),$$

or

$$\frac{V_m}{\sqrt{gl_m}} = \frac{V_p}{\sqrt{gl_p}} \qquad (4.20),$$

where l is a length scale and the subscripts m and p refer to model and prototype, respectively. Prototype velocity and discharge can be computed using (4.20) as follows: assuming an undistorted length scale of 1:100, the prototype velocity is $V_p = V_m\sqrt{\frac{l_p}{l_m}}$, or $10\ V_m$. Since discharge is expressed as Vl^2, then

$$\frac{V_m}{\sqrt{gl_m}}\frac{l_m^2}{l_m^2} = \frac{V_p}{\sqrt{gl_p}}\frac{l_p^2}{l_p^2}, \qquad \text{or}$$

$$Q_m\sqrt{\frac{l_p}{l_m}}\frac{l_p^2}{l_m^2} = Q_p \qquad \text{or} \qquad Q_p = \left(\frac{l_p}{l_m}\right)^{2.5}Q_m \qquad \text{or} \qquad 100{,}000(Q_m).$$

Experimental results are scaled using Froude number similarity to find prototype flow properties.

4.6.1.2 Similarity for sediment transport.

An appropriate scaling factor for sediment transport is the Shields' stress, denoted by

$$\tau^* = \frac{hS_f}{Rd_{50}} \qquad (4.21).$$

Critical Shields' stress is considered to be the minimum value required to initiate general sediment motion, and from Equation (4.21), the critical shear stress value is dependent upon the submerged specific gravity. Prototype bankfull discharges usually exhibit a Shields' stress about 15 times the critical value (Parker, Martinez, and Hills, 1982). The use of crushed walnut shells (R = 1.35) ensures that model and prototype Shields' stresses are of the same order of magnitude. The critical Shields stress for the crushed walnut shells in the experiments is about 0.035. A typical value of Shields' stress for the experiments is 0.47, assuming a flow depth of 0.055 meters and a slope of 0.0020, or 13 times the critical value. Thus experimental and prototype Shields' stresses are of the same order of magnitude, and sediment transport similarity is satisfied.

4.6.2 Three-dimensional Effects

The experiments for this investigation were conducted in a channel where the sluice gate(s) extended completely across the dam. In most prototype situations, the sluice gate(s) represent only a fraction of the flow area. Sluicing operations at such sites exhibit three-dimensional effects; local zones of erosion are present upstream from each sluice gate instead of a uniform scour zone across the entire dam width as observed in the experiments. The numerical model described herein can still be applied to these three-dimensional situations if 1.) the downstream boundary is taken at a location far enough upstream so as to be out of the region of the three-dimensional effects, and 2.) the total width to depth ratio (aspect ratio) is less than about fifteen.

The first restriction applies to all simulations, even those of the laboratory experiments, where three-dimensional effects were generally not present. The restriction is necessary because 1.) flow and sediment transport conditions downstream of the delta lip are not one-dimensional and cannot be modeled with the equations used in this study, and 2.) the St. Venant equations are shallow-water equations, meaning that flow parameters change much more slowly in the direction of flow than in directions transverse to the flow (vertical and lateral). This assumption is clearly violated downstream of the delta lip.

The restriction does not result in excessive limitations to modeling three-dimensional situations. Laboratory experiments showed that the distance upstream from the dam where scour extended to the bottom of the flume (dam) was less than three normal depths. The horizontal distance from the delta toe at this location to the lip is of the same order as the flow depth, since the slope of the delta is at the submerged angle of repose, or about 34°. The total length not modeled therefore, is of the same order of magnitude as the flow depth and represents only a small fraction of the upstream reach affected by the dam.

If the aspect ratio exceeds about fifteen, the flow is likely to split into multiple branches typical of a braided system (Fredsoe, 1978). The one-dimensional St. Venant equations in the form used in this study do not apply to such a system. Care should be taken not to apply the model to a prototype case where the channel width at the dam exceeds about fifteen times the original channel width.

4.7 Summary

It has been demonstrated that the computer model can successfully reproduce observed laboratory profiles for cases of aggradation and degradation, and that it can produce reasonable results when applied to a field-scale case. This research model requires fairly large amounts of computer time as revealed in Table 4.4. Relatively small distance and time steps are required in the case of aggradation to follow the evolution of the delta, and small steps are likewise required during sediment sluicing to accommodate high transport rates. The model has several restrictions, the most important being the use of steady water discharges and steady sediment input for the simulations, and the exclusion of sediment mixtures from the bed.

Case	Seconds of CYBER 855 mainframe time required for solution
Flume: aggradation	422
Flume: sluicing	683
Field case: aggradation	165
Field case: sluicing	333

Table 4.4 Number of computational seconds required for solution

CHAPTER 5 BED RESPONSE TO CHANGES IN CHANNEL WIDTH

The purpose of this chapter is to develop equations for the equilibrium depth, slope, and bed elevation for rectangular channels of prescribed varying width. The motivation for this analysis resulted from the observation that the bed slope in the diverging channel is adverse and is more pronounced near the beginning of the diverging section (see Figure 3.9). A more general analysis is then made for a rectangular channel of arbitrary width. The results are applied to a hypothetical field case.

5.1 Brief Review of Previous Work

Several researchers have developed relationships for depth, width, and slope ratios for rectangular channels with long contractions. Garde and Ranga Raju (1985), for example, summarize the work of Lorenz Straub and others. Assuming that the channel contraction is long enough for the establishment of normal flow, they derive

$$\frac{S_2}{S_1} = \frac{h_1}{h_2}\left(\frac{b_1}{b_2}\right)^{\frac{2}{1+2N}} \qquad (5.1),$$

and

$$\frac{h_2}{h_1} = \left(\frac{b_1}{b_2}\right)^{\frac{12N}{7(1+2N)}} \qquad (5.2),$$

where S = normal slope, h = normal depth, b = channel width, and subscripts 1 and 2 refer to the unperturbed and contracted channels, respectively (see Figure 5.1 for a definition sketch). The exponent N is from the generalized power-law sediment transport relationship

$$q_s = c_4 \tau_b^{\,N} \qquad (5.3),$$

where q_s is sediment transport per unit width of channel and τ_b is total bed shear stress.

The authors illustrate that with an N value of 2.0 - corresponding, they say, to a bedload equation, the exponent in equation (5.2) is 0.686; a value of N of 4.0 (supposedly appropriate for a total load equation) produces an exponent of 0.76. They compare these to a field-observed value of 0.637.

5.2 Equilibrium Depth and Slope in Rectangular Channels of Prescribed Varying Width

A more general relationship is derived for the equilibrium depth and slope of a rectangular channel of prescribed varying width. Normal flow conditions need not prevail for this derivation, but flow is assumed to be steady for a long enough period of time that equilibrium conditions exist throughout the channel length. The wide channel assumption is also invoked; that is, the hydraulic radius is assumed to be equal to the depth.

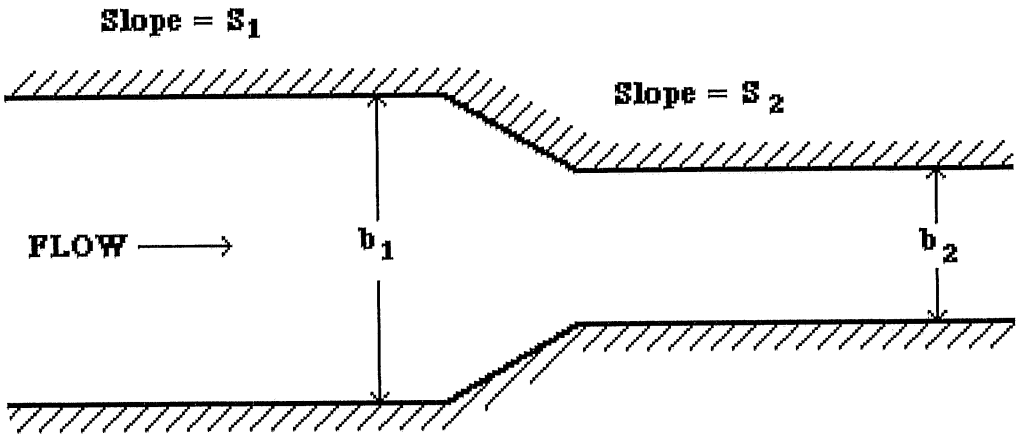

Figure 5.1 Plan view of channel with long contraction

5.2.1 Dimensionless Equations of Motion

For steady flow in a wide rectangular channel, the St. Venant equations for momentum and continuity are

$$\frac{d(u^2 h b)}{dx} = -g b h \frac{\partial \xi}{\partial x} - b C_f u^2 \qquad (5.4),$$

and

$$Q = 2 u h b = \text{constant} \qquad (5.5),$$

where all terms are as defined as in Chapter 2, except b is now taken as the channel half width, and is an explicit function of x (see Figure 5.2). Note that the friction factor, C_f, is assumed to be constant in the reach.

Sediment transport is generalized as in Garde and Ranga Raju, that is,

$$q_s = c_4 \tau_b^N \qquad (5.6).$$

Sediment continuity is simply expressed as

$$Q_s = 2 b q_s = \text{constant} \qquad (5.7).$$

Equations (5.4) through (5.7) are made dimensionless as follows: $\hat{u} = \frac{u}{u_o}$, $\hat{h} = \frac{h}{h_o}$, $\hat{x} = \frac{x}{b_o}$, $\hat{b} = \frac{b}{b_o}$, $\hat{q_s} = \frac{q_s}{q_{so}}$, and $\hat{S} = \frac{S}{S_o}$, where the subscript refers to values in the uniform width channel. Introducing these variables into (5.4) through (5.7) produces the dimensionless momentum equation

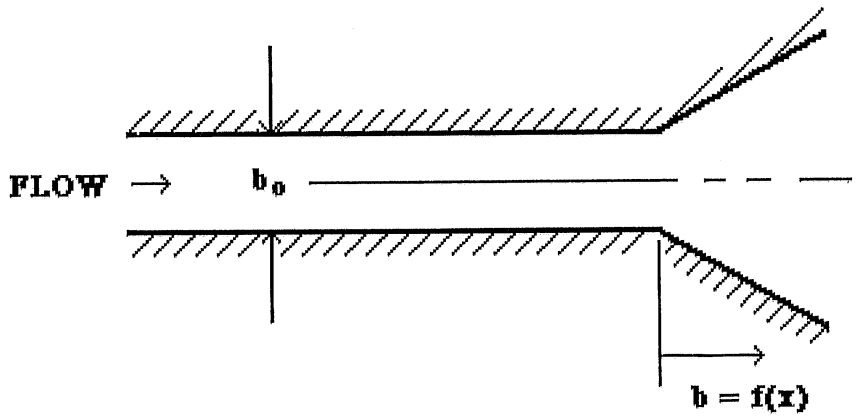

Figure 5.2 Plan view of channel with prescribed varying width

$$\frac{d}{d\hat{x}}(\hat{u}^2\hat{h}\hat{b}) = \varepsilon\hat{S}\hat{b}\hat{h} - \varepsilon\hat{b}\hat{u}^2 - Fr_o^{-2}\hat{b}\hat{h}\frac{d\hat{h}}{d\hat{x}} \quad (5.8),$$

the dimensionless continuity equation

$$\hat{u}\hat{h}\hat{b} = 1 \quad (5.9),$$

and the sediment transport and sediment continuity equations,

$$\hat{q_s} = \hat{u}^{2N} \quad (5.10),$$

and

$$\hat{q_s}\hat{b} = 1 = \hat{u}^{2N}\hat{b} \quad (5.11),$$

where $\varepsilon = \gamma C_f$ with γ defined as the aspect ratio $\frac{b_o}{h_o}$, and Fr_o = the Froude number of the uniform width channel.

5.2.2 Equation Development

Dropping all superscripts for simplicity, and realizing from (5.9) that $u = b^{-1}h^{-1}$, (5.11) may be solved for depth:

$$h = b^{\frac{1-2N}{2N}} \quad (5.12).$$

Substituting into equation (5.8) and differentiating as indicated yields an explicit solution for the slopes in a channel of varying width relative to those of a uniform width channel with the same discharge:

$$S = b^{\frac{2N-3}{2N}} - \frac{1}{\varepsilon}\frac{db}{dx}\left(\frac{1-2N}{2N}F_{r_o}^{-2}\, b^{\frac{1-4N}{2N}} - \frac{1}{2N}b^{\frac{-1-N}{N}}\right) \qquad (5.13).$$

Equation (5.13) holds for any channel width expressed as a function of distance, that is, $b = b(x)$. Bed elevation is now made dimensionless with the variable $\hat{\eta} = \frac{\eta}{b_o}$, and equation (5.13) is integrated for the case that $b = b_0 + mx$ to yield an expression for dimensionless deviation from a uniformly sloping bed:

$$\hat{\eta} = -S_o\left[\frac{1}{m}\left(\frac{2N}{4N-3}\right)\left\{b^{\frac{4N-3}{2N}} - 1\right\} + \frac{1}{\varepsilon}\left\{\frac{1}{2}\left(b^{\frac{-1}{N}} - 1\right) + F_{r_o}^{-2}\left(b^{\frac{1-2N}{2N}} - 1\right)\right\}\right] \qquad (5.14),$$

where the superscript over η has been dropped. Equation (5.14) applies to a channel, such as the laboratory flume, where width varies linearly with distance. A different expression would result from a different functional relationship for width.

Equations (5.12), (5.13), and (5.14) describe the depth, slope and bed elevation of a channel of varying width . Sidewall effects and bedform influences are not included, but the second term of equation (5.13) accounts for the pressure and inertial terms encountered in non-uniform flow. The computer model in Chapter 4 accounts for sidewall and bedform effects and predicted bed elevations in the diverging portion of the flume may be compared to observed elevations in Figures 4.4, 4.10, and 4.13.

Equations (5.12) and (5.13) may be compared to the simple case developed by Garde and Ranga Raju by re-writing (5.1) and (5.2). Equation (5.2) may be substituted into (5.1) yielding

$$\frac{S_2}{S_1} = \left(\frac{b_1}{b_2}\right)^{\frac{14-12N}{7(1+2N)}} \qquad (5.15).$$

To illustrate, use a channel with a long contraction as in the original analysis and let $N = 2$ and 4 in both sets of equations. Then the second term in equation (5.13) is zero, and the dimensionless equilibrium slope is simply a function of the exponent N. Since the right -hand-sides of equations (5.2) and (5.15) are expressed as the inverse of $\frac{b_2}{b_1}$, the sign of the exponents must be reversed. Table 5.1 shows the results, which compare favorably. The physical significance of the signs associated with the exponents is explained with an example. If channel width increases, flow depth decreases (negative exponent) to satisfy continuity, but slope increases (positive exponent) to transport the same amount of sediment and to maintain sediment continuity.

Value of N in sediment transport relationship	Values of exponents in expressions for Slope		Depth	
	Garde and Ranga Raju	Present Analysis	Garde and Ranga Raju	Present Analysis
2	0.29	0.25	-0.686	-0.75
4	0.54	0.625	-0.76	-0.875

Table 5.1 Comparison of exponents in slope-depth equations

5.3 Expression for Slope and Depth for a Rectangular Channel with Sinusoidally Varying Width

A more general expression for slope and depth may be developed by introducing a small pertubation in an otherwise uniform width rectangular channel. For example, suppose a pertubation of the following form is used:

$$b = 1 + Dk \cdot \sin(kx) \qquad (5.16),$$

where k is a wave number defined by $k = \frac{2\pi b}{\lambda}$ with λ defined as wavelength, and Dk is a pertubation amplitude such that $Dk << 1$ (see Figure 5.3). All variables are dimensionless. Note that for a very long wave number (λ approaches infinity), equation (5.16) returns a value of the uniform channel width. Equation (5.16) may be substituted into (5.12) and (5.13) and expanded about $Dk \cdot \sin(kx) = 0$ to produce the following expressions for h and S (to the second order):

$$h = 1 + \omega\left(\frac{1-2N}{2N}\right) + \frac{\omega^2}{2}\left(\frac{1-2N}{2N}\right)\left(\frac{1-4N}{2N}\right) \qquad (5.17),$$

and

$$S = 1 + \omega\left(\frac{2N-3}{2N}\right) + \frac{\omega^2}{2}\left(\frac{2N-3}{2N}\right)\left(\frac{-3}{2N}\right) + \frac{1}{\varepsilon}\frac{d\omega}{dx}\left[F_{r_o}^2\left(\frac{1-2N}{2N}\right)\left(1 + \omega\left(\frac{1-4N}{2N}\right) - \frac{1}{2N}\left\{1 + \omega\left(\frac{-2-2N}{2N}\right)\right\}\right)\right] \qquad (5.18),$$

where $\omega = Dk \cdot \sin(kx)$. Retaining only first order terms and performing the differentiation in (5.18) results in

$$h = 1 + Dk \cdot \sin(kx)\left(\frac{1-2N}{2N}\right) \qquad (5.19),$$

and

$$S = 1 + \psi(\sin(kx) + \beta\cos(kx)) \qquad (5.20),$$

where $\psi = (\frac{2N-3}{2N})Dk$, and

$$\beta = \frac{2Nk}{\varepsilon(2N-3)}(\frac{Fr_o^2(1-2N)-1}{2N}) \qquad (5.21).$$

Now if we let $\beta = \tan B$, we can rewrite (5.20) using trigonometric identities to produce

$$S = 1 + \alpha\sin(kx + B) \qquad (5.22),$$

where

$$\alpha = Dk(\frac{2N-3}{2N})(1 + \beta^2)^{\frac{1}{2}} \qquad (5.23)$$

and is equal to the amplitude of the slope pertubation, and $B = \tan^{-1}\beta$, and equals the phase lead or lag in equation (5.22). Equation 5.23 may be integrated to yield the deviation from normal bed elevations:

$$\eta = S_o[\frac{\alpha}{k}\cdot\cos(kx + B) - x] \qquad (5.24),$$

where all variables are dimensionless.

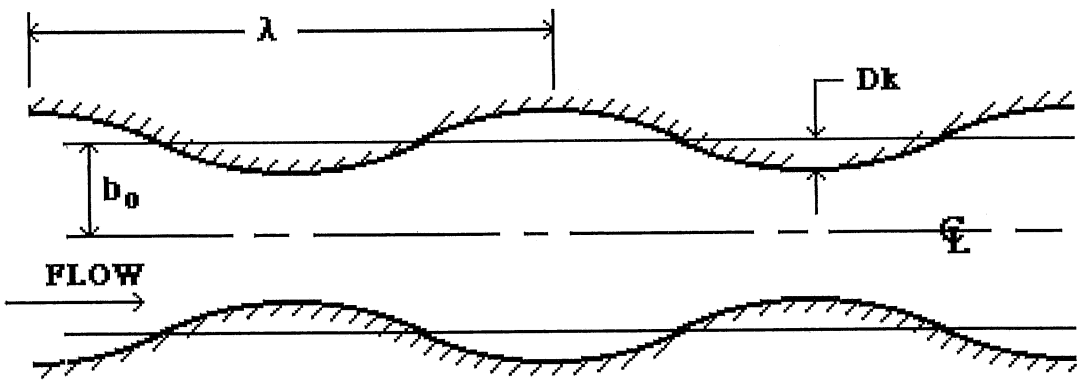

PLAN VIEW

Figure 5.3 Uniform rectangular channel with a sinusoidal pertubation in width

The form of equation (5.24) indicates that the bed elevation response to a sinusoidal change in width is expressed by a cosine function with a phase lead or lag. If

the phase lead is zero, for example, the deepest part of the channel is at a point where the maximum rate of change in width occurs in the contracting portion of the channel.

5.3.1 Application to Hypothetical Field Case

It was once thought that during floods, there was a general lowering of bed elevations in varying-width channels. Lane and Borland, in Schumm (1954), dispelled that belief using observed flood data from the Rio Grande. The data show that during periods of increasing discharge the bed scours at narrow sections and deposits at wide sections. Equation (5.21) may be used to demonstrate this phenomenon.

5.3.1.1 Approach

A hypothetical field case is used for demonstration. The critical parameter to examine is the phase angle, B, which is a function of geometric, hydraulic and sediment transport properties. Geometric factors are bed width and pertubation wavelength. Hydraulic factors include steady flow depth, Froude number, and friction factor, and sediment transport is characterized by the exponent N in the sediment transport power law, equation (5.6).

Steady flow depths, Froude numbers, and friction factors are computed using the Engelund-Hansen equation. The Engelund-Hansen equation accounts for variations in the friction factor with discharge, and provides the estimates of total bed shear stress and grain shear stress necessary to determine the sediment power law exponent, N. The dimensionless grain shear stress from the Engelund-Hansen equation is used in the Parker equation to compute dimensionless sediment transport. The sediment transport value is plotted on log-log paper versus the corresponding value of total dimensionless shear stress from the Engelund-Hansen equation. Repeating this process for several depths we can fit a curve through the points of sediment transport versus total shear stress. The local slope of the curve at a point is the value of the exponent N in the sediment power law.

5.3.1.2 Solution

The Minnesota River near Granite Falls, Minnesota, is used to illustrate the procedure. The same site was used in Chapter 4 to illustrate a field-scale application of the numerical model. For the purposes of this illustration, however, it is assumed the dam does not alter upstream flow. Channel half-width at this location is 40 meters, and the meander wavelength, modeled with the pertubation wavelength, is estimated at 800 meters (Johannesson, 1988). A pertubation amplitude (Dk) of 0.10 is used. Observed bankfull depth is about 1 meter (Schneider, 1966). Three discharges were selected for analysis: a relatively low value, exceeded 50 per cent of the time, the mean annual discharge, and bankfull discharge, The hydraulic parameters, N values, and resulting phase lags are summarized in Table 5.2

5.3.1.3 Discussion

Results are plotted graphically in the plan view of the perturbed channel shown in Figure 5.4. Bed elevations relative to the bed in a uniform channel are plotted along the channel centerline. For example, if there were no phase lag involved, the bed relative to a uniform bed is deepest at the point of maximum rate of change of width in the contracting portion of the channel and is most shallow at the point of maximum curvature as the channel expands. Depth is equal to uniform depth at the widest and narrowest sections. These locations are displaced 90 degrees from those of the maximum deviation in slope, the result of integrating a sine curve (slope) to obtain a cosine curve (bed elevation).

Normal depth meters	Discharge m^3/sec	Velocity m/sec	Froude Number	Friction Factor	Aspect Ratio	Exponent in sediment transport power law	β	Phase lag degrees
0.21	7.1	0.42	0.30	0.0105	190	2.58	-0.099	-6
0.43	22.4	0.65	0.32	0.0090	93	2.58	-0.248	-14
1.04	135	1.62	0.51	0.0035	38	1.63	-14.25	-86

Table 5.2 Hydraulic and sediment transport parameters and angle shifts for hypothetical field case

The results of the pertubation analysis clearly show that the point of maximum depth migrates downstream with increasing discharge, until at bankfull conditions, maximum depth is found at the narrowest section and minimum depth at the widest section. This conclusion confirms Lane and Borland's observations of the Rio Grande. It also explains why stream gaging stations and river crossings such as bridges typically located at narrow channel sections, experience extreme scour during floods.

The present analysis assumes that each discharge event lasts long enough to produce equilibrium beds in the channel reach. This is most likely achieved in large watersheds where increasing runoff is produced by snowmelt, producing a very slowly increasing discharge hydrograph during the melt season. It also assumes the one-dimensional equations of motion apply, meaning that even at the low discharges, water is evenly distributed across the entire cross section. It does not account for effects of secondary flow in the meander bends. Finally, the effect of bedforms was considered in determining depth, discharge, and sediment transport, but bedform effects on the phase lag itself are not considered. Nonetheless, this first-order analysis gives a picture of the general behavior of rectangular channels of varying width during increasing discharge, and replicates the essence of reported field observations.

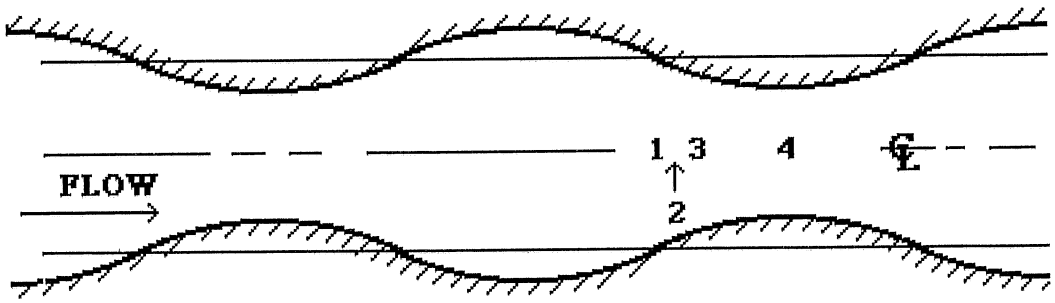

LOCATION OF MAXIMUM DEPTH	Phase Lag, degrees
1 Assuming phase lag = zero	0
2 Median annual discharge	4
3 Average annual discharge	14
4 Bankfull discharge	86

Figure 5.4 Phase angle shifts and effects on bed elevations in rectangular channel with a sinusoidal pertubation in width

CHAPTER 6 SUMMARY

It has been shown that for reservoirs dominated by bedload transport, sedimentation and sediment sluicing can be successfully modeled with laboratory and numerical models.

The laboratory experiments revealed the basic processes of reservoir aggradation and degradation. Aggradation is accompanied by the formation of a delta which essentially divides the reservoir into two hydraulic regimes: a segment upstream of the delta lip and a segment downstream of the delta lip. Flow conditions upstream of the delta lip for the laboratory experiments display nearly uniform flow depth and slope for a constant width rectangular channel. Flow conditions downstream are unaffected by the delta; sediment transport rate is zero, and flow conditions remain unchanged until the delta advances into the region. Modeling a field case with the computer reveals that without the restriction of a short laboratory flume, the backwater zone extends itself upstream as aggradation occurs in the reservoir, and that the sediment transport rate decreases downstream as the flow approaches the delta lip. Conditions are not uniform, and bed slopes are about one-half to two-thirds the value far upstream. This was shown to be consistent with field observations of Borland (1971).

For the case of the laboratory experiments, which were conducted in a narrow, rectangular flume, the depth of deposit or scour is ultimately equal to the amount by which the water surface was raised or lowered at the dam. Since the headwater elevation at a dam can be predicted during sluicing using the orifice equation, the ultimate amount of scour in response to sluicing can also be predicted using the orifice equation. Thus a relatively simple equation can be used to predict the amount by which the bed upstream will be lowered in response to sluicing.

The development and migration of the aggradational delta were successfully modeled with the quasi-steady one-dimensional equations of motion and the sediment continuity and transport equations. The accuracy of the predicted delta migration speed is linearly dependent upon the accuracy of the sediment transport equation. Predictions of reservoir filling time for a field case were well within the range of available data.

The numerical model is restriced to subcritical flow conditions. This means that supercritical flow during rapid drawdown cannot be modeled. This is a limiting factor when considering small scale experiments such as those performed in a laboratory flume, where sluicing proceeds very rapidly in response to relatively small changes in gate opening. But on a field scale, the restriction ensures that sluicing will take place in a controlled fashion without catastrophic amounts of sediment being introduced rapidly into the downstream channel.

Further work on the numerical model should incorporate sediment mixtures, the effects of cohesive sediments on sluicing, supercritical flow, and the consideration of temporal width variations in the channel. These additions will allow evaluations of the effects of sorting, armoring, cohesion, and width variation to be included in the analysis of sediment sluicing.

REFERENCES

Annandale, G.W.. 1987. Reservoir Sedimentation. Volume 29 in Developments in Water Science. Amsterdam, Netherlands: Elsevier Science Publishers.

Asada, Hiroshi. 1973. Some Examples of Bed Profile Calculation of Sedimentation in Reservoirs in Mountainous Region. Proceedings of 15th Congress of the International Association of Hydraulic Research, vol. 1, p. 581-588.

Ashida, K. 1980. How to Predict Reservoir Sedimentation. In Proceedings of the International Symposium on River Sedimentation, Vol. 2, p. 821-846. Beijing, China: March 24-29.

Barr Engineering. 1986. Emergency Action Plan submitted for Granite Falls. U.S. Federal Energy Regulatory Commission Project No. 8423. November.

Bell, Robert G., and Alex J. Sutherland. 1983. Nonequilibrium Bedload Transport by Steady Flows. American Society of Civil Engineers, Journal of Hydraulics, Vol. 109, No. 3, March, p. 351-367.

Bhamidipaty, Suryanarayana, and Hsieh W. Shen. 1971. Laboratory Study of Degradation and Aggradation. American Society of Civil Engineers Harbors and Coastal Engineering Division, vol. 97, No. WW4, November, p. 615-630.

Bogardi, Jonaos. 1974. Sediment Transport in Alluvial Streams. Budapest: Akademiai Kiado.

Bondurant, Donald C. 1955. Report on Reservoir Delta Reconaissance. U.S. Army Corps of Engineers Missouri River District Sediment Series No. 6, June.

Borland, Whitney M.. 1971. Reservoir Sedimentation. In River Mechanics, Vol. II. H.W. Shen, editor. Fort Collins, Colorado: Water Resources Publications.

Bouchard, J.P. 1987. A Mathematical Model of Sedimentation and Erosion in Reservoirs. Abstract in Proceedings of EUROMECH, Mechanics of Sediment Transport in Fluvial and Marine Environments. Genoa, Italy: Sept. 15-19, p. 119.120.

Brownlie, William R. 1981. Prediction of Flow Depth and Sediment Discharge in Open Channels. Pasadena, California: W.M. Keck Laboratory of Hydraulics and Water Resources Report No. KH-R-43A.

Brune, G.M. 1953. Trap Efficiency of Reservoirs. Transactions of the American Geophysical Union, Volume 34, No. 3..

Cao, Ruxuan, and Jingliang Chen. 1980. Erosion and Sedimentation of Flow at Hyperconcentration in Reservoirs. In Proceedings of the International Symposium on River Sedimentation, Volume 2, p. 791-792 (abstract in English). Beijing, China: March 24-29.

Cao, Shuyou, Duo Fang, Xinnian Liu, and Jiayang Chen. 1988. Mathematical Modeling of Delta Deposits and Retrogressive Erosion in Reservoirs. 1988. Proceedings of American Society of Civil Engineers National Conference on Hydraulic Engineering. Colorado Springs, Colorado: August 8-12, p. 503-509.

Cavor, Rajko. (no date). Mathematical Modeling of Reservoir Flushing. Belgrade, Yugoslavia: Energoprojekt-energodata Co.

Chang, Howard H.. 1984. Modeling of River Channel Changes. American Society of Civil Engineers Journal of Hydraulics, vol. 110, No.2, February, p. 157-172.

Chee, S.P., and A.P. Sweetman. 1971. An Experimental Investigation of Reservoir Sedimentation. Proceedings of 14th Congress of the International Association of Hydraulic Research, vol. 1, p. 21-24, Paris, France.

Chee, S.P.. 1983. Influence of Dams on Sediment Bed Formation on Reservoirs and Rivers. Proceedings of the 20th Congress of the International Association of Hydraulic Research, vol. 2, p. 297-301.

Chen, Y.H. 1979. Water and Sediment Routing in Rivers. In Modeling of Rivers, Hsieh Wen Shen, editor. New York: John Wiley and Sons.

Chen, Yung Hai, Jose L. Lopez, and Everett V. Richardson. 1978. Mathematical Modeling of Sediment in Reservoirs. American Society of Civil Engineers Journal of Hydaulics, vol. 104, No. HY12, December , p. 1605-1616.

Chen, Yung Hai. 1988. Development of a Quasi-nonequilibrium Reservoir Sedimentation Model: RESSED. Prepared for Second Seminar on Stream Sedimentation Models, Sponsored by Sedimentation Committee, Interagency Advisory Committee on Water Data, Denver, Colorado, October 19-20.

Chitale, S.V., V.G. Galgali, and K.N. Appukuttan. 1975. Simulation of Delta Building Process. Proceedings of Symposium on Modeling Techniques, vol. 2, 2nd Annual Symposium of the American Society of Civil Engineers Waterways, Harbors and Coastal Engineering Division, San Francisco, September 3-5.

Chow, Ven Te, David R. Maidment, and Larry W. Mays. 1988. Applied Hydrology. New York: McGraw-Hill Book Company.

Crickmore, Maurice J. 1970. Effect of Flume Width on Bed-Form Characteristics.American Society of Civil Engineers, Journal of Hydraulics, Vol. 96, No. HY2, February, p. 473 - 496.

Cunge, J.A., F.M. Holly Jr., and J. Verwey. 1983. Practical Aspects of Computational River Hydraulics. London, England: Pitman Publishing Ltd.

Cunge, Jean A. 1988. Wrap-up Discussion. Prepared for Second Seminar on Stream Sedimentation Models, Sponsored by Sedimentation Committee, Interagency Advisory Committee on Water Data, Denver, Colorado, October 19-20.

Einstein, Hans A., and Nicholas L. Barbarossa. 1952. River Channel Roughness. American Society of Civil Engineers Transactions, vol. 117, paper 2528, p. 1121-1132.

Einstein, Hans Albert. The Bed-Load Function for Sediment Transportation in Open Channel Flows. 1950. Washington, D.C.: United States Department of Agriculture Soil Conservation Service Technical Bulletin No. 1026, September.

Engelund, F. and E.D. Hansen. 1967. A Monograph on Sediment Transport on Alluvial Streams. Copenhagen: Teknisk Vorlag.

Evrard, J. 1983. Technical and Economic Impact of Reservoir Sedimentation. In Methods of Computing Sedimentation in Lakes and Reservoirs. Project A.2.6.1 of the International Hydrological Programme. Paris, France: UNESCO.

Fan, Jiahua. 1983. Methods of Preserving Reservoir Capacity. In Methods of Computing Sedimentation in Lakes and Reservoirs. Project A.2.6.1 of the International Hydrological Programme. Paris, France: UNESCO.

Fredsoe, J. 1978. Meandering and Braiding of Rivers. Journal of Fluid Mechanics, v. 84, p. 609-624.

Gake, Loyal, Rodrick Garver, John Gulliver, and Richard Renaud. 1981. Feasibility of Hydropower Capacity Additions at the Granite Falls Dam MN 00510. Minneapolis, Minnesota: University of Minnesota St. Anthony Falls Hydraulic Laboratory Project Report No. 203.

Garde, R.J., and K.G. Ranga Raju. 1985. Mechanics of Sediment Transportation and Alluvial Stream Problems. New Delhi, India: Wiley Eastern Limited.

Gill, Mohammad Akram. 1988. Hyperbolic Model for Aggrading Channels. American Society of Civil Engineers Journal of Engineering Mechanics, vol. 114, No.7, July, p. 1245-1255.

Graf, W.H.. 1977. Reservoir Sedimentation. Bethlehem, Pennsylvania: Lehigh University Hydraulic Laboratory .

Graf, Walter Hans. 1971. Hydraulics of Sediment Transport. New York, New York: McGraw Hill Book Company.

Granger, Robert A. 1985. Fluid Mechanics. New York: Holt, Rinehart and Winston.

Han, Qiwei. 1980. A Study on the Non-equilibrium Transport of Suspended Load. In the Proceedings of the International Symposium on River Sedimentation, Vol. 2, p. 793 - 802 (abstract in English). Beijing, China: March 24 - 29.

Hwang, Li-San, and David Divoky. 1971. Discussion of "Effect of Flume Width on Bed-Form Characteristics." American Society of Civil Engineers, Journal of Hydraulics, Vol. 97, No. HY2, February, p. 353 - 358.

Ikeda, Syunsuke and Takashi Asaeda. 1983. Sediment Suspension with Rippled Bed. American Society of Civil Engineers, Journal of Hydraulics, Vol. 109, No. 3, March, p. 409 - 423.

Jaramillo, Wilson F., and Subhash C. Jain. 1984. Aggradation and Degradation of Alluvial-Channel Beds. American Society of Civil Engineers, Journal of Hydraulics, Vol. 110, No. 8, August, p. 1072-1085.

Johannesson, Helgi. 1988. Theory of River Meanders. University of Minnesota Graduate School: Ph.d. Thesis.

Johnson, J.W. and W.L. Minaker. 1944. Movement and Deposition of Sediment in the Vicinity of Debris-Barriers. Transactions of the American Geophysical Union, Part VI, p. 901-905.

Johnson, Joe W. 1942. The Importance of Considering Side-Wall Friction in Bed-Load Investigations. Civil Engineering, vol. 12, no. 6, June.

Karaushev, A.V., I.V. Boguliubova, and T.B. Tabakaeva. 1981. Model for River-Type Reservoirs Sedimentation. Proceedings of the 19th Congress of the International Association of Hydraulic Research. New Delhi: vol. 2, p. 9-13.

Li, Ru-Min, Robert A. Massetter, and Thomas R. Grindeland. 1988. Sediment Routing Model HEC2SR. Prepared for Second Seminar on Stream Sedimentation Models, Sponsored by Sedimentation Committee, Interagency Advisory Committee on Water Data, Denver, Colorado, October 19-20.

Lopez, Jose Luis S.. 1978. Mathematical Modeling of Sediment Deposition in Reservoirs. Hydrology Papers No. 95. Fort Collins, Colorado: Colorado Statue University.

Mahmood, K.. 1987. Reservoir Sedimentation: Impact, Extent, and Mitigation. World Bank Technical Paper no. 71. Washington, D.C.: The World Bank.

Meyer-Peter, E., and R. Muller. 1948. Formulas for Bed-Load Transport. International Association of Hydraulic Research, 2nd meeting, Stockholm.

Mikhalev, M.A.. 1971. Control of Silting in Reservoirs on Mountain Rivers. Proceedings of the International Association of Hydraulic Research, Volume 5, p.101-1 to 101-3.

Mukhamedov, Amin. 1981. Silting Upstream of Dam and Scour Methods. In the Proceedings of the International Association of Hydraulic Research 19th Congress, Volume 2, p. 35 -42. New Delhi, India.

Nordin, Carl. 1988. Some Closing Comments. Prepared for Second Seminar on Stream Sedimentation Models, Sponsored by Sedimentation Committee, Interagency Advisory Committee on Water Data, Denver, Colorado, October 19-20.

Oral communication with Alan Ridels, 1989.

Parker, Gary, Ismael Martinez, and Randall Hills, 1982. Model Study of the Minnesota River near Trunk Highway No. 169 Bridge, Minnesota. Project Report No. 213. University of Minnesota: St. Anthony Falls Hydraulic Laboratory. September.

Parker, Gary. 1976. On the cause and Characteristic Scales of Meandering and Braiding in Rivers. Journal of fluid Mechanics, Volume 76, part 3, pp. 457-480.

Parker, Gary. 1978. Self-formed straight rivers with equilibrium banks and mobile bed. Part 2. The gravel river. Journal of Fluid Mechanics, Vol 89, part 1, pp. 127-146.

Paul, T.C., and G.S. Dhillon. 1988. Sluice Dimensioning for Desilting Reservoirs. Water Power and Dam Construction, May , p. 40-44.

Razvan, Ernest H., and Carlos Lloret Ramos. 1981. Sedimentation of River Impoundments Behind Medium-high Dams. Proceedings of the 19th Congress of the International Association of Hydraulic Research. New Delhi: vol. 2, p. 73-85.

Ribberink, and van der Sande. 1985. Aggradation in Rivers due to Overloading. Delft University of Technology Report No. 84-1.

Sanoyan, V.G.. 1971. Calculation of the Process of Sedimentation and Hydraulic Washout of River Reservoir. In the Proceedings of the International Association of Hydraulic Research 14th Congress, Vol. 1, p. 5-8. Paris, France.

Schneider, John. 1966. A Biological Reconnaissance of the Minnesota River from Lac Qui Palre dam to Mankato. Minnesota Department of Conservation Division of Game and Fish Section of Technical Services Special Publication No. 37. September.

Schumm, Stanley A. (editor). 1972 Benchmark Papers in Geology: River Morphology. Stroudsburg, Pennsylvania: Dowden, Hutchinson, and Ross, Inc.

Strand, Robert I. and Ernest L. Pemberton. 1982. Reservoir Sedimentation: Technical Guideline for Bureau of Reclamation. Sedimentation and River Hydraulics Section, Hydrology Branch, Division of Planning and Technical Services. Denver, Colorado.

Street, Robert L. 1973. The Analysis of Partial Differential Equations. Monterey, California: Brooks/cole Publishing Co.

Sugio, Sutesaburo, Michio Hashino, and Eiji Sasaki. 1973. Debris Slopes Above Sand Barriers. In the Proceedings of the International Association of Hydraulic Research International Symposium on River Mechanics, p. A5-1 to A5-12. Bangkok, Thailand: January 9 - 12.

Sugio, Sutesaburo. 1966. Discussion of "Channel Gradients Above Guly-control Structures." American Society of Civil Engineers, Journal of Hydraulics, Vol. 92, No. HY1, p. 108 - 120.

Sugio, Sutesaburo. 1972. Discussion of "Laboratory Study of Degradation and Aggradation." American Society of Civil Engineers Journal of the Waterways Division, WW4, November, p. 588-591.

Thomas, William A., and Alan L. Prasuhn. 1977. Mathematical Modeling of Scour and Deposition. American Society of Civil Engineers, Journal of Hydraulics, Vol. 103, No. HY8, August, p. 851 - 863.

United States Geological Survey. 1965. Granite Falls Quadrangle Minnesota 7.5 minute series.

Vanoni, Vito A., and Norman H. Brooks. 1957. Laboratory Studies of the Roughness and Suspended Load of Alluvial Streams. Pasadena, California: California Institute of Technology Sedimentation Laboratory Report No. E-68, December.

Vanoni, Vito, (editor). 1975. Sedimentation Engineering. American Society of Civil Engineers Manuals and Reports on Engineering Practice No. 54.

Vries, J.J. de, W. Hartman, and F. Amorocho. 1980. Sediment Modeling for the Sacramento River Diversion to the Peripheral Canal. In Proceedings of the American Society of Civil Engineers Specialty Conference on Computer and Physical Modeling in Hydraulic Engineering. Chicago, Illinois: August 6 - 8.

Vries, M. de. 1973. River-bed Variations - Aggradation and Degradation. Delft Hydraulics Laboratory Publication No. 107, April.

Wang, Flora C., Yu-hwa Wang, Panagiotis D. Scarlatos, and William H. McAnally, Jr.. 1983. Analytical Analysis of River-Delta Interaction. In Proceedings of the International Association of Hydraulic Research 20th Congress, Volume 2, p. 262-272.

White, W.R., and R. Bettes. 1984. The Feasibility of flushing Sediments Through Reservoirs. In the Proceedings of Harare Symposium, Challenges in African Hydrology and Water Resources, IAHS Publ. no. 144, p. 577 - 587.

White, W.R., H. Milli and A.D. Crabbe. 1973. Sediment Transport: An Appraisal of Available Methods. Volume 1: Summary of Existing Theories. Wallingford, England: Hydraulics Research Station Report No. INT 119, November.

Woolhiser, David A., and Arno T. Lenz. 1965. Channel Gradients Above Gully-control Structures. American Society of Civil Engineers, Journal of Hydraulics, Vol. 91, No. HY3, May, p. 165 - 187.

Xia, Mai-Ding and Zenghai Ren. 1980. Methods of Sluicing Sediment from Heisonglin Reservoir and it Utilization Downstream. In Proceedings of the International Symposium on River Sedimentation, Vol. 2, p. 725-726 (abstract in English). Beijing, China: March 24-29.

Xia, Zhenhuan and Qiwei Han. 1980. The Long-term Capacity of a Reservoir. In Proceedings of the International Symposium on River Sedimentation, Vol. 2, p. 761-762 (abstract in English). Beijing, China: March 24-29.

Yan, Jinghai, and Guoguan Xu. 1980. Layout of Intakes with Respect to Sediment Prevention for Waterpower and Irrigation Projects. In Proceedings of the International Symposium on River Sedimentation, Volume 2, p. 781 - 782 (abstract in English). Beijing, China: March 24-29.

Yucel, Oner, and Walter H. Graf. 1973. Bed Load Deposition in Reservoirs. In Proceedings of the International Association of Hydraulic Research 15th Congress, Volume 1, p. 271-278

Yucel, Oner. 1977. Investigation of Reservoir Delta Formations in a Laboratory Flume. In Proceedings of the International Association of Hydraulic Research 17th Congress, Volume 1, p. 159-164

Zhang, Hao, Mai-Ding Xia, Shi-Ji Chen, Zhen-Wu Li, and Heng-Bin Xia. 1976. Regulation of Sediments in Some Medium- and Small-Sized Reservoirs on Heavily Silt-Laden Streams in China. Transactions of the Twelfth International Congress on Large Dams, Vol. III, Q.47R.32, p. 1223-1243. Mexico City: March 29-April 2.

Zhang, Qishun, Yuqian Long, and Enze Jiao. 1980. Sediment Problems of Sanmenxia Reservoir. In Proceedings of the International Symposium on River Sedimentation, Volume 2, p. 715-716 (abstract in English). Beijing, China: March 24-29.

APPENDICES

APPENDIX 1 SIDEWALL AND BEDFORM CORRECTION PROCEDURE

Resistance to flow in stream channels is provided by the channel bed and stream banks, or sidewalls. In natural streams the sidewalls may be either more or less rough than the bed. In glass-walled laboratory flumes the sediment-covered bed generally provides much more resistance to flow than do the sidewalls. Channel beds, in turn, provide both grain (skin) and form resistance. Grain resistance is due to flow over individual sediment particles, while form resistance is due to irregularities in the bed, such as ripples, dunes, and other bedforms. Only that portion of energy expended on overcoming grain resistance is effective in producing bedload transport. Sediment transport predictions require estimates of this grain resistance, or grain shear stress.

If bed and sidewall roughness are not equal, the total resistive shear force is not equally distributed across the wetted perimeter. A procedure is needed to estimate channel bed shear stress and subsequently grain shear stress. In this investigation, the sidewall correction procedure of Johnson (1942) is used to separate bed shear stress from total shear stress, and the Einstein-Barbarossa method (1952) is used to find grain shear stress. These procedures are used differently for the three flow conditions encountered:

1. steady, uniform flow where all hydraulic parameters are known,
2. steady, uniform flow when channel depth and roughness are not known, and
3. steady, non-uniform flow when the depth is known but the energy slope and roughness are not.

The correction procedures for these conditions have been incorporated into the computer program presented in Chapter 4 and listed in the procedure named "CORRECT" in Appendix 3.

A1.1 Steady, Uniform Flow with Known Depth

In this case laboratory flume measurements are available for steady, uniform flow conditions.

A1.1.1 Bed Friction Factor and Shear Stress

The Johnson sidewall correction procedure partitions the total cross-sectional flow area, A, into flow areas pertaining to the wall, A_w, and the bed, A_b, where the streamwise gravity force is resisted by shear forces on the bed and walls, respectively (Figure A1.1). It is assumed that the mean velocity and energy slope are the same for both flow areas, and that the hypothetical boundaries between A_b and A_w are considered surfaces of zero shear and are not included in calculations of wetted perimeters (Vanoni and Brooks, 1957). It is further assumed that the Darcy-Weisbach relation can be applied to each subsection as well as the whole. It follows (Vanoni, 1975) that

$$\frac{u^2}{S_f} = \frac{8gA}{fp} = \frac{8gA_b}{f_b p_b} = \frac{8gA_w}{f_w p_w} \qquad \text{(A1.1)}$$

where p is the wetted perimeter, f is the Darcy-Weisbach friction coefficient, and the subscripts b and w refer to the bed and sidewalls, respectively. Note that

$$C_f = \frac{f}{8}, \quad C_b = \frac{f_b}{8}, \text{ and } C_w = \frac{f_w}{8} \qquad \text{(A1.2)}$$

where C_f is a modified Darcy-Weisbach friction factor. From the requirement that

$$A = A_b + A_w \qquad \text{(A1.3)},$$

equations (A1.1) and (A1.2) are used to obtain the result

$$C_b = \frac{C_f - C_w p_w}{p_b} \qquad \text{(A1.4)}.$$

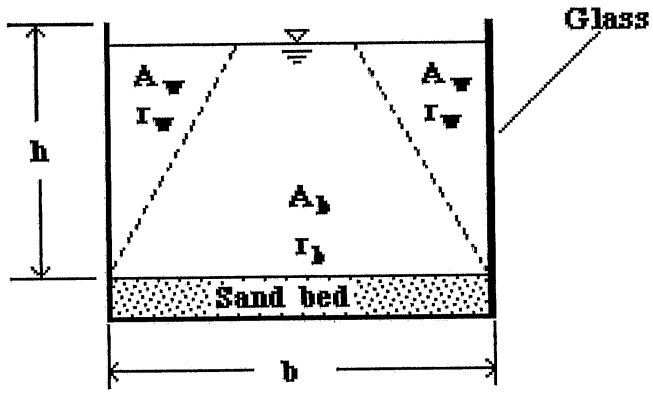

Figure A1.1 Hypothetical division of bed and wall hydraulic parameters

For a rectangular channel, since $p_w = 2h$, where h is the mean depth, and $p_b = b$, where b is the width, (A1.4) may be written as

$$C_b = C_f + \frac{2h}{b}(C_f - C_w) \qquad \text{(A1.5)}.$$

The wall friction factor, C_w, is the only unknown on the right hand side of (A1.5). To find its value, consider the Reynolds number for each section:

$$Re = \frac{4ru}{\nu}, \quad Re_b = \frac{4r_b u}{\nu}, \text{ and } Re_w = \frac{4r_w u}{\nu} \qquad \text{(A1.6)},$$

where r is the hydraulic radius and is equal to $\frac{A}{p}$. Substituting for the values of r from (A1.1) and assuming equality of u and S_f for all sections, (A1.6) becomes

$$\frac{Re}{C_f} = \frac{Re_b}{C_b} = \frac{Re_w}{C_w} \qquad \text{(A1.7).}$$

Since Re and C_f are known from the experimental data, they can be used to compute $\frac{Re}{C_f}$ and thus $\frac{Re_w}{C_w}$. The wall friction factor may be found from the well known Moody diagram for smooth turbulent flow. That is, $C_w = f(Re_w)$, or

$$\frac{1}{\sqrt{C_w}} = 2.211 \cdot \ln\left(\frac{Re_w}{6.9}\right) \qquad \text{(A1.8),}$$

from Granger, 1985. Since $Re_w = Re\frac{C_w}{C_f}$, equation (A1.8) may be re-written as

$$\frac{1}{\sqrt{C_w}} = 2.211 \cdot \ln\left(Re\frac{C_w}{6.9C_f}\right) \qquad \text{(A1.9).}$$

Equation (A1.9) may be solved iteratively for C_w, after which C_b may be found from (A1.5). The bed shear stress, τ_b, is then found from

$$\tau_b = \rho C_b u^2 \qquad \text{(A1.10).}$$

A1.1.2 Grain Shear Stress

The grain friction factor for flume conditions is found using the Einstein-Barbarossa method (1952):

$$\frac{1}{\sqrt{C_g}} = 2.5\ln\left(12.3\frac{r_g}{k_s}X\right) \qquad \text{(A1.11),}$$

where k_s is a roughness height, taken as the median sediment diameter, d_{50}, in this investigation, and X is a correction factor for non-fully rough turbulent flows, expressed as $X = f(\frac{k_s}{\delta})$, where δ is the laminar sublayer thickness, defined by $\delta = \frac{11.6\nu}{u_{*g}}$, and u_{*g} is the grain shear velocity, equal to $\sqrt{gr_gS_f}$. For values of $\frac{k_s}{\delta}$ greater than 10, flow is considered to be fully rough turbulent, and X = 1.0. For values of $\frac{k_s}{\delta}$ of less than approximately 0.256 the flow is smooth and may be described by (Einstein, 1950)

$$\frac{1}{\sqrt{C_g}} = 2.5\ln\left(3.67\frac{r_g u_{*g}}{\nu}\right) \qquad \text{(A1.12).}$$

For values of $\frac{k_s}{\delta}$ between 0.256 and 10, X may be found using Figure 4 in Einstein (1950), or from the following analytic expression taken from White, Milli, and Crabbe (1973):

$$X = 1.90 + 0.7383\ln\left(\frac{k_s}{\delta}\right) \quad \text{for } 0.265 \le \frac{k_s}{\delta} < 0.5,$$

$$X = 1.615 - 0.407\left(\left|\ln\left(\frac{k_s}{\delta}\right)\right|\right)^{1.6} \quad \text{for } 0.5 \le \frac{k_s}{\delta} < 2.35,$$

$$X = 1 + 0.926\left(1 - 0.434\ln\left(\frac{k_s}{\delta}\right)\right)^{2.43} \quad \text{for } 2.35 \le \frac{k_s}{\delta} < 10 \qquad \text{(A1.13)}$$

For wide open channel conditions it is assumed the sidewalls do not contribute significantly to the resistive force. This means that the assumption of a wide channel applies, so that the hydraulic radius is simply equal to the depth. It is also assumed that flow is fully turbulent rough. The grain friction factor for these conditions is found using the Engelund-Hansen relationship (Brownlie, 1981)

$$\frac{1}{\sqrt{C_g}} = 2.5\ln\left(11\frac{r_g}{2d_{50}}\right) \qquad \text{(A1.14).}$$

Equations (A1.11) or (A1.12) for flume conditions or (A1.14) for wide open channel conditions contain two unknowns, C_g and r_g. The second equation for closure is

$$C_g u^2 = g r_g S_f \qquad \text{(A1.15).}$$

Equations (A1.11) or (A1.12) for flume conditions or (A1.14) for open channel conditions and (A1.15) may be solved iteratively for values of C_g and r_g. Sediment transport is then found using τ_g from the relation

$$\tau_g = \rho C_g u^2 \qquad \text{(A1.16).}$$

A1.2 Steady, Uniform Flow with Unknown Roughness and Depth

The computer code developed in Chapter 4 initializes computations by estimating normal depth and sediment transport based on known values of channel discharge, width, and slope, and a sediment roughness factor and water temperature. If a flume experiment is being reproduced, both the sidewall and bedform correction procedures are needed. If a field case is simulated, only bedform roughness need be considered. Since the channel depth and friction factor are not known beforehand, an iterative procedure with 5 equations is used. Unknowns are the normal depth, h_N, composite friction factor for the flume, C_f, wall friction factor, C_w, grain friction factor, C_g, and bed friction factor, C_b.

Depth is related to composite friction factor by

$$g S_f r_N = C_f u^2 \qquad \text{(A1.17),}$$

where $r_N = \frac{A}{p} = \frac{bh_N}{b + 2h_N}$.

From the sidewall correction procedure C_f may be expressed as a function of the wall and bed friction factors using (A1.5):

$$C_f = \frac{2h_N C_w + bC_b}{b + 2h_N} \qquad \text{(A1.18).}$$

The wall friction factor is found as in the sidewall correction procedure using (A1.9). Note that an estimate of h_N is needed to compute r_N and Re in (A1.9).

A1.2.1 Flume Conditions

The Einstein-Barbarossa method is used again for estimating the value of the grain roughness factor. Since r_g in (A1.11) and (A1.12) is unknown, the equations are re-written recognizing that

$$r_N \frac{r_g}{r_N} = r_N \frac{C_g}{C_f} \qquad \text{(A1.19)}$$

where C_f is expressed using (A1.18). Equation (A1.11) and (A1.12) become

$$\frac{1}{\sqrt{C_g}} = 2.5\ln\left(12.3\frac{r_N C_g}{k_s C_f}X\right) \qquad \text{(A1.20)}$$

and

$$\frac{1}{\sqrt{C_g}} = 2.5\ln\left(3.67\frac{r_N u_{*g} C_g}{\nu C_f}\right) \qquad \text{(A1.21),}$$

respectively.

The grain shear velocity in (A1.20) and (A1.21) is expressed as

$$u_{*g} = \sqrt{C_g}\, u^2 \qquad \text{(A1.22).}$$

Bed shear stress is expressed in dimensionless form as

$$\tau_b^* = \frac{\rho C_b u^2}{\rho g R d_{50}} = C_b u^{*2} \qquad \text{(A1.23),}$$

where R is the submerged specific gravity of the sediment and $u^{*2} = \frac{u^2}{\rho g R d_{50}}$. The following expression relating τ_b^* and τ_g^* was derived in Chapter 3:

$$\tau_g^* = \tau_b^* \text{ if } \tau_b^* \le 0.0626,$$

$$\tau_g^* = 0.06 + 2.14\tau_b^{*2.43} \text{ for } 0.0626 \le \tau_b^* \le 0.541, \text{ and}$$

$$\tau_g^* = \tau_b^* \text{ if } \tau_b^* > 0.541 \qquad \text{(A1.24).}$$

Substituting (A1.23) in (A1.24) and solving for $C_b u^{*2}$ yields

$$C_b u^{*2} = C_g u^{*2} \text{ for } C_g u^{*2} < 0.0626 \text{ or } C_g u^{*2} > 0.541, \text{ and}$$

$$C_b u^{*2} = \left(\frac{C_g u^{*2} - 0.06}{2.14}\right)^{0.41} \text{ otherwise} \qquad \text{(A1.25).}$$

Initial estimates of h_N, C_f, C_w, C_g, and C_b are used in equations (A1.17), (A1.18), (A1.9), (A1.20) or (A1.21), and (A1.25). Final values are found by iteration. Sediment transport is then predicted using equation (3.12) from Chapter 3.

A1.2.2 Wide Open Channel Conditions

The procedure for open channel conditions is very similar except Equations (A1.20) and (A1.24) are replaced by equations appropriate for fully rough turbulent flow in wide open channels. The grain friction factor is written as

$$\frac{1}{\sqrt{C_g}} = 2.5\ln\left(11\frac{r_N C_g}{2d_{50}C_f}\right) \qquad \text{(A1.26)}$$

from Equation (A1.14). The relationship between grain shear stress and bed shear stress is taken from Engelund and Hansen (1967), which after modifying in a fashion similar to (A1.23) and (A1.24) becomes:

$$C_b u^{*2} = C_g u^{*2} \text{ for } C_g u^{*2} < 0.0615 \text{ or } C_g u^{*2} \geq 2.435, \text{ and}$$

$$C_b u^{*2} = 1.581\sqrt{C_g u^{*2} - 0.06} \text{ for } 0.0615 \leq C_g u^{*2} < 2.435 \qquad \text{(A1.27).}$$

Note that the transition between lower regime and upper regime bedforms is not modeled in this investigation, as mentioned in Chapter 4.

A1.3 Steady, Non-uniform Flow with Unknown Energy Slope and Friction Factor

The energy slope, S_f, in non-uniform flow such as a reservoir backwater zone is not equal to the channel slope or water surface slope. It may be found using (A1.17), or, solving for S_f,

$$S_f = \frac{C_f u^2}{gr} \qquad \text{(A1.28),}$$

where C_f is the composite friction factor, a function of C_w and C_b as expressed in (A1.18). Thus S_f may be found from

$$S_f = \frac{u^2 2h}{gr}\left(\frac{C_w + bC_b}{b + 2h}\right) \qquad \text{(A1.29).}$$

Note that the subscripts signifying normal flow have been dropped. The wall friction factor, C_w, may be found from (A1.9) using the sidewall correction procedure, but since C_f is unknown, (A1.9) must be written using (A1.18) as

$$\frac{1}{\sqrt{C_w}} = 2.211 \cdot \ln\left(\mathrm{Re}\,\frac{C_f}{\frac{2h_N C_w + bC_b}{b + 2h_N}}\right) \qquad \text{(A1.30)}$$

For flume conditions, the bed friction factor is estimated using (A1.25) and an estimate of C_g from (A1.20) or (A1.21). For open channels, C_g and C_b are estimated from (A1.26) and (A1.27), respectively. After convergence, final values of C_w, C_b, and C_g are obtained, and S_f may be found from (A1.29) and used in the standard step backwater method for finding water surface profiles. The values of S_f and C_g are used to compute grain shear stress and sediment transport.

APPENDIX 2 EXPERIMENTAL DATA

Table A2.1 Centerline velocity profile data (follows)

DATE: 11 Aug 1987 RUN NUMBER: 1

DISCHARGE, l/sec: 1.5 SEDIMENT DISCHARGE, gr/min 150

GATE OPENING, cm: open NO. OF GATES OPEN: -

WATER SURFACE SLOPE: .0020 BED SLOPE: .0020

WATER TEMPERATURE, °C: 26 BEDFORM AMPLITUDE, cm: 0.8

Distance upstream of sluice gate(s), cm: 11.3

Water surface elevation, cm: 81.28 Elevation at top of bedform, cm: 84.35

Point	1	2	3	4	5	6	7	8
Elevation, cm	81.56	82.04	82.83	83.21	83.59	83.77	83.97	84.15
Velocity, cm/sec	35.5	33.8	32.7	29.3	29.0	29.8	27.0	23.5

Notes:

Distance upstream of sluice gate(s), cm: 15.0

Water surface elevation, cm: 81.71 Elevation at top of bedform, cm: 84.53

Point	1	2	3	4	5	6	7	8
Elevation, cm	81.86	82.42	83.11	83.46	83.82	84.00	84.17	84.35
Velocity, cm/sec	34.1	33.8	32.1	31.2	28.7	28.4	27.3	25.5

Notes:

Distance upstream of sluice gate(s), cm: 22.5

Water surface elevation, cm: 81.71 Elevation at top of bedform, cm: 84.58

Point	1	2	3	4	5	6	7	8
Elevation, cm	81.86	82.42	83.16	83.51	83.87	84.05	84.22	84.40
Velocity, cm/sec	34.5	33.6	31.2	30.7	29.1	28.0	27.4	25.6

Notes:

Distance upstream of sluice gate(s), cm: 30

Water surface elevation, cm: 81.71 Elevation at top of bedform, cm: 84.50

Point	1	2	3	4	5	6	7	8
Elevation, cm	81.96	82.42	83.11	83.46	83.79	83.97	84.15	84.33
Velocity, cm/sec	34.8	34.3	31.2	29.8	29.2	28.6	27.1	26.6

Notes:

RUN 1 (continued)
Distance upstream of sluice gate(s), cm: 37.5

Water surface elevation, cm: 81.66 Elevation at top of bedform, cm: 84.40

Point	1	2	3	4	5	6	7	8
Elevation, cm	81.84	82.34	83.03	83.39	83.72	83.89	84.07	84.22
Velocity, cm/sec	34.8	34.7	31.8	31.4	29.5	29.0	27.5	26.7

Notes:

Distance upstream of sluice gate(s), cm: 45

Water surface elevation, cm: 81.02 Elevation at top of bedform, cm: 83.89

Point	1	2	3	4	5	6	7	8
Elevation, cm	81.18	81.73	82.47	82.83	83.18	83.36	83.54	83.72
Velocity, cm/sec	33.4	31.9	30.4	28.6	27.8	27.2	26.3	24.7

Notes:

Distance upstream of sluice gate(s), cm: 75

Water surface elevation, cm: 80.97 Elevation at top of bedform, cm: 84.05

Point	1	2	3	4	5	6	7	8
Elevation, cm	81.13	81.73	82.52	82.90	83.28	83.46	83.67	83.84
Velocity, cm/sec	34.1	32.4	29.3	28.4	26.1	25.4	24.9	22.2

Notes:

Distance upstream of sluice gate(s), cm: 120

Water surface elevation, cm: 80.97 Elevation at top of bedform, cm: 83.97

Point	1	2	3	4	5	6	7	8
Elevation, cm	81.13	81.73	82.47	82.85	83.23	83.41	83.59	83.79
Velocity, cm/sec	33.0	32.1	29.7	28.9	26.3	26.5	24.0	22.0

Notes:

Distance upstream of sluice gate(s), cm: 180

Water surface elevation, cm: 80.74 Elevation at top of bedform, cm: 83.69

Point	1	2	3	4	5	6	7	8
Elevation, cm	80.90	81.48	82.22	82.60	82.95	83.13	83.34	83.51
Velocity, cm/sec	33.4	32.0	30.2	29.2	27.0	26.4	24.4	24.2

Notes:

RUN 1 (continued)

Distance upstream of sluice gate(s), cm: 300

Water surface elevation, cm: 80.57 Elevation at top of bedform, cm: 83.44

Point	1	2	3	4	5	6	7	8
Elevation, cm	80.72	81.28	82.01	82.37	82.73	82.90	83.08	83.26
Velocity, cm/sec	34.2	32.2	29.9	28.7	27.7	26.0	25.4	23.1

Notes:

Distance upstream of sluice gate(s), cm: 450

Water surface elevation, cm: 80.29 Elevation at top of bedform, cm: 83.13

Point	1	2	3	4	5	6	7	8
Elevation, cm	80.44	81.00	81.71	82.06	82.42	82.60	82.78	82.95
Velocity, cm/sec	33.8	33.4	30.4	28.4	27.8	27.1	25.9	24.1

Notes:

Distance upstream of sluice gate(s), cm:

Water surface elevation, cm: Elevation at top of bedform, cm:

Point	1	2	3	4	5	6	7	8
Elevation, cm								
Velocity, cm/sec								

Notes:

Distance upstream of sluice gate(s), cm:

Water surface elevation, cm: Elevation at top of bedform, cm:

Point	1	2	3	4	5	6	7	8
Elevation, cm								
Velocity, cm/sec								

Notes:

Distance upstream of sluice gate(s), cm:

Water surface elevation, cm: Elevation at top of bedform, cm:

Point	1	2	3	4	5	6	7	8
Elevation, cm								
Velocity, cm/sec								

Notes:

DATE: 18 Aug 1987 RUN NUMBER: 2

DISCHARGE, l/sec: 1.5 SEDIMENT DISCHARGE, gr/min 150

GATE OPENING, cm: 5.64 NO. OF GATES OPEN: 1/1

WATER SURFACE SLOPE: .0021 BED SLOPE: .0017

WATER TEMPERATURE, °C: 26 BEDFORM AMPLITUDE, cm: 0.8

Distance upstream of sluice gate(s), cm: 30

Water surface elevation, cm: 81.51 Elevation at top of bedform, cm: 84.45

Point	1	2	3	4	5	6	7	8
Elevation, cm	81.81	82.24	82.98	83.36	83.72	83.89	84.10	84.27
Velocity, cm/sec	34.4	32.4	31.8	30.3	29.7	27.8	26.4	25.6

Notes:

Distance upstream of sluice gate(s), cm: 120

Water surface elevation, cm: 81.51 Elevation at top of bedform, cm: 84.33

Point	1	2	3	4	5	6	7	8
Elevation, cm	81.66	82.22	82.93	83.26	83.61	83.79	83.97	84.15
Velocity, cm/sec	34.4	32.7	30.7	30.4	27.8	26.9	26.4	24.0

Notes:

Distance upstream of sluice gate(s), cm: 180

Water surface elevation, cm: 81.23 Elevation at top of bedform, cm: 84.25

Point	1	2	3	4	5	6	7	8
Elevation, cm	81.38	81.99	82.75	83.11	83.49	83.69	83.87	84.07
Velocity, cm/sec	34.1	33.3	30.8	30.8	28.2	26.4	26.4	23.9

Notes:

Distance upstream of sluice gate(s), cm:

Water surface elevation, cm: Elevation at top of bedform, cm:

Point	1	2	3	4	5	6	7	8
Elevation, cm								
Velocity, cm/sec								

Notes:

DATE: 29 Sept 1987 RUN NUMBER: 5

DISCHARGE, l/sec: 1.5 SEDIMENT DISCHARGE, gr/min 150

GATE OPENING, cm: 0.69 NO. OF GATES OPEN: 1/1

WATER SURFACE SLOPE: .0018 BED SLOPE: .0018

WATER TEMPERATURE, °C: 20 BEDFORM AMPLITUDE, cm: 0.8

Distance upstream of sluice gate(s), cm: 47.5

Water surface elevation, cm: 59.77 Elevation at top of bedform, cm: 62.51

Point	1	2	3	4	5	6	7	8
Elevation, cm	59.9	60.46	61.14	61.50	61.83	62.01	62.18	62.34
Velocity, cm/sec	34.7	33.4	31.1	29.7	27.8	27.1	26.0	25.1

Notes:

Distance upstream of sluice gate(s), cm: 120

Water surface elevation, cm: 59.64 Elevation at top of bedform, cm: 62.62

Point	1	2	3	4	5	6	7	8
Elevation, cm	59.80	60.38	61.14	61.50	61.88	62.06	62.24	62.44
Velocity, cm/sec	34.5	34.4	32.0	30.9	29.0	28.5	26.9	25.0

Notes:

Distance upstream of sluice gate(s), cm: 300

Water surface elevation, cm: 59.36 Elevation at top of bedform, cm: 62.13

Point	1	2	3	4	5	6	7	8
Elevation, cm	59.49	60.05	60.74	61.09	61.45	61.63	61.78	61.96
Velocity, cm/sec	36.3	33.9	32.8	32.2	29.6	29.7	27.3	25.8

Notes:

Distance upstream of sluice gate(s), cm:

Water surface elevation, cm: Elevation at top of bedform, cm:

Point	1	2	3	4	5	6	7	8
Elevation, cm								
Velocity, cm/sec								

Notes:

DATE: 10 July 1987 RUN NUMBER: 6

DISCHARGE, l/sec: 1.5 SEDIMENT DISCHARGE, gr/min 300

GATE OPENING, cm: open NO. OF GATES OPEN: -

WATER SURFACE SLOPE: .0025 BED SLOPE: .0025

WATER TEMPERATURE, °C: 26 BEDFORM AMPLITUDE, cm: 0.5

Distance upstream of sluice gate(s), cm: 15

Water surface elevation, cm: 80.79 Elevation at top of bedform, cm: 83.28

Point	1	2	3	4	5	6	7	8
Elevation, cm	80.92	81.46	82.14	82.47	82.80	82.95	83.13	
Velocity, cm/sec	38.3	35.9	33.8	31.4	29.2	29.2	27.7	

Notes: 8th point was too close to the bed to sample

Distance upstream of sluice gate(s), cm: 22.5

Water surface elevation, cm: 80.85 Elevation at top of bedform, cm: 83.47

Point	1	2	3	4	5	6	7	8
Elevation, cm	81.00	81.56	82.27	82.60	82.95	83.13	83.31	
Velocity, cm/sec	37.0	36.7	34.2	32.3	29.8	27.9	25.0	

Notes: 8th point was too close to the bed to sample

Distance upstream of sluice gate(s), cm: 30

Water surface elevation, cm: 80.62 Elevation at top of bedform, cm: 83.31

Point	1	2	3	4	5	6	7	8
Elevation, cm	80.74	81.30	82.96	82.29	82.65	82.80	82.98	83.13
Velocity, cm/sec	37.6	36.7	34.7	32.7	32.6	30.3	27.9	26.6

Notes: ---

Distance upstream of sluice gate(s), cm: 37.5

Water surface elevation, cm: 80.72 Elevation at top of bedform, cm: 83.28

Point	1	2	3	4	5	6	7	8
Elevation, cm	80.85	81.35	82.01	82.32	82.65	82.80	82.95	83.13
Velocity, cm/sec	38.8	37.5	34.1	32.4	30.2	29.3	28.8	27.1

Notes: ---

RUN 6 (continued)

Distance upstream of sluice gate(s), cm: 45

Water surface elevation, cm: 80.62 Elevation at top of bedform, cm: 83.24

Point	1	2	3	4	5	6	7	8
Elevation, cm	80.77	81.33	82.04	82.37	82.73	82.90	83.08	
Velocity, cm/sec	39.2	36.0	35.1	32.9	31.6	29.3	26.9	

Notes: 8th point was too close to the bed to sample

Distance upstream of sluice gate(s), cm: 75

Water surface elevation, cm: 80.97 Elevation at top of bedform, cm: 83.87

Point	1	2	3	4	5	6	7	8
Elevation, cm	81.20	81.71	82.42	82.78	83.13	83.34	83.51	
Velocity, cm/sec	39.5	38.1	35.5	35.0	32.0	30.4	28.7	

Notes: 8th point was too close to the bed to sample

Distance upstream of sluice gate(s), cm:

Water surface elevation, cm: Elevation at top of bedform, cm:

Point	1	2	3	4	5	6	7	8
Elevation, cm								
Velocity, cm/sec								

Notes:

Distance upstream of sluice gate(s), cm:

Water surface elevation, cm: Elevation at top of bedform, cm:

Point	1	2	3	4	5	6	7	8
Elevation, cm								
Velocity, cm/sec								

Notes:

Distance upstream of sluice gate(s), cm:

Water surface elevation, cm: Elevation at top of bedform, cm:

Point	1	2	3	4	5	6	7	8
Elevation, cm								
Velocity, cm/sec								

Notes:

DATE: 30 July 1987 RUN NUMBER: 7

DISCHARGE, l/sec: 1.5 SEDIMENT DISCHARGE, gr/min 300

GATE OPENING, cm: 6.76 NO. OF GATES OPEN: 1/1

WATER SURFACE SLOPE: .0026 BED SLOPE: .0024

WATER TEMPERATURE, °C: 26 BEDFORM AMPLITUDE, cm: 0.5

Distance upstream of sluice gate(s), cm: 12

Water surface elevation, cm: 81.46 Elevation at top of bedform, cm: 84.3

Point	1	2	3	4	5	6	7	8
Elevation, cm	81.61	82.17	82.88	83.23	83.59	83.77	83.94	84.12
Velocity, cm/sec	37.8	36.7	34.5	32.6	31.1	29.5	27.7	25.7

Notes:

Distance upstream of sluice gate(s), cm: 75

Water surface elevation, cm: 81.40 Elevation at top of bedform, cm: 84.10

Point	1	2	3	4	5	6	7	8
Elevation, cm	81.53	82.09	82.75	83.08	83.44	83.59	83.77	83.92
Velocity, cm/sec	37.9	36.1	33.7	32.8	29.9	29.1	27.6	25.3

Notes:

Distance upstream of sluice gate(s), cm: 180

Water surface elevation, cm: 81.15 Elevation at top of bedform, cm: 83.82

Point	1	2	3	4	5	6	7	8
Elevation, cm	81.28	81.81	82.47	82.83	83.16	83.31	83.49	83.64
Velocity, cm/sec	37.6	36.2	34.0	33.6	30.9	30.0	28.5	26.4

Notes:

Distance upstream of sluice gate(s), cm:

Water surface elevation, cm: Elevation at top of bedform, cm:

Point	1	2	3	4	5	6	7	8
Elevation, cm								
Velocity, cm/sec								

Notes:

DATE: 3 Aug 1987 RUN NUMBER: 11

DISCHARGE, l/sec: 1.5 SEDIMENT DISCHARGE, gr/min 300

GATE OPENING, cm: 2.05 NO. OF GATES OPEN: 1/1

WATER SURFACE SLOPE: .0024 BED SLOPE: .0024

WATER TEMPERATURE, °C: 26 BEDFORM AMPLITUDE, cm: 0.5

Distance upstream of sluice gate(s), cm: 22

Water surface elevation, cm: 79.07 Elevation at top of bedform, cm: 81.71

Point	1	2	3	4	5	6	7	8
Elevation, cm	79.35	79.73	80.39	80.72	81.05	81.20	81.38	81.53
Velocity, cm/sec	38.4	37.1	35.8	34.0	32.9	31.8	30.3	28.8

Notes:

Distance upstream of sluice gate(s), cm: 120

Water surface elevation, cm: 78.86 Elevation at top of bedform, cm: 81.58

Point	1	2	3	4	5	6	7	8
Elevation, cm	79.27	79.55	80.24	80.57	80.90	81.07	81.25	81.40
Velocity, cm/sec	38.0	36.6	35.8	33.1	32.0	30.6	28.4	26.8

Notes:

Distance upstream of sluice gate(s), cm: 300

Water surface elevation, cm: 78.31 Elevation at top of bedform, cm: 81.13

Point	1	2	3	4	5	6	7	8
Elevation, cm	78.64	79.02	79.73	80.06	80.41	80.59	80.77	80.95
Velocity, cm/sec	38.7	36.9	34.8	33.5	30.5	30.2	28.2	25.6

Notes:

Distance upstream of sluice gate(s), cm:

Water surface elevation, cm: Elevation at top of bedform, cm:

Point	1	2	3	4	5	6	7	8
Elevation, cm								
Velocity, cm/sec								

Notes:

DATE: 5 Feb 1988 RUN NUMBER: 13

DISCHARGE, l/sec: 3.0 SEDIMENT DISCHARGE, gr/min 150

GATE OPENING, cm: 1.96 NO. OF GATES OPEN: 1/1

WATER SURFACE SLOPE: .0019 BED SLOPE: .0014

WATER TEMPERATURE, °C: 3 BEDFORM AMPLITUDE, cm: 1.5

Distance upstream of sluice gate(s), cm: 45

Water surface elevation, cm: 67.18 Elevation at top of bedform, cm: 72.69

Point	1	2	3	4	5	6	7	8
Elevation, cm	67.71	68.55	69.92	70.63	71.32	71.65	72.01	72.34
Velocity, cm/sec	38.0	37.5	37.7	34.6	31.9	32.0	29.3	26.4

Notes:

Distance upstream of sluice gate(s), cm: 120

Water surface elevation, cm: 67.13 Elevation at top of bedform, cm: 72.36

Point	1	2	3	4	5	6	7	8
Elevation, cm	67.51	68.45	69.75	70.41	71.04	71.37	71.70	72.03
Velocity, cm/sec	37.5	37.9	37.0	34.2	34.3	33.0	31.9	28.1

Notes:

Distance upstream of sluice gate(s), cm: 300

Water surface elevation, cm: 66.62 Elevation at top of bedform, cm: 71.88

Point	1	2	3	4	5	6	7	8
Elevation, cm	66.95	67.94	69.26	69.90	70.56	70.89	71.22	71.55
Velocity, cm/sec	37.8	37.2	34.9	35.5	33.8	30.7	28.5	29.5

Notes:

Distance upstream of sluice gate(s), cm:

Water surface elevation, cm: Elevation at top of bedform, cm:

Point	1	2	3	4	5	6	7	8
Elevation, cm								
Velocity, cm/sec								

Notes:

DATE: 19 May 1988 RUN NUMBER: 14

DISCHARGE, l/sec: 3.0 SEDIMENT DISCHARGE, gr/min 150

GATE OPENING, cm: 7.97 NO. OF GATES OPEN: 1/1

WATER SURFACE SLOPE: .0017 BED SLOPE: .0017

WATER TEMPERATURE, °C: 16 BEDFORM AMPLITUDE, cm: 0.6

Distance upstream of sluice gate(s), cm: 30

Water surface elevation, cm: 76.48 Elevation at top of bedform, cm: 82.65

Point	1	2	3	4	5	6	7	8
Elevation, cm	76.78	78.03	79.55	80.34	81.10	81.48	81.89	82.27
Velocity, cm/sec	39.6	39.2	37.6	35.8	33.0	31.6	29.4	23.9

Notes:

Distance upstream of sluice gate(s), cm: 120

Water surface elevation, cm: 76.37 Elevation at top of bedform, cm: 82.13

Point	1	2	3	4	5	6	7	8
Elevation, cm	76.80	77.82	79.24	79.97	80.69	81.04	81.42	81.78
Velocity, cm/sec	39.4	39.8	37.8	36.2	33.4	32.1	29.9	27.5

Notes:

Distance upstream of sluice gate(s), cm:

Water surface elevation, cm: Elevation at top of bedform, cm:

Point	1	2	3	4	5	6	7	8
Elevation, cm								
Velocity, cm/sec								

Notes:

Distance upstream of sluice gate(s), cm:

Water surface elevation, cm: Elevation at top of bedform, cm:

Point	1	2	3	4	5	6	7	8
Elevation, cm								
Velocity, cm/sec								

Notes:

DATE: 19 Jan 1988 RUN NUMBER: 15

DISCHARGE, l/sec: 3.0 SEDIMENT DISCHARGE, gr/min 300

GATE OPENING, cm: 7.24 NO. OF GATES OPEN: 1/1

WATER SURFACE SLOPE: .0019 BED SLOPE: .0018

WATER TEMPERATURE, °C: 3 BEDFORM AMPLITUDE, cm: 1.0

Distance upstream of sluice gate(s), cm: 15

Water surface elevation, cm: 78.83 Elevation at top of bedform, cm: 84.34

Point	1	2	3	4	5	6	7	8
Elevation, cm	79.11	80.18	81.60	82.29	82.97	83.30	83.66	83.99
Velocity, cm/sec	41.9	42.1	40.9	39.0	36.8	35.3	32.5	28.8

Notes:

Distance upstream of sluice gate(s), cm: 120

Water surface elevation, cm: 79.06 Elevation at top of bedform, cm: 83.89

Point	1	2	3	4	5	6	7	8
Elevation, cm	79.29	80.25	81.47	81.96	82.69	82.97	83.28	83.58
Velocity, cm/sec	42.4	43.0	41.9	39.6	36.3	35.9	34.8	31.2

Notes:

Distance upstream of sluice gate(s), cm: 300

Water surface elevation, cm: 78.20 Elevation at top of bedform, cm: 82.97

Point	1	2	3	4	5	6	7	8
Elevation, cm	78.43	79.39	80.58	81.19	81.73	82.08	82.39	82.64
Velocity, cm/sec	43.2	43.2	42.0	39.5	37.9	37.1	34.3	33.3

Notes:

Distance upstream of sluice gate(s), cm:

Water surface elevation, cm: Elevation at top of bedform, cm:

Point	1	2	3	4	5	6	7	8
Elevation, cm								
Velocity, cm/sec								

Notes:

DATE: 28 Jan 1988 RUN NUMBER: 16

DISCHARGE, l/sec: 3.0 SEDIMENT DISCHARGE, gr/min 300

GATE OPENING, cm: 1.67 NO. OF GATES OPEN: 1/1

WATER SURFACE SLOPE: .0018 BED SLOPE: .0021

WATER TEMPERATURE, °C: 3 BEDFORM AMPLITUDE, cm: 0.8

Distance upstream of sluice gate(s), cm: 45

Water surface elevation, cm: 64.77 Elevation at top of bedform, cm: 69.52

Point	1	2	3	4	5	6	7	8
Elevation, cm	65.00	65.97	67.16	67.25	68.33	68.63	68.94	69.22
Velocity, cm/sec	43.1	44.1	41.2	40.6	39.1	36.2	35.2	32.4

Notes:

Distance upstream of sluice gate(s), cm: 120

Water surface elevation, cm: 64.32 Elevation at top of bedform, cm: 69.40

Point	1	2	3	4	5	6	7	8
Elevation, cm	64.7	65.59	66.86	67.49	68.13	68.46	68.76	69.09
Velocity, cm/sec	43.9	43.6	43.6	41.2	38.3	36.4	34.3	31.5

Notes:

Distance upstream of sluice gate(s), cm: 300

Water surface elevation, cm: 64.01 Elevation at top of bedform, cm: 68.91

Point	1	2	3	4	5	6	7	8
Elevation, cm	64.32	65.23	66.45	67.09	67.70	68.00	68.30	68.61
Velocity, cm/sec	43.2	42.7	42.1	39.8	37.5	34.5	33.3	31.3

Notes:

Distance upstream of sluice gate(s), cm:

Water surface elevation, cm: Elevation at top of bedform, cm:

Point	1	2	3	4	5	6	7	8
Elevation, cm								
Velocity, cm/sec								

Notes:

DATE: 29 June 1988 RUN NUMBER: 17

DISCHARGE, l/sec: 3.0 SEDIMENT DISCHARGE, gr/min 150

GATE OPENING, cm: 5.60 NO. OF GATES OPEN: 1/3

WATER SURFACE SLOPE: .0017 BED SLOPE: .0017

WATER TEMPERATURE, °C: 25 BEDFORM AMPLITUDE, cm: 1.1

Distance upstream of sluice gate(s), cm: 30

Water surface elevation, cm: 77.43 Elevation at top of bedform, cm: 79.67

Point	1	2	3	4	5	6	7	8
Elevation, cm	77.76	77.99	78.55	78.83	79.11	79.24	79.39	79.54
Velocity, cm/sec	30.7	30.1	29.0	28.0	27.5	26.1	25.9	24.5

Notes:

Distance upstream of sluice gate(s), cm: 120

Water surface elevation, cm: 82.34 Elevation at top of bedform, cm: 77.54

Point	1	2	3	4	5	6	7	8
Elevation, cm	77.87	78.73	79.95	80.53	81.14	81.45	81.73	82.03
Velocity, cm/sec	34.8	34.3	33.4	31.8	31.8	28.8	27.6	27.1

Notes:

Distance upstream of sluice gate(s), cm:

Water surface elevation, cm: Elevation at top of bedform, cm:

Point	1	2	3	4	5	6	7	8
Elevation, cm								
Velocity, cm/sec								

Notes:

Distance upstream of sluice gate(s), cm:

Water surface elevation, cm: Elevation at top of bedform, cm:

Point	1	2	3	4	5	6	7	8
Elevation, cm								
Velocity, cm/sec								

Notes:

DATE: 27 June 1988 RUN NUMBER: 19

DISCHARGE, l/sec: 3.0 SEDIMENT DISCHARGE, gr/min 150

GATE OPENING, cm: 1.70 NO. OF GATES OPEN: 1/3

WATER SURFACE SLOPE: .0019 BED SLOPE: .0016

WATER TEMPERATURE, °C: 25 BEDFORM AMPLITUDE, cm: 0.6

Distance upstream of sluice gate(s), cm: 450

Water surface elevation, cm: 64.18 Elevation at top of bedform, cm: 69.97

Point	1	2	3	4	5	6	7	8
Elevation, cm	64.46	65.63	67.08	67.79	68.53	68.88	69.26	
Velocity, cm/sec	36.3	35.9	33.9	34.4	31.9	28.5	28.2	

Notes: 8th point was too close to the bed to sample

Distance upstream of sluice gate(s), cm: ______

Water surface elevation, cm: ______ Elevation at top of bedform, cm: ______

Point	1	2	3	4	5	6	7	8
Elevation, cm								
Velocity, cm/sec								

Notes: ______

Distance upstream of sluice gate(s), cm: ______

Water surface elevation, cm: ______ Elevation at top of bedform, cm: ______

Point	1	2	3	4	5	6	7	8
Elevation, cm								
Velocity, cm/sec								

Notes: ______

Distance upstream of sluice gate(s), cm: ______

Water surface elevation, cm: ______ Elevation at top of bedform, cm: ______

Point	1	2	3	4	5	6	7	8
Elevation, cm								
Velocity, cm/sec								

Notes: ______

CENTERLINE VELOCITY PROFILES

Q = 1.5 l/sec **Q_s = 150 gr/min**

h_g/h_N = 1.55 **lip = <12 cm from gate**

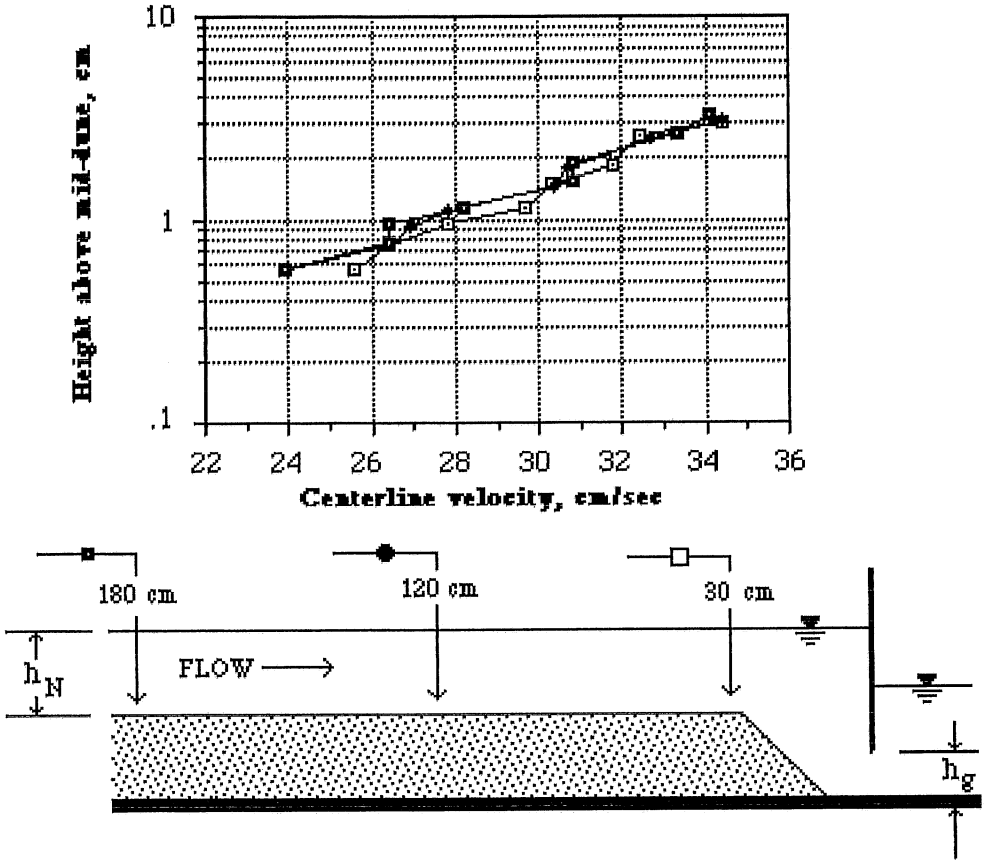

Figure A2.1 Centerline velocity profiles for Run 2

CENTERLINE VELOCITY PROFILES

Q = 1.5 l/sec **Q_s = 150 gr/min**

h_g/h_N = 0.2 **lip = 47.5 cm from gate**

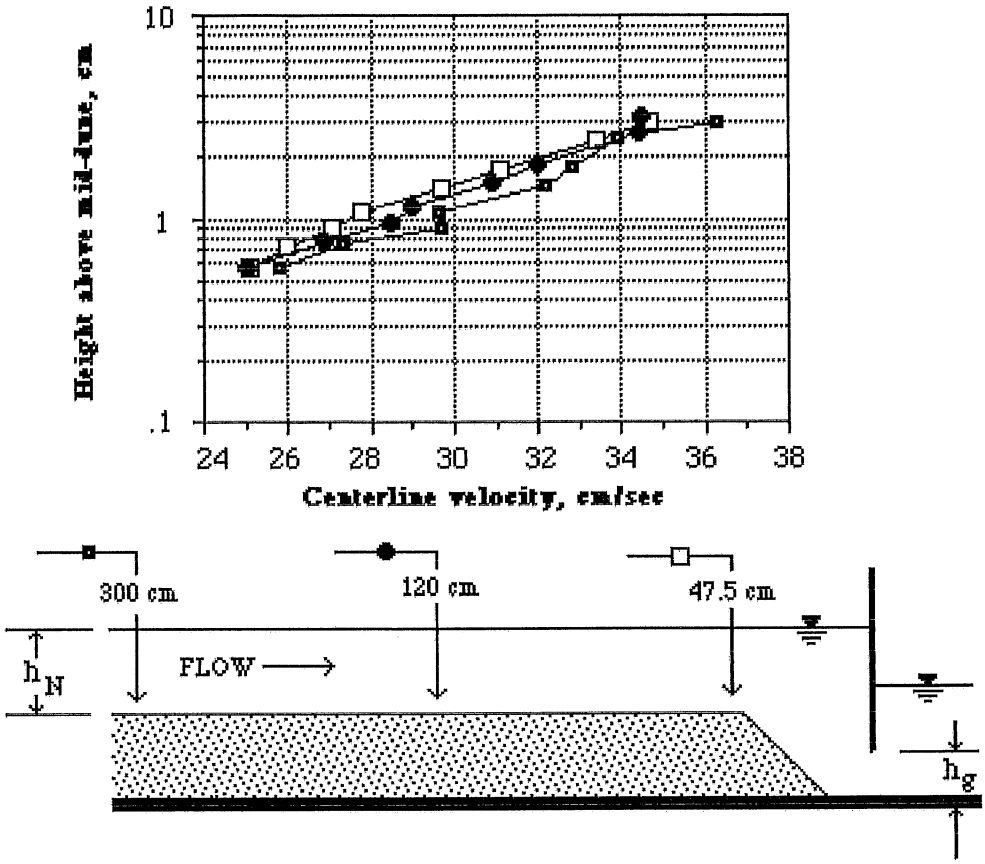

Figure A2.2 Centerline velocity profiles for Run 5

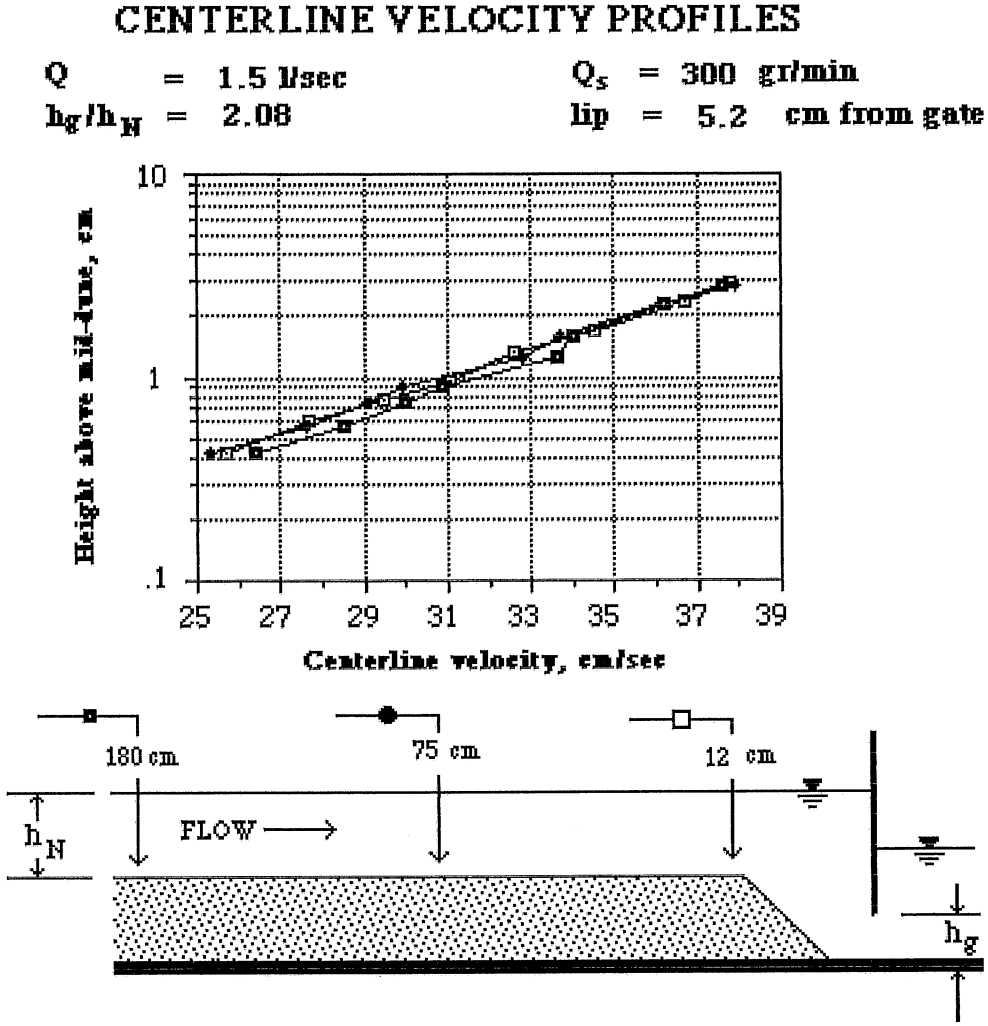

Figure A2.3 Centerline velocity profiles for Run 7

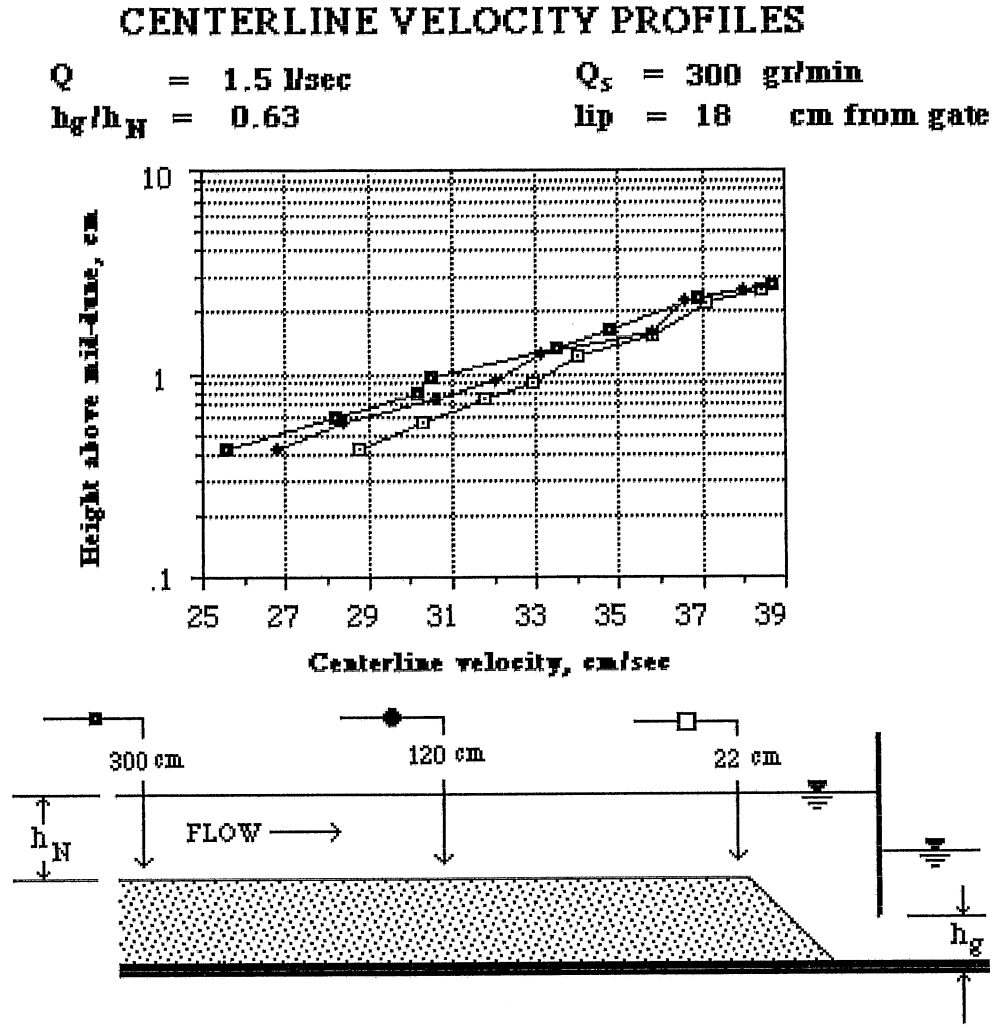

Figure A2.4 Centerline velocity profiles for Run 11

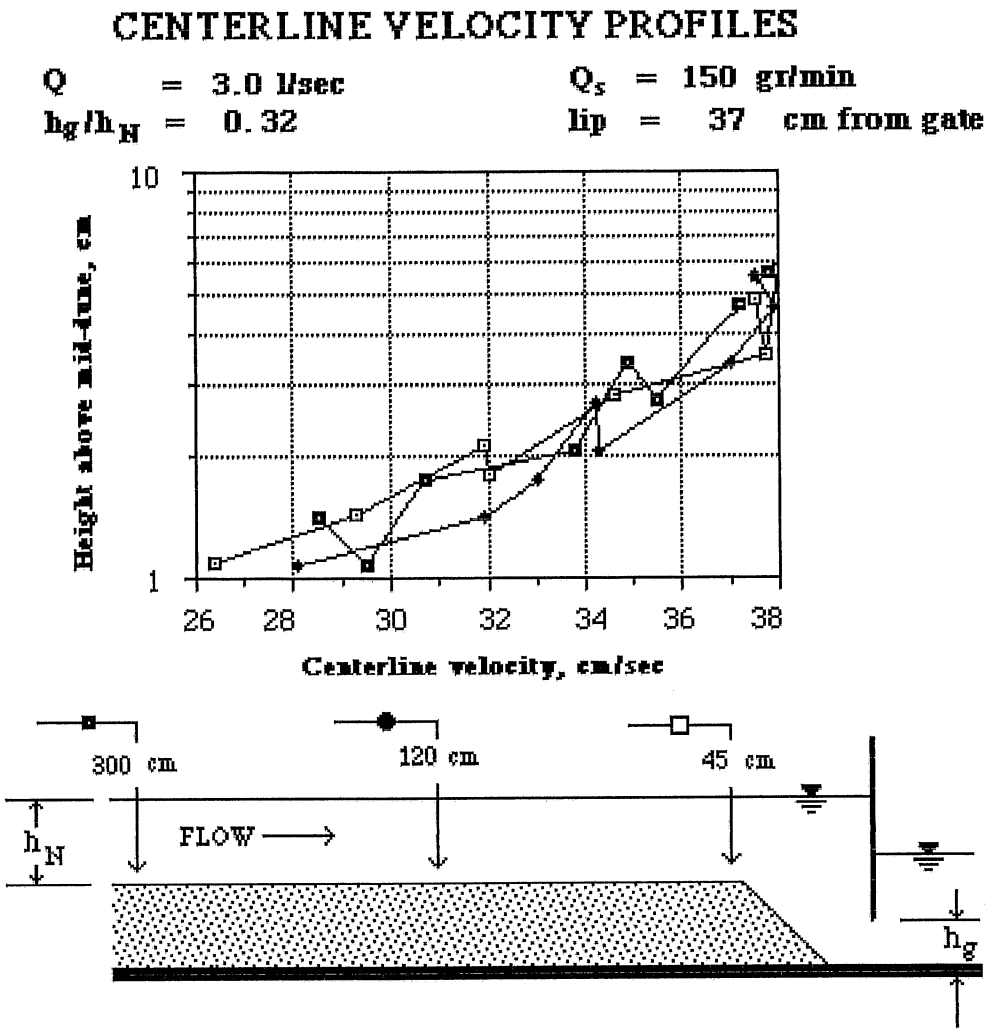

Figure A2.5 Centerline velocity profiles for Run 13

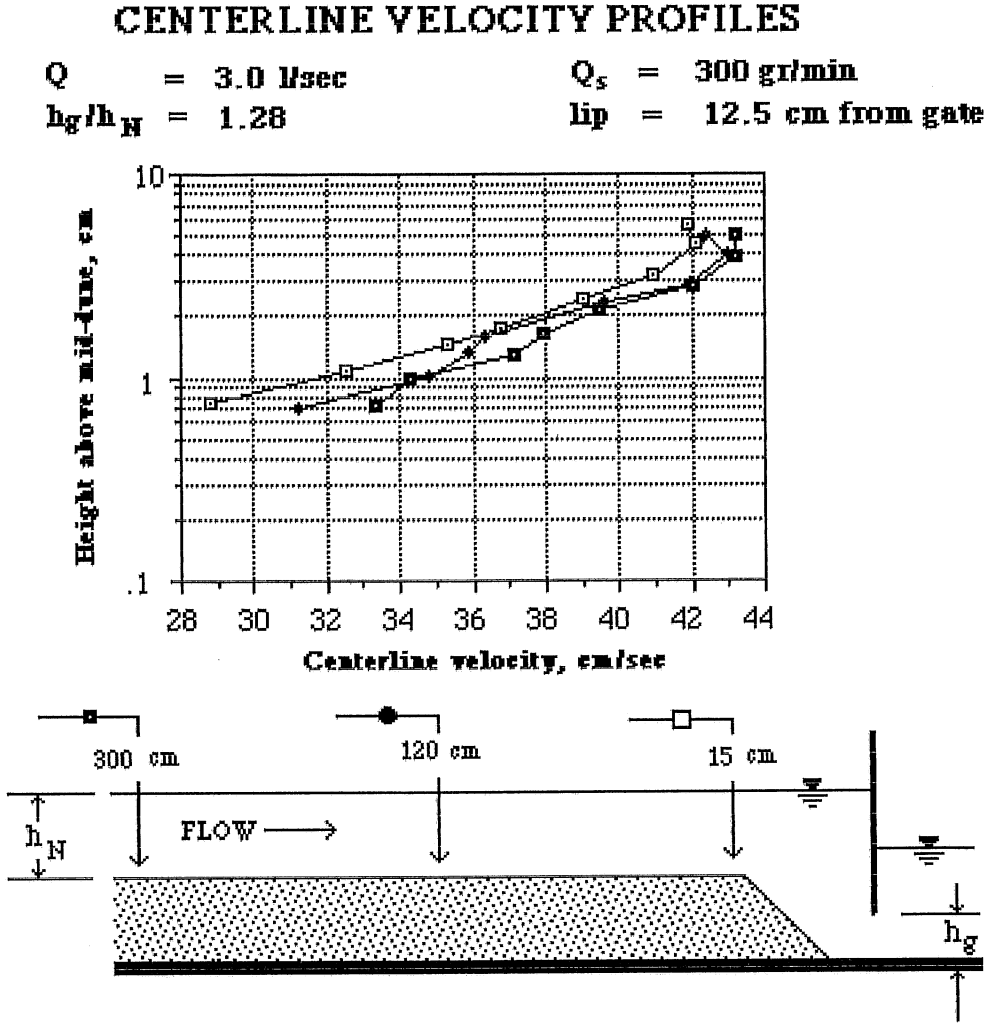

Figure A2.6 Centerline velocity profiles for Run 15

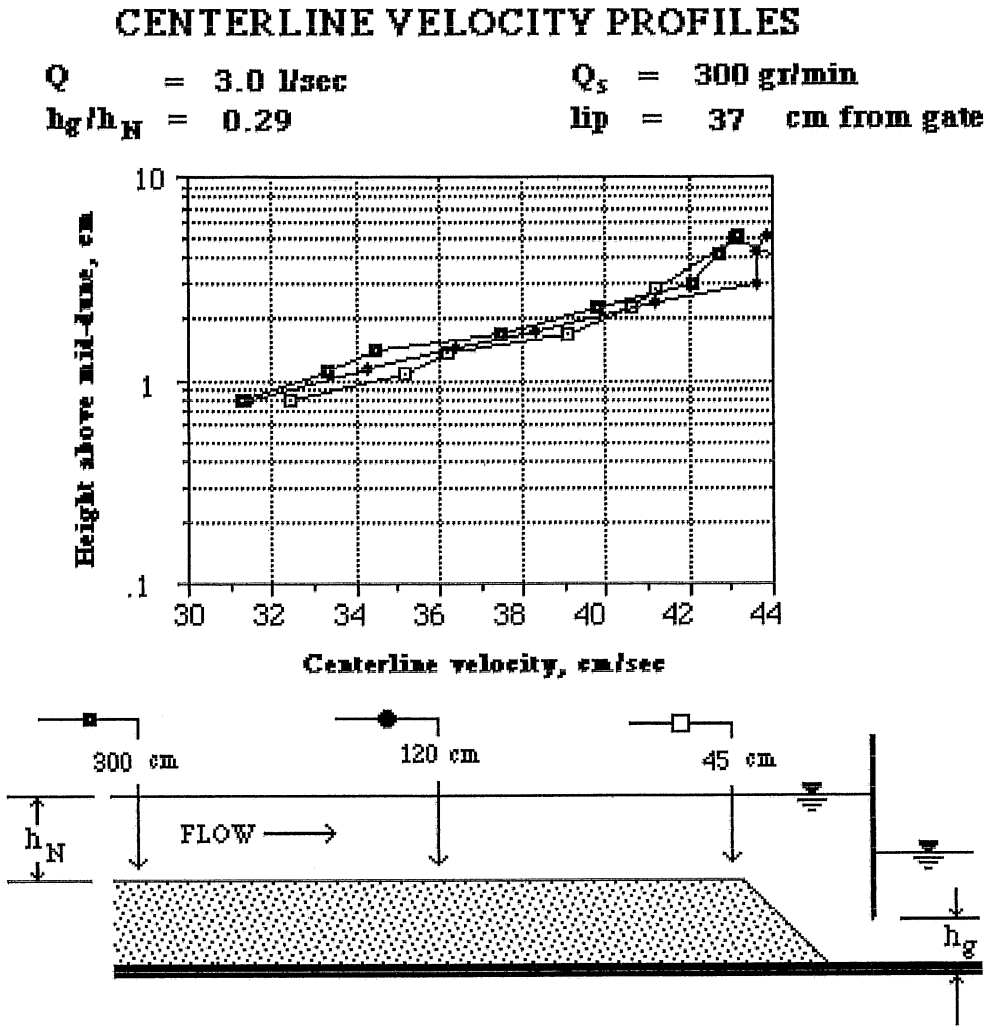

Figure A2.7 Centerline velocity profiles for Run 16

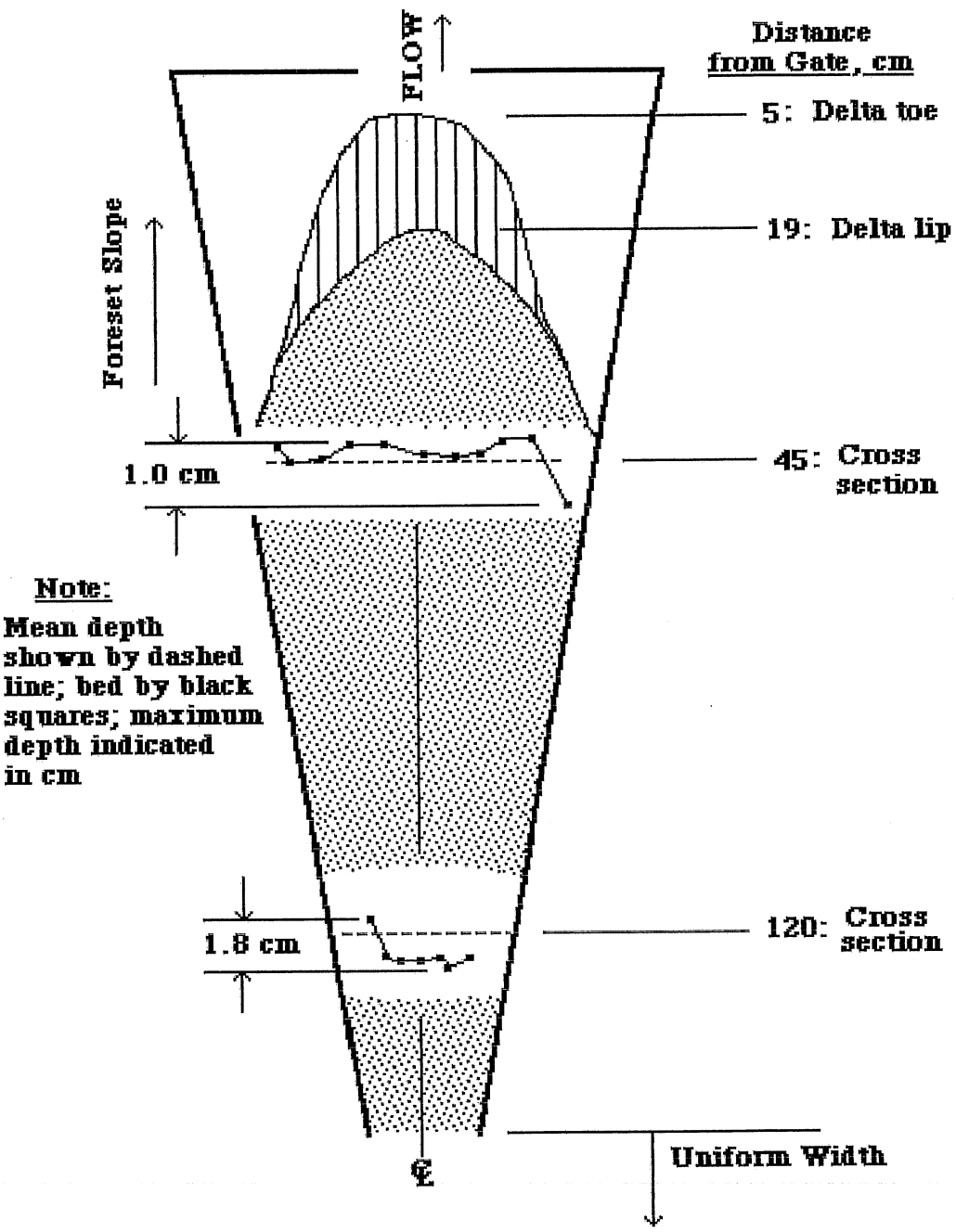

Figure A2.8 Plan view of expanding region upstream of dam for Run 17

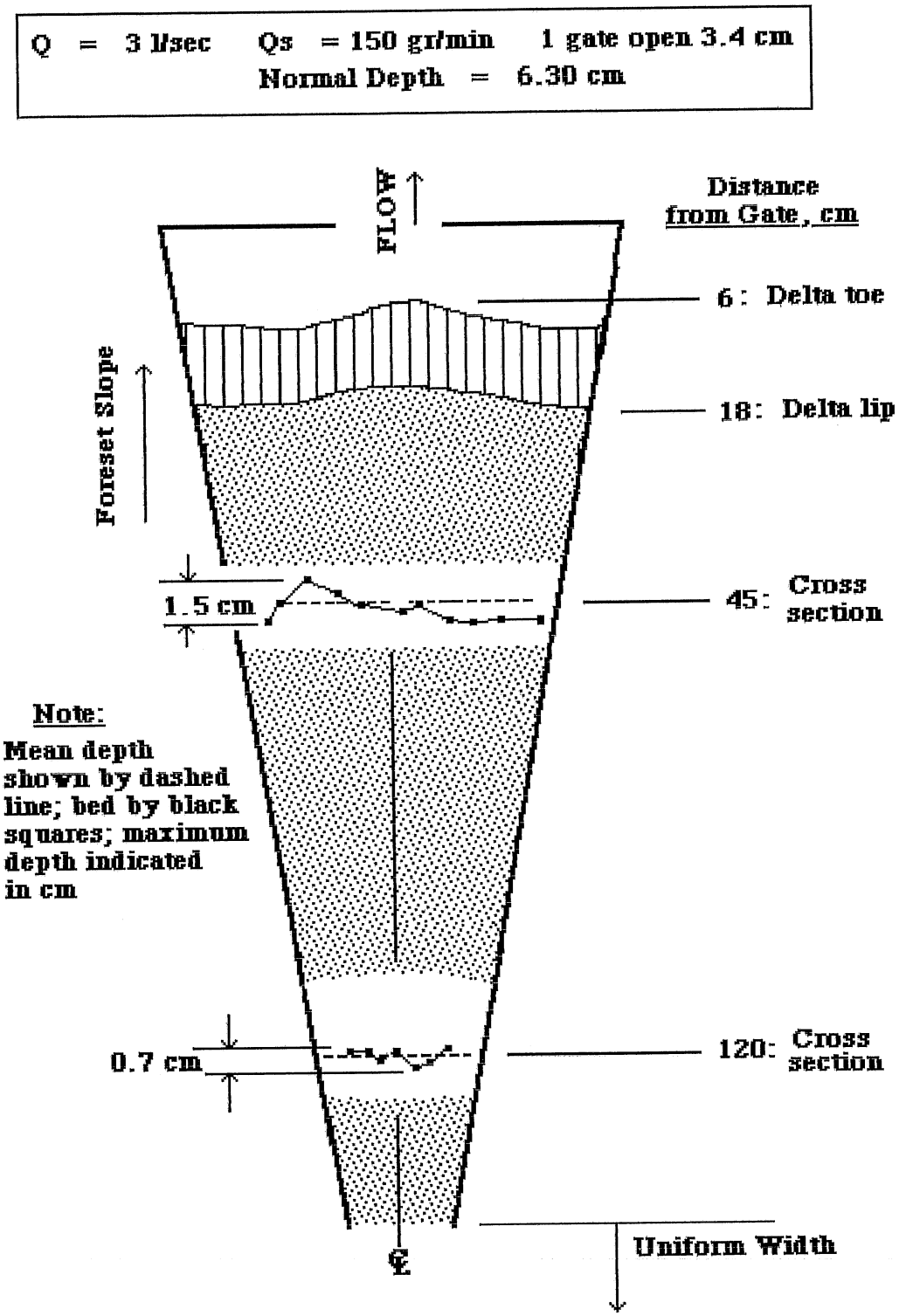

Figure A2.9 Plan view of expanding region upstream of dam for Run 18

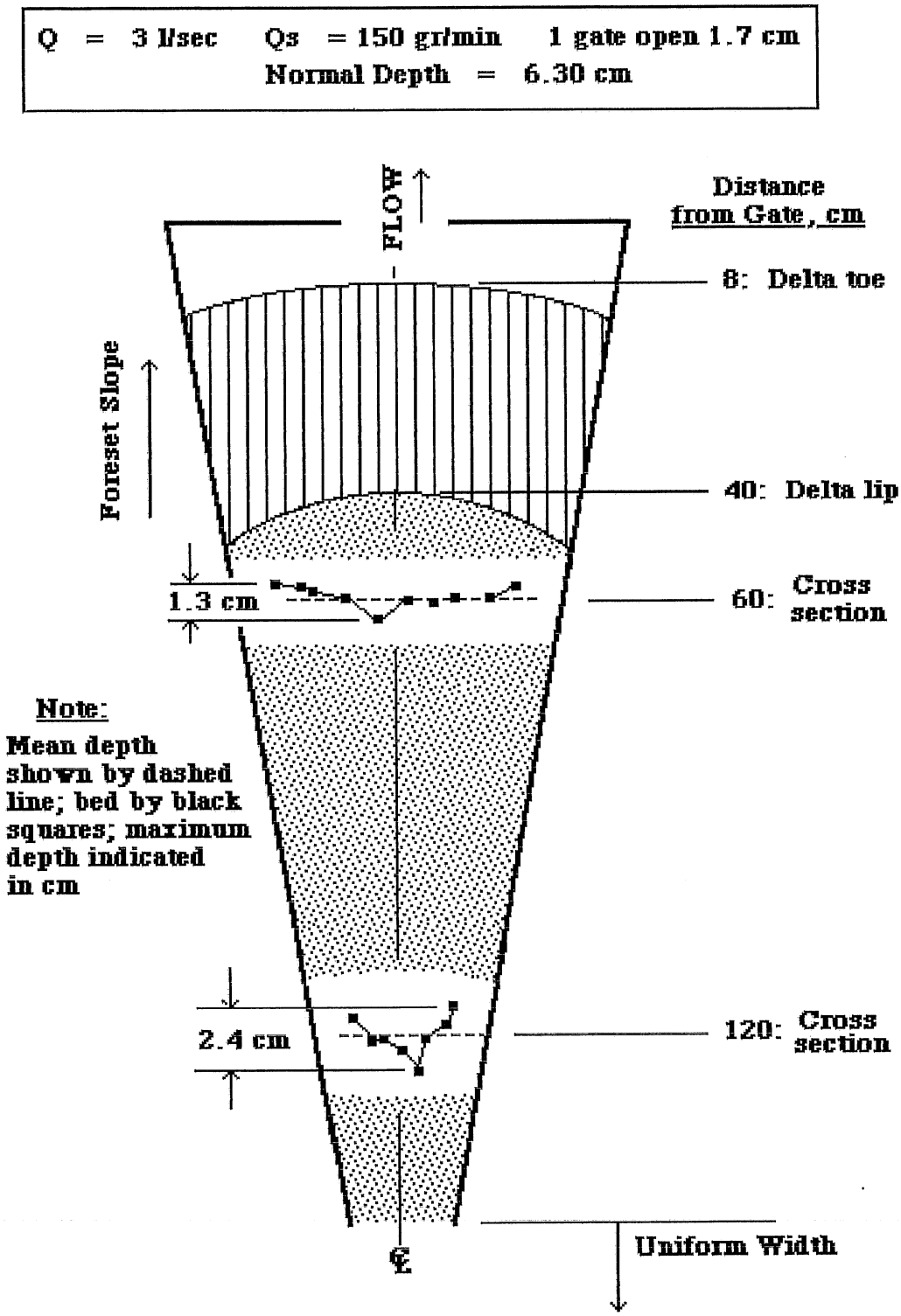

Figure A2.10 Plan view of expanding region upstream of dam for Run 19

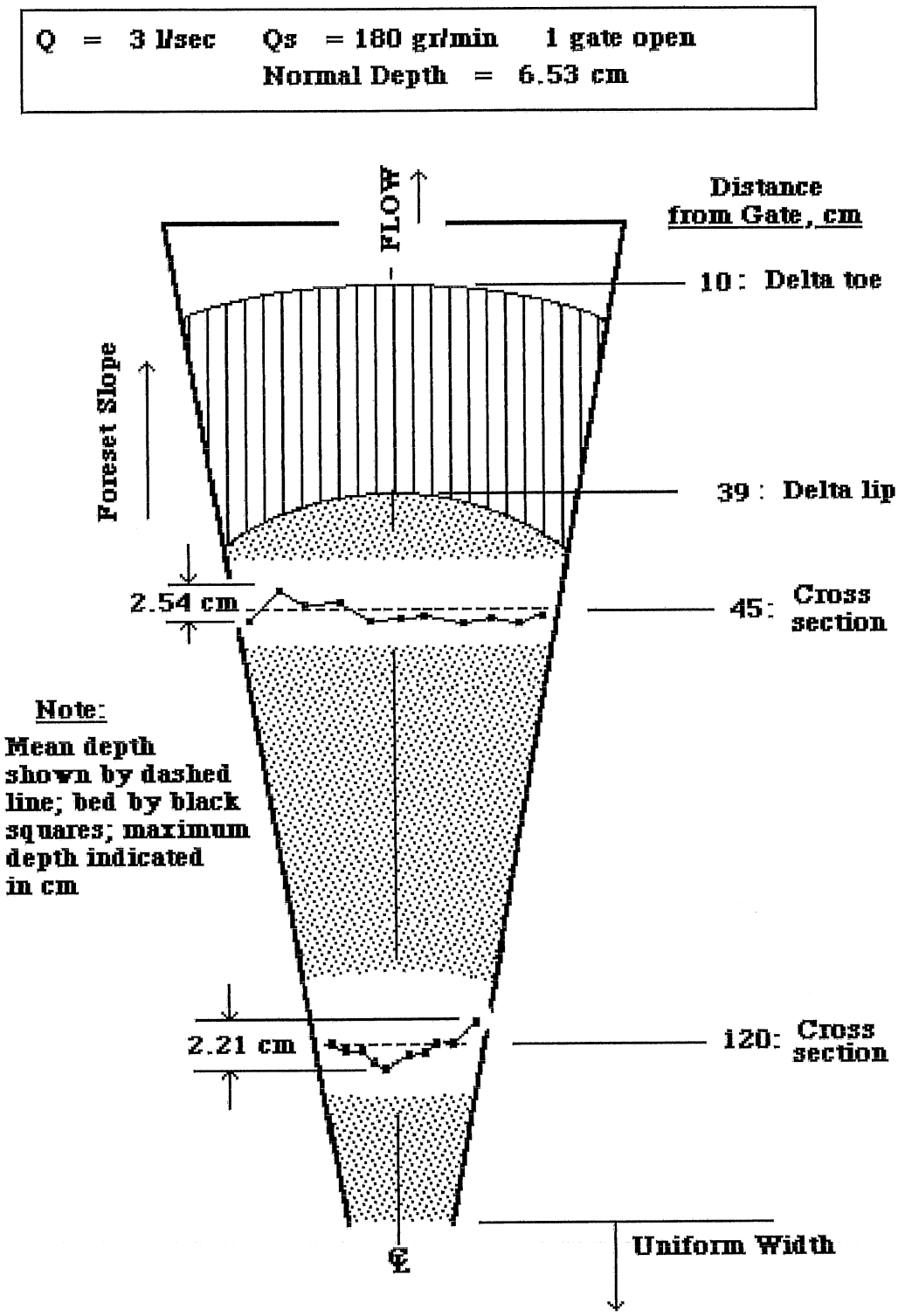

Figure A2.11 Plan view of expanding region upstream of dam for Run 28

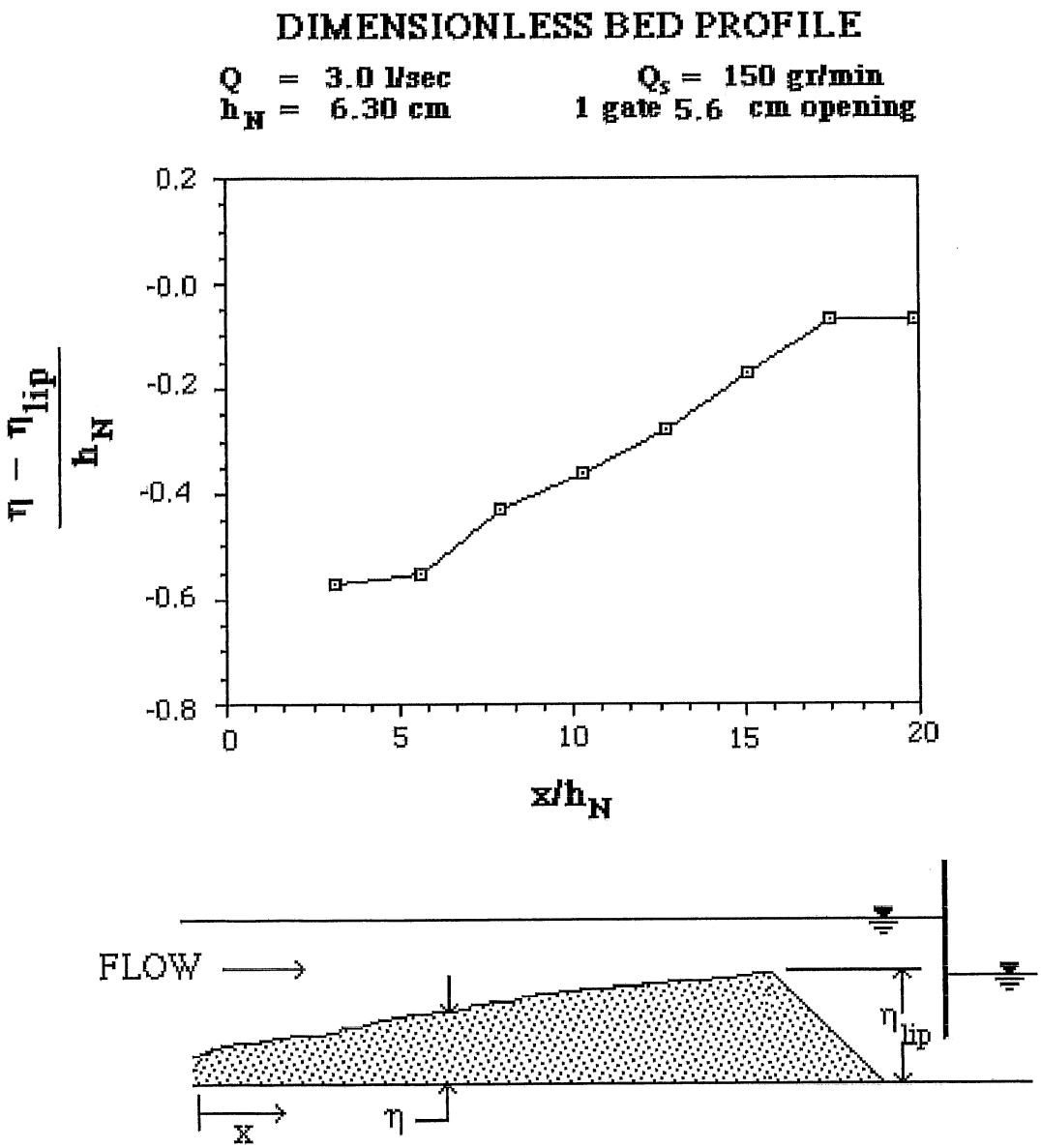

Figure A2.12 Dimensionless longitudinal bed profile in expanding region upstream of dam for Run 17

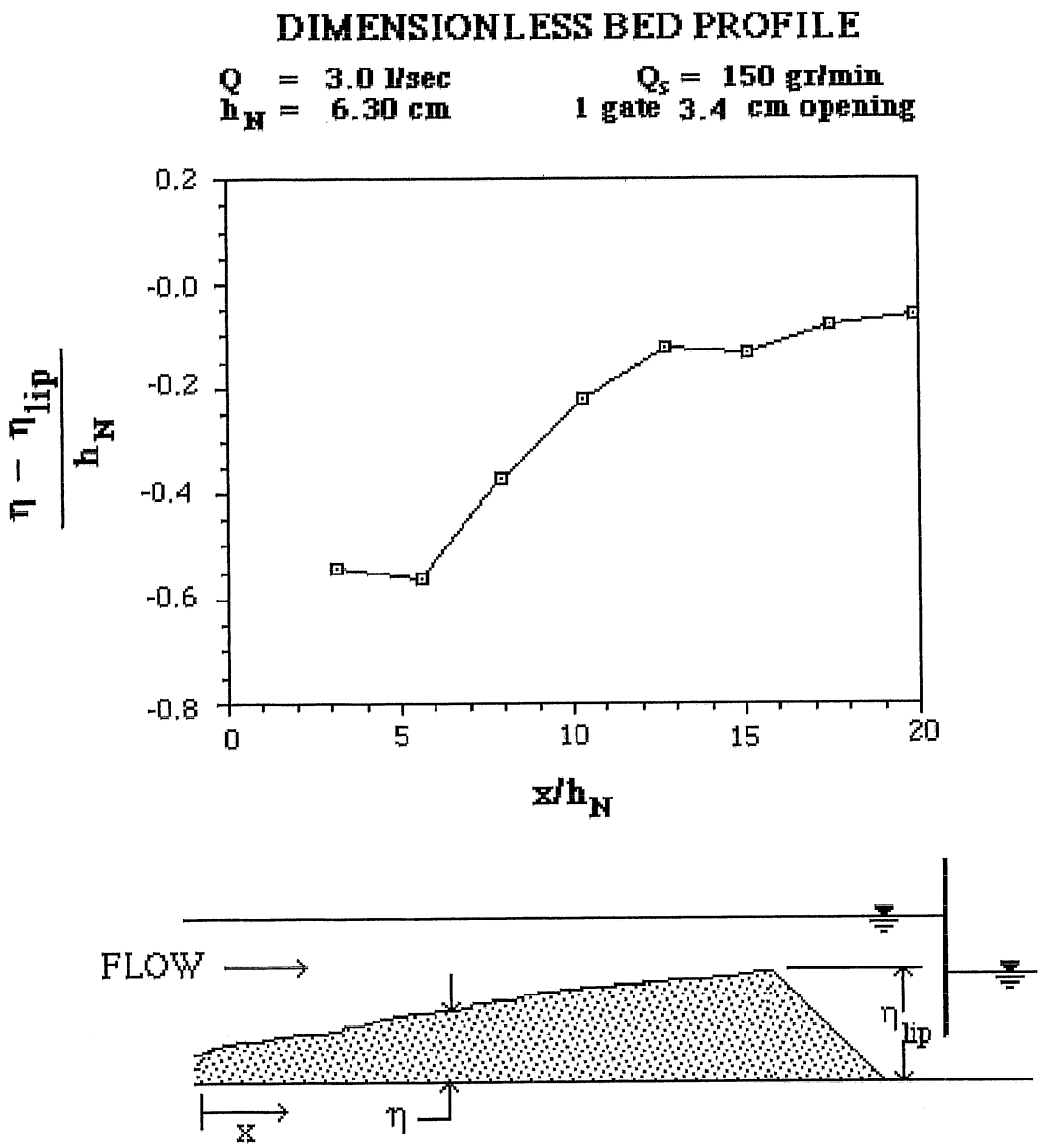

Figure A2.13 Dimensionless longitudinal bed profile in expanding region upstream of dam for Run 18

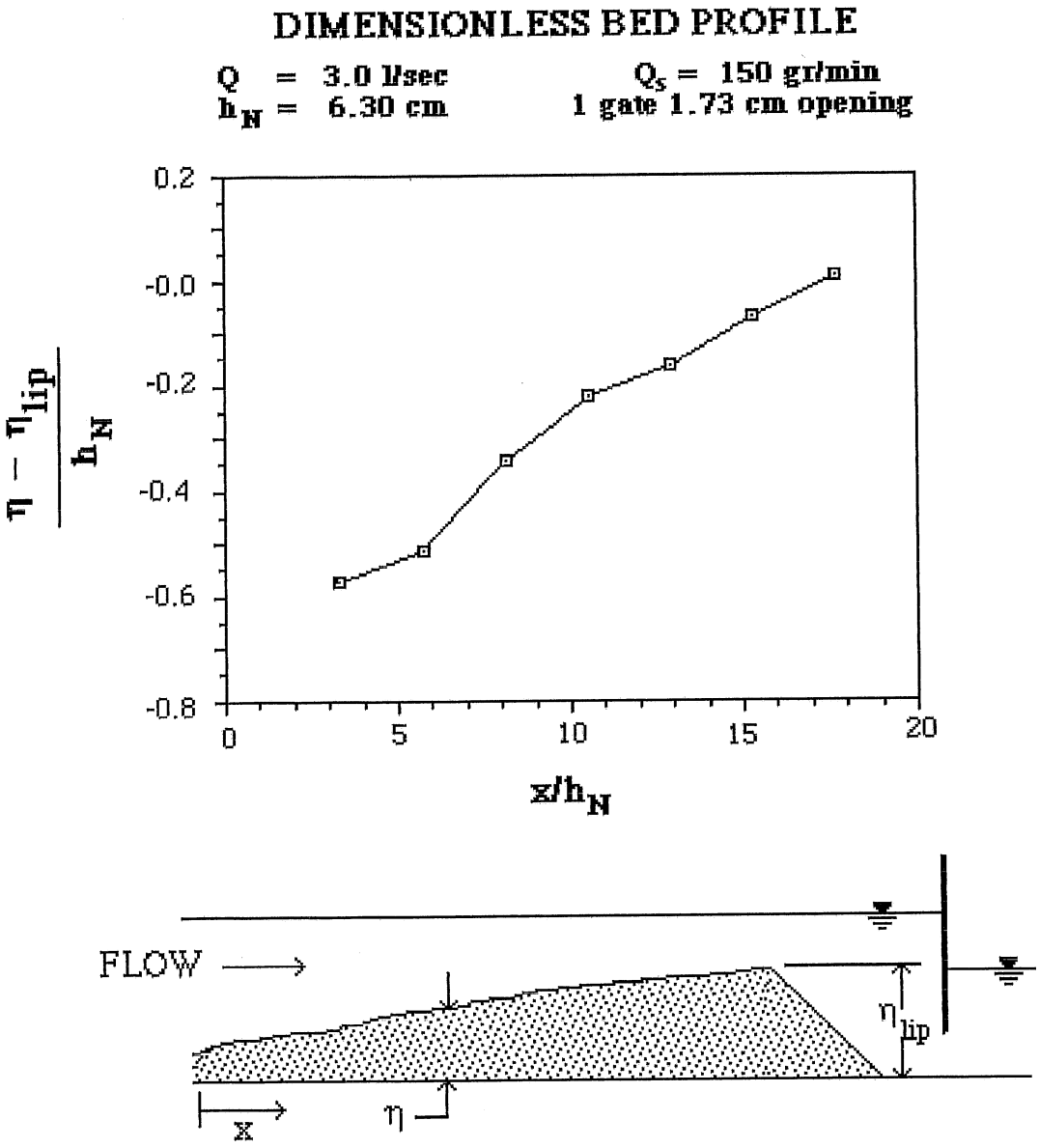

Figure A2.14 Dimensionless longitudinal bed profile in expanding region upstream of dam for Run 19

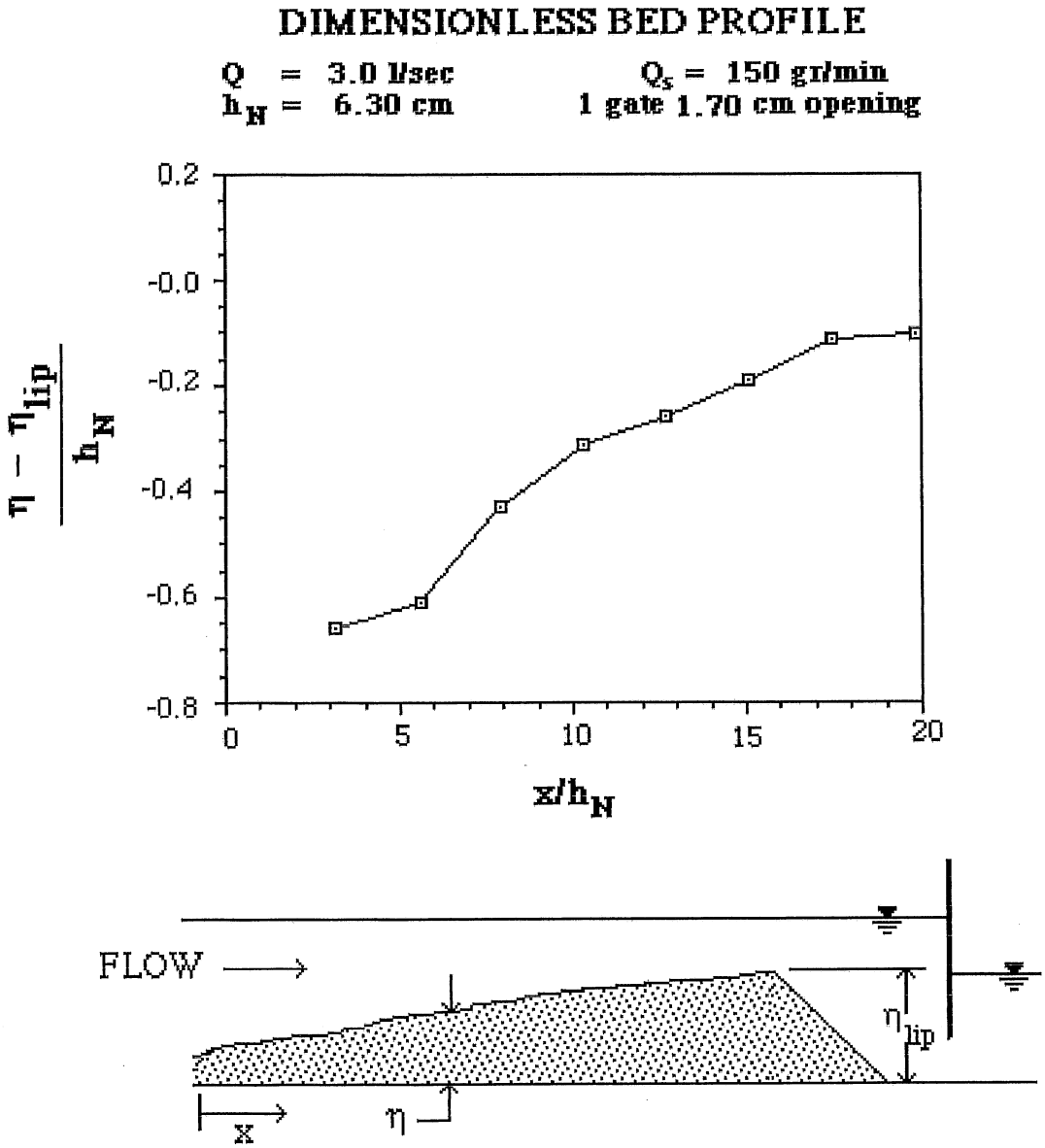

Figure A2.15 Dimensionless longitudinal bed profile in expanding region upstream of dam for Run 20

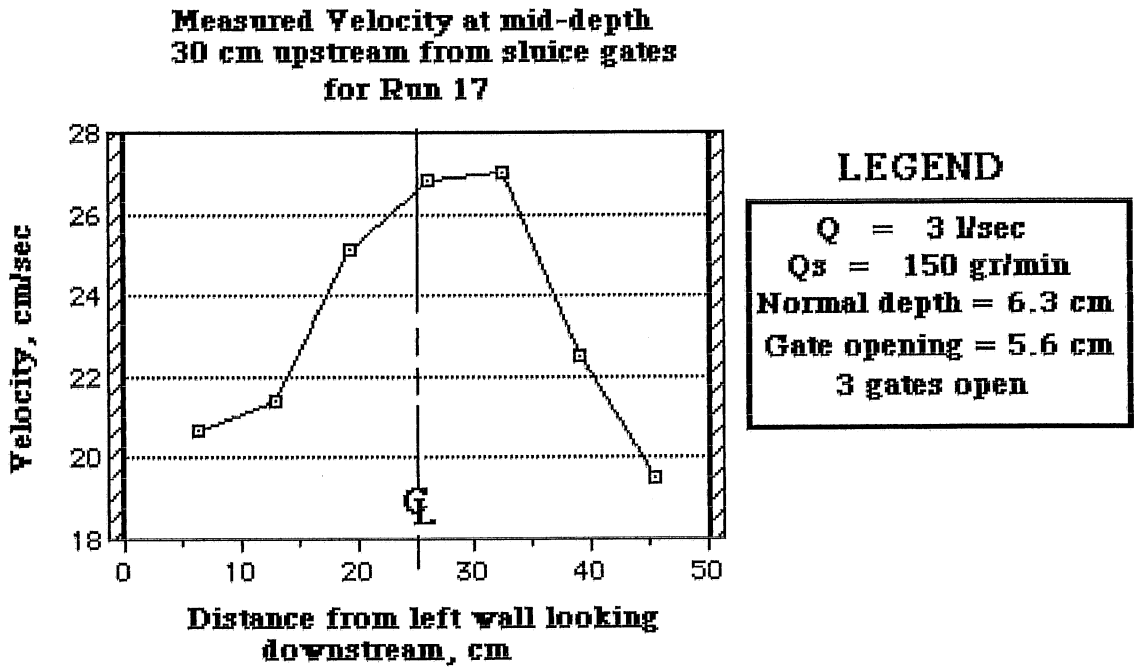

Figure A2.16 Mean velocity at one-half depth at a location 30 cm upstream from sluice gates in diverging flume for Run 17

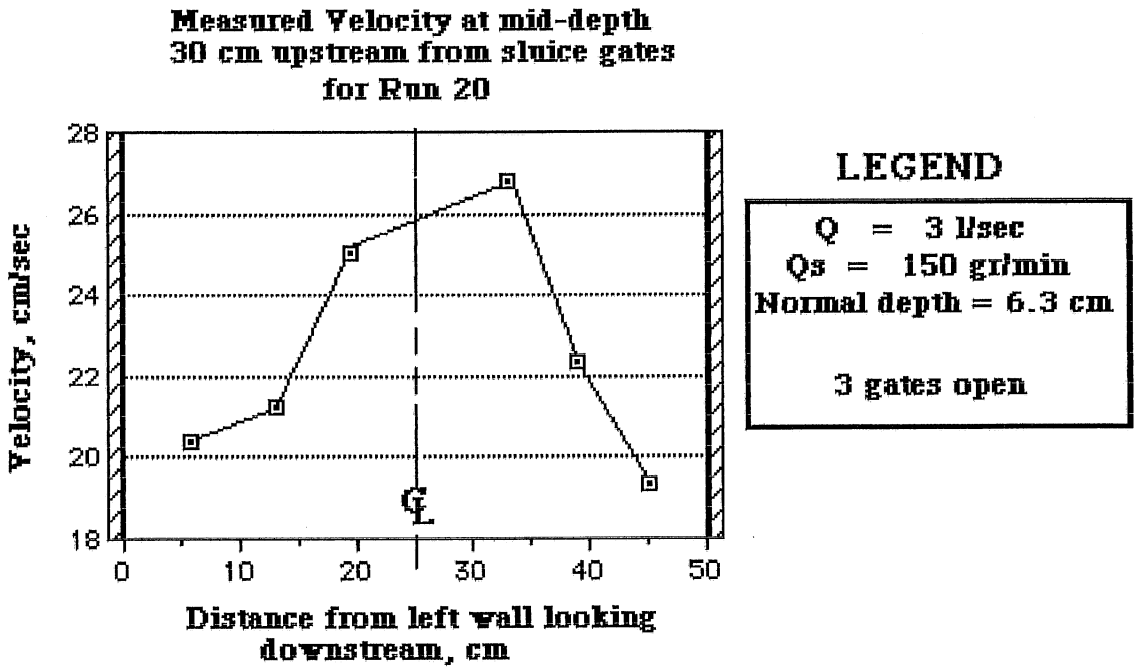

Figure A2.17 Mean velocity at one-half depth at a location 30 cm upstream from sluice gates in diverging flume for Run 20

APPENDIX 3 LISTING OF COMPUTER PROGRAM DELTA

Three Tables describe the program code DELTA. Table A3.1 is a listing of the program source code, written in Pascal-6000 for a CYBER 855 mainframe computer. Table A3.2 lists and describes the code procedures. Table A3.3 lists the name, type, location of appearance, and definition of each code variable.

Table A3.1 Listing of program code DELTA

```
PROGRAM DELTA(INPUT/,OUTPUT);

    (* 26 JUNE ADDED AUTOMATIC BW EXTENSION AND LENGTH      MULTIPLIER
    24 JUNE ADDED PARKER FIELD EQUATION WITH TAUSR = 0.03
    REVERSED HORIZONTAL AXIS
    8 JUNE CHANGED PARKER TO 0.04 AND 18
    6 JUNE WILL NOT ALLOW DEPTH < 1.01*CRITICAL
    2 JUNE ALWAYS GOES TO CORRECT, NOT JUST IF FLUME = TRUE
    2 JUNE ALLOWS FOR OPEN CHANNEL OR FLUME BEDFORM CORRECTION
    1 JUNE COMBINED SDELTA AND SDIF
    30 MAY MODIFIED ENABLING FLUME EXPERIMENTS
    17 MAY PGM FOR FINDING AND MOVING DELTA.  USING CALIBRATED
    SED. TRANSPORT EQUATION.
    MAY 15 PUT INITIAL STUFF INTO INITIALIZATION AND HEADER
    PROCEDURES
    MAY 9 INCLUDED CORRECTION FOR SIDEWALL AND BEDFORMS.
    MARCH 13 TOOK OUT TAU, X, Q ARRAYS.
    FEB 20 BW HAS N + 1 IN IT.  REMOVED REFERENECES TO READING
    FILES
    FEB 3 CHANGED XIEND TO REALLY BE WATER SURFACE, NOT DEPTH!
    FEB 1 INCORPORATED VARIABLE WIDTH AND TOOK OUT EXTENDNODES
    JAN 25 1989: INCREASED TAUMIN FROM 0.0747 TO 0.0748
    MODIFIED ON 24 JAN 1989
    NO EXTENSION OF BACKWATER CURVE
    TOOK OUT EVERYTHING ASSOCIATED WITH IT  *)

CONST
    G = 9.81;
TYPE
    VEC =  ARRAY[1..1000] OF REAL;

VAR
    DELTA,EXTENDRUN,FIRSTDELTA,FIRSTTIME,FLUME,INITIAL,
    NEARNORMAL,SHOCK,WARNING:  BOOLEAN;

    BEND,BLIP,B0,CBT,CDT,CGT,COEFF,CRITICAL,CWT,DETA,DT,DX,
    DXIEND,D50,ETALIP,ETALIPOLD,ETAOLD,ETATOE,FR2,HBEND,HIN,
    HLIP,I,INITIALDEPTH,H,KS,LOCDELTA,M,POR,QDOWN,QS,QSIN,
    QSLIMIT,QT,QUP,QW,R,SG,SINIT,TAUG,TAUMIN,TAUSR,TEMP,TIME,
    TOTIME,TOTX,TP,TPRINT,TSTART,UNODE,VISC,VSFILL,VSVOID,W,XB,
    XDAM,XIEND,XIENDF,XL:  REAL;

    B,ETA,H,TAU,X:  VEC;

    ANSWER,BWLM,DNODE,J,LIMIT,LMULT,MULT,N,NB:  INTEGER;

PROCEDURE LOADR;  (* SED. TRANSPORT PER MODIFIED PARKER *)

    VAR
```

```
        XX,XT: REAL;

    BEGIN
        XT:= TAUG/R/G/D50;
        IF XT <= TAUMIN THEN XX:= 0.0
        ELSE XX:= COEFF * XT * SQRT(XT) * EXP(4.5 * LN(1-0.853 *
            TAUSR/XT));
        QS:= XX * SQRT(R * G * D50) * D50  (* MAKE QS DIMENSIONAL *)
    END;

PROCEDURE RESULTS;

    VAR

        I: INTEGER;

    BEGIN
        WRITELN(J:8,',',TIME:10:5);
        WRITELN('TOTAL BW DISTANCE = ',DX*N/1000:10:4);
        IF WARNING = TRUE THEN
            BEGIN
                WARNING:= FALSE;
                WRITELN('****  WARNING:  BED SHEAR STRESS IN
            UPPER REGIME');
                WRITELN('          NOT PROPERLY ACCOUNTED FOR
                ****')
            END;
        FOR I:= 1 TO N + 1 DO
            BEGIN
                TAUG:= TAU[I];
                LOADR;
                WRITELN(XDAM + DX*(I-1):10:1,',',B[I]:10:4,',',
                ETA[I]:10:4,',',
                ETA[I] + H[I]:10:4,',',H[I]:10:4,',',QS*B[I]:10:7);
                IF DELTA = TRUE THEN
                IF I = LIMIT THEN
                    BEGIN
                        WRITELN(LOCDELTA:10:4,',',BLIP:10:4,',',
                            ETATOE:10:4,',',ETALIP + HLIP:10:4,',',
                            ETALIP-ETATOE+HLIP:10:4);
                        WRITELN(LOCDELTA +
                        0.001:10:4,',',BLIP:10:4,',',
                            ETALIP:10:4,',',ETALIP +
                        HLIP:10:4,',',HLIP:10:4)
                    END
        END
    END;

PROCEDURE SETBED;  (* COMPUTE BED ELEV & WIDTH FOR ALL NODES *)

    VAR

        I: INTEGER;
```

```
BEGIN
    IF FIRSTTIME = TRUE THEN
        BEGIN
            FOR I:= 1 TO NB DO
            B[I]:= B0 + (NB - I) * DX * M;
            FOR I:= NB TO N + 1 DO
                BEGIN
                    ETA[I]:= ETA[NB] + DX * SINIT * (I - NB);
                    B[I]:= B0
                END
        END
    ELSE
        BEGIN
            B[N+1]:= B0;
            ETA[N+1]:= ETA[N] + DX * SINIT
        END
END;


PROCEDURE CORRECT (VAR XQ,XH,XW,XXS,XXH:  REAL);
        (*  CORRECT FOR SIDEWALL AND BEDFORM EFFECTS  *)

    VAR

        CB,CBUSTAR,CD,CF,CG,CGINV,CGUSTAR,CW,ER,FC,
        FCG,FCW,FDELTA,FRE,H,HN,HTT,HYRADIUS,P,RE,U:  REAL;

        ALLTRUE,CBK,CGK,CTEST,CWK,HK,K:  INTEGER;
        CONV,BOMB:  BOOLEAN;

    PROCEDURE DEPTH;  (*  FIND NORMAL DEPTH *)

        VAR

            KK:  INTEGER;
            CCONV,BBOMB:  BOOLEAN;
        BEGIN
            KK:= 1;
            CCONV:= FALSE;
            BBOMB:= FALSE;
            REPEAT
                HN:= HTT - (HTT*(G*SINIT*B0*HTT*HTT - 2*XQ*XQ*CW)
                    - XQ*XQ*B0*CB)
                    /(3*G*SINIT*B0*HTT*HTT - 2*XQ*XQ*CW);
                ER:= ABS(2*(HN - HTT)/(HN + HTT));
                IF ER < 0.001 THEN CCONV:= TRUE
                ELSE IF KK > 50 THEN
                    BEGIN
                        BBOMB:= TRUE;
                        WRITELN('BOMBED IN INITIAL DEPTH')
                    END
                ELSE
                    BEGIN
                        KK:= KK + 1;
```

```
                        HTT:= HN
                    END
            UNTIL CCONV OR BBOMB
    END;

PROCEDURE FREYNOLDS;  (* FIND F FOR SMOOTH WALL  *)
    BEGIN
        FRE:=  1.0/SQR(0.78*LN(RE*FCW/6.9))
    END;

PROCEDURE FD;  (*  FIND X IN EINSTEIN-BARBAROSSA EQUATION  *)

    VAR

        D50DEL: REAL;

    BEGIN
        D50DEL:= D50*SQRT(CGT)*U/11.6/VISC;
        IF D50DEL < 0.265 THEN FDELTA:= 0;
        IF D50DEL >= 0.265 THEN FDELTA:= 1.9 + 0.7383*LN(D50DEL);
        IF D50DEL >= 0.5 THEN FDELTA:= 1.615 - 0.407 *
            EXP(1.6*LN(ABS(LN(D50DEL))));
        IF D50DEL >= 2.35 THEN
        IF D50DEL >= 10.0 THEN FDELTA:= 1.0
        ELSE FDELTA:= 1.0 + 0.926 *
        EXP(2.43*LN(1.0- 0.434*LN(D50DEL)))
    END;

BEGIN
    HK:= 0;
    CBK:= 0;
    CGK:= 0;
    CWK:= 0;
    CONV:= FALSE;
    BOMB:= FALSE;
    IF INITIAL = TRUE THEN ALLTRUE:= 4
    ELSE ALLTRUE:= 3;
    U:= XQ/XH;
    IF FLUME = TRUE THEN P:= XW + 2*XH
    ELSE P:= XW;
    HYRADIUS:= XH*XW/P;
    RE:= 4*U*HYRADIUS/VISC;
    K:= 0;
    REPEAT
        K:= K + 1;
        IF FLUME = TRUE THEN
            BEGIN
                FC:= (2*XH*CWT + XW*CBT)/P;
                FCW:= CWT/FC;
                FREYNOLDS;
                CW:= FRE/8;
                FCG:= CGT/FC;
                FD;
                ER:= ABS((CW - CWT)/CW);
```

```
            IF ER <= 0.005 THEN CWK:= 1
        END
ELSE
        BEGIN
            CWK:= 1;
            CW:= 0;
            FCG:= CGT/CBT
        END;
IF FDELTA = 0 THEN
CGINV:=
SQR(2.5*LN(3.67*HYRADIUS*FCG*U*SQRT(CGT)/VISC))
ELSE IF FLUME = TRUE THEN
CGINV:= SQR(2.5*LN(12.3*HYRADIUS*FCG*FDELTA/D50))
ELSE CGINV:= SQR(2.5*LN(11*HYRADIUS*FCG/2.5/D50));
CG:= 1/CGINV;
CGUSTAR:= CG*U*U/R/G/D50;
IF FLUME = TRUE THEN
        BEGIN
            IF CGUSTAR < 0.0626 THEN CBUSTAR:= CGUSTAR;
            IF CGUSTAR >= 0.0626 THEN CBUSTAR:=
            EXP(0.412*LN((CGUSTAR - 0.06)/2.14));
            IF CGUSTAR >= 0.541 THEN CBUSTAR:= CGUSTAR
        END
ELSE
        BEGIN
            IF CGUSTAR < 0.0615 THEN CBUSTAR:= CGUSTAR;
            IF CGUSTAR >= 0.0615 THEN CBUSTAR:=
            1.581*SQRT(CGUSTAR - 0.06);
            IF CGUSTAR >= 2.435 THEN CBUSTAR:= CGUSTAR
        END;
CB:= CBUSTAR*R*G*D50/U/U;
CD:= CB - CG;
ER:= ABS((CB - CBT)/CB);
IF ER <= 0.005 THEN CBK:= 1;
ER:= ABS((CG - CGT)/CG);
IF ER <= 0.005 THEN CGK:= 1;
CTEST:= CWK + CBK + CGK;
IF INITIAL = TRUE THEN
        BEGIN
            HTT:= XH;
            DEPTH;
            ER:= ABS((HN - XH)/HN);
            IF ER <= 0.005 THEN HK:= 1;
            CTEST:= CTEST + HK;
            XH:= HN;
            U:= XQ/XH;
            IF FLUME = TRUE THEN P:= 2*XH + B0
            ELSE P:= B0;
            HYRADIUS:= B0*XH/P;
            RE:= 4*U*HYRADIUS/VISC;
            HK:= 0
        END;
IF CTEST = ALLTRUE THEN CONV:= TRUE
ELSE IF K > 50 THEN
```

```
                    BEGIN
                        BOMB:= TRUE;
                        WRITELN('BOMB IN CCT XW,XQ ',XW:10:4,XQ:10:4);
                        WRITELN('XH,CG,CW,CB=
                            ',XH:10:4,CG:10:4,CW:10:4,CB:10:4);
                        WRITELN('CGK,CWK,CBK,HK=
                                ',CGK,CWK,CBK,HK)
                    END
                ELSE
                    BEGIN
                        CGT:= CG;
                        CBT:= CB;
                        CWT:= CW;
                        CDT:= CD
                    END
            UNTIL CONV OR BOMB;
            XXH:= XH;
            IF FLUME = TRUE THEN P:= 2*XXH + XW
            ELSE P:= XW;
            HYRADIUS:= XXH*XW/P;
            CF:= (CW*2*XXH + CB*XW)/P;
            XXS:= CF*U*U/G/HYRADIUS;
            TAUG:= CG*U*U;
            IF CGUSTAR >= 0.541 THEN WARNING:= TRUE
        END;

PROCEDURE SLOPHEAD (VAR XQ,XW,XH,XETA,XS,XTH:  REAL);
            (*  FIND FR,SF, AND TOTAL H  *)

        VAR

            XDUMMY:  REAL;

        BEGIN
            XTH:= SQR(XQ)/2/G/SQR(XH) + XETA + XH;
            FR2:= SQR(XQ)/G/SQR(XH)/XH;
            CORRECT(XQ,XH,XW,XS,XDUMMY)
        END;

PROCEDURE BACKWATER;  (*  COMPUTE BACKWATER PROFILE  *)

        VAR

            CRIT,DXX,ETC,HN,HT,SD,SU,THD,THU:   REAL;
            I,IB:  INTEGER;

        PROCEDURE CALCH;  (*  FIND DEPTH AT NEXT U.S. NODE  *)

            VAR

                CONV,BOMB:  BOOLEAN;

                ER:  REAL;
```

```
        K: INTEGER;

    BEGIN
        CONV:= FALSE;
        BOMB:= FALSE;
        K:= 1;
        REPEAT
            SLOPHEAD(QW,W,HT,ETC,SU,THU);
            HN:= HT - (THU - THD - DXX/2 * (SU + SD))/
            (1 - FR2 + 3/2 * DXX * SU/HT);
            IF HN <= CRIT THEN
                BEGIN
                    HN:= 1.01 * CRIT;
                    SLOPHEAD(QW,W,HN,ETC,SU,THU);
                    CONV:= TRUE
                END;
            ER:= ABS(2 * (HN - HT)/(HN + HT));
            IF ER < 0.001 THEN CONV:= TRUE
            ELSE IF K > 50 THEN
                BEGIN
                    BOMB:= TRUE;
                    WRITELN('BOMBED IB = ',IB)
                END
            ELSE
                BEGIN
                    K:= K + 1;
                    HT:= HN
                END
        UNTIL CONV OR BOMB
    END;

PROCEDURE EXTENDBW; (*  EXTEND BACKWATER ZONE U.S. 1 NODE
*)

    VAR

        I,IB:  INTEGER;

    BEGIN
        QW:= QT/B0;
        SLOPHEAD(QW,B0,H[N],ETA[N],SD,THD);
        HT:= H[N];
        ETC:= ETA[N+1];
        W:= B0;
        DXX:= DX;
        CRIT:= EXP(1/3 * LN(QW*QW/G));
        IF HT < CRIT THEN HT:= 1.01 * CRIT;
        CALCH;
        H[N+1]:= HN;
        TAU[N+1]:= TAUG
    END;

BEGIN
    IF FIRSTTIME = FALSE THEN EXTENDBW
```

```
ELSE
    BEGIN
        DXX:= DX;
        QW:= QT/B[LIMIT];
        IF LIMIT = 1 THEN
        IF ((DXIEND < 0) AND (DETA < 0)) THEN
            BEGIN
                XIEND:= XIEND + DETA;
                IF XIEND < XIENDF THEN XIEND:= XIENDF
            END;
        H[1]:= XIEND - ETA[1];
        IF H[1] < CRITICAL THEN
            BEGIN
                H[1]:= 1.01 * CRITICAL;
                ETA[1]:= XIEND - H[1]
            END;
        SLOPHEAD(QW,B[LIMIT],H[LIMIT],ETA[LIMIT],SD,THD);
        TAU[LIMIT]:= TAUG;
        HT:= H[LIMIT];
        IF ((DXIEND > 0) AND (DELTA = TRUE)) THEN
            BEGIN
                QW:= QT/BLIP;
                ETC:= ETALIP;
                W:= BLIP;
                DXX:= LOCDELTA - XDAM - DX*(LIMIT-1);
                CRIT:= EXP(1/3 * LN(QW*QW/G));
                IF HT < CRIT THEN HT:= 1.01 * CRIT;
                CALCH;
                HLIP:= HN;
                HT:= HLIP;
                DXX:= DX*LIMIT - (LOCDELTA - XDAM);
                SD:= SU;
                THD:= THU
            END;
        FOR I:= LIMIT + 1 TO N + 1  DO
            BEGIN
                QW:= QT/B[I];
                ETC:= ETA[I];
                CRIT:= EXP(1/3 * LN(QW*QW/G));
                IF HT < CRIT THEN HT:= 1.01 * CRIT;
                W:= B[I];
                CALCH;
                H[I]:= HN;
                TAU[I]:= TAUG;
                HT:= HN;
                DXX:= DX;
                SD:= SU;
                THD:= THU
            END
        END
    END;

PROCEDURE INPUTDATA;    (* INPUT DATA TO PROGRAM *)
```

```
VAR

      I: INTEGER;    (* COUNTER *)

BEGIN
      WRITELN('IS THIS FOR A FLUME 1 = YES, 2 = NO');
      READLN;
      READ(ANSWER);
      IF ANSWER = 1 THEN FLUME:= TRUE
      ELSE FLUME:= FALSE;
      WRITELN('DO YOU WANT A SHOCK FIT TO THE DELTA?  1 = YES, 2
      =      NO');
      READLN;
      READ(ANSWER);
      IF ANSWER = 1 THEN SHOCK:= TRUE
      ELSE SHOCK:= FALSE;
      WRITELN('INPUT MULT FACTOR');
      READLN;
      READ(MULT);
      WRITELN('INPUT LENGTH MULTIPLIER');
      READLN;
      READ(LMULT);
      WRITELN('INPUT BW LENGTH MULTIPLIER');
      READLN;
      READ(BWLM);
      WRITELN('INPUT QT IN M3/S, D50 IN MM, INIT SLOPE,
      ROUGHNESS IN M');
      READLN;
      READ(QT,D50,SINIT,KS);
      WRITELN('INPUT SPECIFIC GRAVITY, POROSITY,WATER TEMP
      DEG. C.');
      READLN;
      READ(SG,POR,TEMP);
      WRITELN('INPUT DX IN M, DT IN SEC, TOTAL TIME IN SEC,
TSTART');
      READLN;
      READ(DX,DT,TOTTIME,TSTART);
      WRITELN('INPUT TPRINT, TO PRINT EVERY TPRINT SECONDS');
       READLN;
      READ(TPRINT);
      WRITELN('INPUT INITIAL NUMBER OF INCREMENTS');
      READLN;
      READ(N);
      WRITELN('INPUT DISTANCE AT DAM, M');
      READLN;
      READ(XDAM);
      WRITELN('INPUT UN. WIDTH, CHANGE FACTOR, BREAK PT DIST,
      M');
      READLN;  (* IF UN. WIDTH, CH.FCTR = 0 AND BK PT DIST = TOT
      LENGTH *)
      READ(B0,M,XB);
      NB:= ROUND((XB - XDAM)/DX + 1);
      WRITELN('INPUT WATER SURFACE CHANGE, M:  + FOR UP, - FOR
      DOWN');
```

```
READLN;
READ(DXIEND);
IF M <> 0 THEN
      BEGIN
            WRITELN('INPUT UNPERTURBED DEPTH AT D.S.
            SECTION, M');
            READLN;
            READ(HBEND)
      END;
WRITELN('INPUT BED ELEVATION AT DAM');
READLN;
READ(ETA[1]);
WRITELN('IS THIS AN EXTENDED RUN 1 = YES, 2 = NO');
READLN;
READ(ANSWER);
IF ANSWER <> 1 THEN  (* STARTING A NEW RUN *)
      BEGIN
            EXTENDRUN:= FALSE;
            DELTA:= FALSE;
            IF M <> 0 THEN
            BEGIN
                  FOR I:= 1 TO NB DO
                  READ(ETA[I])  (* READ BED ELEV IN CHANGING
                        WIDTH *)
            END
      END
ELSE
      BEGIN
            EXTENDRUN:= TRUE;
            IF SHOCK = TRUE THEN
                  BEGIN
                        WRITELN('IS THERE A DELTA 1 = YES, 2 = NO');
                        READLN;
                        READ(ANSWER);
                        IF ANSWER = 1 THEN
                              BEGIN
                                    DELTA:= TRUE;
                                    WRITELN('INPUT DELTA,M');
                                    READLN;
                                    READ(LOCDELTA);
                                    WRITELN('INPUT LIP, TOE EL, LIP
                                    WIDTH, M');
                                    READLN;
                                    READ(ETALIP,ETATOE,BLIP)
                              END
                  END
            ELSE DELTA:= FALSE;
            I:= 0;
            WHILE NOT EOF DO
                  BEGIN
                        I:= I + 1;
                        READLN(X[I],B[I],ETA[I])  (* READ  BED &
                        WIDTH *)
                  END;
```

```
                N:= I - 1 (* NO. OF INCREMENTS IS (NO. OF NODES) - 1 *)
            END
        END;

PROCEDURE INITIALIZATION;

    VAR

        HFLUME,HGUESS,SDUMMY:  REAL;

    BEGIN
        DETA:= 0.0;
        HLIP:= 0.0;
        D50:=  D50/1000;  (* D50 NOW IN METERS *)
        R:= SG - 1;
        XL:= N*DX;
        TIME:= TSTART;
        IF DELTA = FALSE THEN LOCDELTA:= XDAM;
        HIN:= 0.285 * EXP(-0.3*LN(G)) * EXP(0.1*LN(KS)) *
              EXP(0.6*LN(QT/B0)) * EXP(-0.3*LN(SINIT));  (* MANNING-
        TYPE LAW *)
        BEND:= B0 + M * XB;
        LIMIT:= 1;
        CBT:= 0.005;  (* INITIAL GUESSES *)
        CDT:= 0.001;
        CGT:= 0.004;
        CWT:= 0.002;
        IF FLUME = TRUE THEN
            BEGIN
                COEFF:= 18;
                TAUSR:= 0.04;
                TAUMIN:= 0.03412
            END
        ELSE
            BEGIN
                COEFF:= 11.2;
                TAUSR:= 0.03;
                TAUMIN:= 0.02559
            END;
        VISC:= 0.00000179/(1 + 0.03368*TEMP + 0.000221*TEMP*TEMP);
        QW:= QT/B0;
        HGUESS:= HIN;
        W:= B0;
        INITIAL:= TRUE;
        CORRECT(QW,HGUESS,W,SDUMMY,HFLUME);  (* FIND NORMAL
        DEPTH *)
        HIN:= HFLUME;
        INITIAL:= FALSE;
        LOADR;
        QSIN:= QS;  (* U.S. BOUNDARY CONDITION ON SEDIMENT FEED *)
        IF M<> 0 THEN INITIALDEPTH:= HBEND
        ELSE INITIALDEPTH:= HIN;
        CRITICAL:= EXP(1/3 * LN(QT*QT/BEND/BEND/G));
        XIEND:= INITIALDEPTH + ETA[1];
```

```
            XIENDF:= XIEND + DXIEND;
            IF INITIALDEPTH + DXIEND < CRITICAL THEN XIEND:=
                  XIEND - (INITIALDEPTH - 1.01 * CRITICAL)
            ELSE XIEND:= XIENDF;
            H[1]:= XIEND - ETA[1];
            TOTX:= DX*N/1000;
            FIRSTTIME:= TRUE;
            FIRSTDELTA:= FALSE;
            WARNING:= FALSE;
            IF EXTENDRUN = TRUE THEN BACKWATER
            ELSE
                  BEGIN
                        NEARNORMAL:= FALSE;
                        REPEAT
                              SETBED;
                              BACKWATER;
                              IF ((ABS((H[N+1] - HIN)/HIN) <= 0.02) AND (N MOD
                              MULT = 0))
                              THEN NEARNORMAL:= TRUE
                              ELSE
                                    BEGIN
                                          FIRSTTIME:= FALSE;
                                          N:= N + 1
                                    END
                        UNTIL NEARNORMAL;
                        FIRSTTIME:= TRUE;
                        N:= BWLM*N;
                        SETBED;
                        BACKWATER
                  END;
            TOTX:= DX*N/1000;  (* INITIAL TOTAL DISTANCE IN KILOMETERS
            *)
            TP:  0;
            J:= 0;
            IF ((DXIEND > 0) AND (DELTA = TRUE)) THEN
                  BEGIN
                        LIMIT:= TRUNC((LOCDELTA - XDAM)/DX) + 1;
                        VSVOID:= 0;
                        VSFILL:= 0;
                        ETALIPOLD:= ETALIP;
                        ETAOLD:= ETA[LIMIT + 1]
                  END
            ELSE DELTA:= FALSE;
            IF DXIEND < 0 THEN DELTA:= FALSE
      END;

PROCEDURE HEADER;
      BEGIN
            WRITELN('************************************************
                  **********');
            WRITELN('AGGRADATION AND DEGRADATION IN RESERVOIRS');
            WRITELN('LAST MODIFIED  ON 26 JUNE 1989');
            WRITELN('SOURCE CODE FILENAME IS SDTEST8');
```

```
        WRITELN('**********************************************
        **********');
        WRITELN;
        IF FLUME = TRUE THEN WRITELN('THIS RUN IS FOR A FLUME');
        IF SHOCK = TRUE THEN WRITELN('A SHOCK WILL BE FIT TO THE
        DELTA');
        WRITELN('ITERATING BW IS ',BWLM,' TIMES INITIAL BW
    DISTANCE');
        WRITELN('FINAL BW CAN BE ',LMULT,' TIMES INITIAL
        DISTANCE');
        IF SHOCK = TRUE THEN WRITELN('MULTIPLY DX BY ',MULT,'
        >SHOCK');
        WRITELN('QT = ',QT:5:3,' M3/S    D50 = ',D50:8:6,' M');
        WRITELN('INITIAL UNIFORM SLOPE = ',SINIT:8:6,'   ROUGHNESS =
        '                    ,KS:6:4, ' M');
        WRITELN('SPECIFIC GRAVITY = ',SG:3:2,'   POROSITY = ',POR:3:2);
        WRITELN('DX = ',DX:6:3,' M    DT = ',DT:8:2,
              ' SECONDS');
        WRITELN('UNIFORM WIDTH = ',B0:5:2, 'M    CHANGE FACTOR =
        ',M:6:4, '  B.P. DIST. = ',XB:10:4,' M');
        WRITELN('INITIAL DEPTH = ',HIN:6:4, '  D.S. CHANGE =
        ',DXIEND:6:4,'                M');
        IF M<> 0 THEN
              WRITELN('INITIAL DEPTH AT LIP = ', HBEND:6:4,'  M');
        WRITELN('INITIAL LOAD = ',QSIN*B0:8:6,' M3/S');
        WRITELN('DAM LOCATION, M ',XDAM:10:6);
        WRITELN('INITIAL BW DISTANCE = ',TOTX:10:5,' KM   LENGTH
        MULT FACTOR = LMULT);
        WRITELN('STARTTIME = ',TSTART:6:4,'TOTAL TIME =
              ',TOTTIME:10:2)
    END;

PROCEDURE DELTAMOVE;  (*  MOVE THE SHOCK  *)

    VAR

        DDT,DELT,DN,DPDT,D1,ER,N1,N3,S1,S2,VSIN,VMOVE,W1,XM:
        REAL;

        BOMB,CONV:  BOOLEAN;

        K:  INTEGER;

    BEGIN
        S1:= (ETA[LIMIT + 2] - ETA[LIMIT + 1])/DX;
        ETALIP:= ETA[LIMIT + 1] - S1*(LIMIT*DX - (LOCDELTA - XDAM));
        IF ETALIP < ETALIPOLD THEN ETALIP:= ETALIPOLD;
        VSVOID:= VSVOID + (1 - POR) *
              0.25*(ETA[LIMIT + 1] - ETAOLD + ETALIP - ETALIPOLD)
              * (BLIP + B[LIMIT + 1])*(LIMIT*DX - (LOCDELTA - XDAM));
        VSIN:= QSLIMIT * DT * B[LIMIT + 1];
        VSFILL:= VSFILL + VSIN;
        VMOVE:= (VSFILL - VSVOID)/(1-POR);
        IF VMOVE > 0 THEN
```

```
BEGIN
        VSFILL:= 0;
        VSVOID:= 0;
        N1:= ETALIP;
        N3:= ETATOE;
        D1:= N1 - N3;
        W1:= BLIP;
        IF LOCDELTA - XDAM - DX*(LIMIT - 1) = 0 THEN
                S2:=(ETA[LIMIT - 1] - ETA[LIMIT - 2])/DX
        ELSE S2:= (ETATOE - ETA[LIMIT])/
                (LOCDELTA - XDAM - DX*(LIMIT - 1));
        DELT:= VMOVE/D1/W1;
        K:= 1;
        IF LOCDELTA > XB THEN XM:=0.0
        ELSE XM:= M;
        REPEAT
                DDT:= VMOVE - 0.25*DELT*(D1 + N1 - S1*DELT - N3
        +S2*DELT) *(2*W1 + XM*DELT);
                DPDT:= 0.25*((2*D1 + 2*N1 - 2*N3)*(W1 +XM*DELT) +
                (S1 - S2)*(-4*DELT*W1 - 3*XM*DELT*DELT));
                DN:= DELT - DDT/DPDT;
                ER:= ABS(2*(DN - DELT)/(DN + DELT));
                IF ER < 0.001 THEN CONV:= TRUE
                ELSE IF K > 50 THEN
                        BEGIN
                                BOMB:= TRUE;
                                WRITELN('DELTAMOVE BOMBED')
                        END
                ELSE
                        BEGIN
                                K:= K + 1;
                                DELT:= DN
                        END
        UNTIL CONV OR BOMB;
        LOCDELTA:= LOCDELTA - DN;
        ETATOE:= ETATOE - S2*DN;
        IF LOCDELTA < XB THEN BLIP:= BLIP + M*DN
        ELSE BLIP:= B0;
        IF LOCDELTA - XDAM < DX*(LIMIT - 1) THEN
                BEGIN
                        ETAOLD:= ETA[LIMIT + 1]- DX*(ETA[LIMIT + 1] -
                                ETALIP/(DX*LIMIT - (LOCDELTA - XDAM)
                                - DN);
                        LIMIT:= LIMIT - 1;
                        ETA[LIMIT + 1]:= ETAOLD
                END
        ELSE ETAOLD:= ETA[LIMIT + 1];
        ETALIP:= ETALIP - S1*DN
    END
ELSE ETAOLD:= ETA[LIMIT + 1];
ETALIPOLD:= ETALIP;
IF LOCDELTA - XDAM < 0 THEN
    BEGIN
        RESULTS;
```

```
                    DELTA:= FALSE;
                    LIMIT:= 1
                END
            END;

PROCEDURE DELTAHT; (* FIND THE HEIGHT OF THE SHOCK *)

    VAR

        FP,FX,FX1,FX2,FX3,P:  REAL;

    BEGIN
        FX:= ETA[DNODE + 6];
        FX1:= ETA[DNODE + 16];
        ETALIP:= FX - (FX1 - FX)*6/10;
            (* LOCATE TOE WITH LINEAR EXTRAPOLATION FROM 5
            NODES
        FX:= ETA[DNODE - 6];
        FX1:= ETA[DNODE - 5];
        ETATOE:= FX1 + 5*(FX1 - FX)
    END;

PROCEDURE CHECKDELTA;  (* CHECK FOR A DELTA *)
    VAR

        XEND: BOOLEAN;

        XSLOPE: REAL;

        I,K: INTEGER;

    BEGIN
        XEND:= FALSE;
        I:= N + 1 - 16;
        REPEAT
            XSLOPE:= (ETA[I] - ETA[I-1])/DX;
            IF ((XSLOPE >= 5*SINIT) AND (I > 6)) THEN
                BEGIN
                    DELTA:= TRUE;
                    FIRSTDELTA:= TRUE;
                    DNODE:= I - 1;
                    LOCDELTA:= (DNODE - 1)*DX + XDAM;
                    BLIP:= B[DNODE];
                    DELTAHT;
                    RESULTS;
                    N:= N DIV MULT;
                    DX:= DX*MULT;
                    DT:= DT*MULT;
                    LIMIT:= (DNODE*10 + 8*MULT) DIV (MULT*10);
                    FOR K:= 1 TO N + 1 DO
                        BEGIN
                            B[K]:= B[(K-1)*MULT +1];
                            H[K]:= H[(K-1)*MULT +1];
                            ETA[K]:= ETA[(K-1)*MULT +1];
```

```
                                    TAU[K]:= TAU[(K-1)*MULT +1]
                                END;
                            ETALIPOLD:= ETALIP;
                            ETAOLD:= ETA[LIMIT + 1];
                            RESULTS;
                            VSFILL:= 0;
                            VSVOID:= 0
                        END
                    ELSE
                        BEGIN
                            I:= I - 1;
                            IF I < 7 THEN XEND:= TRUE
                        END
                UNTIL DELTA OR XEND
                END;

PROCEDURE DUMPR; (* ADJUST BED ELEVATIONS *)

    VAR

        I,IEND: INTEGER;

    BEGIN
        IF SHOCK = TRUE THEN
        IF ((DXIEND > 0) AND (DELTA = FALSE)) THEN
        IF N > 22 THEN CHECKDELTA;
        IF ((DXIEND > 0) AND (DELTA = TRUE)) THEN IEND:= LIMIT + 1
        ELSE IEND:= 1;
        QUP:= QSIN;
        FOR I:= N + 1 DOWNTO IEND DO
            BEGIN
                TAUG:= TAU[I];
                LOADR;
                QDOWN:= QS;
                IF I = N+1 THEN ETA[I]:= ETA[I] + DT/DX/(1-POR)*(QUP-
                QDOWN)
                ELSE
                    BEGIN
                        DETA:= DT/DX/(1 - POR)/B[I]*
                            (B[I+1]*QUP - B[I]*QDOWN);
                        ETA[I]:= ETA[I] + DETA
                    END;
                QUP:= QDOWN
            END;
        QSLIMIT:= QUP;
        IF ((DELTA = TRUE) AND (FIRSTDELTA = FALSE)) THEN
        IF LOCDELTA > 0 THEN DELTAMOVE;
        IF ((DELTA = TRUE) AND (FIRSTDELTA = TRUE)) THEN
    FIRSTDELTA:=FALSE
    END;

BEGIN
    INPUTDATA;
    INITIALIZATION;
```

```
        HEADER;
        RESULTS;
        WHILE TIME < TOTTIME DO
              BEGIN
                    J:= J + 1;
                    TIME:= TIME + DT;
                    FIRSTTIME:= TRUE;
                    NEARNORMAL:= FALSE;
                    REPEAT
                          BACKWATER;
                          IF ((ABS((H[N+1] - HIN)/HIN) <= 0.02) AND (N MOD MULT
                          = 0))
                          THEN NEARNORMAL:= TRUE
                          ELSE
                                BEGIN
                                      IF N < TOTX*1000*LMULT/DX THEN
                                            BEGIN
                                                  N:= N + 1;
                                                  FIRSTTIME:= FALSE;
                                                  SETBED
                                            END
                                      ELSE NEARNORMAL:= TRUE
                                END
                    UNTIL NEARNORMAL;
                    TP:= TP + DT;
                    IF  TP >= TPRINT THEN
                          BEGIN
                                RESULTS;
                                TP:= 0
                          END;
                    DUMPR
              END
END.
```

Table A3.2 Procedure names and descriptions

Procedure Name	Function
Backwater	Controls options for computing backwater curves. Checks for rate of drawdown for sluicing, forces depths to remain one per cent above critical at all nodes.
Calch	Calculates depth at next upstream node using the standard step backwater equation (Chapter 4).
Checkdelta	Computes bed slope for all nodes and checks to see if slope exceeds five times the equilibrium slope. If it does, a shock is fit (see Deltaht).
Correct	Finds normal depth in an open channel or flume and corrects for sidewall and bedform influences.
Deltaht	Computes the elevation of the top and bottom of the vertical shock face the first time it is fit to the bed (simulates a delta).
Deltamove	Computes new elevations of top and bottom of the vertical shock face and the distance the shock is moved forward for each time step.
Depth	Computes the normal depth in an open channel or flume.
Dumpr	Adjusts all bed elevations using the sediment continuity equation for each time step.
Extendbw	Extends the backwater profile upstream by one node. Used when the water depth at the current upstream limit of the backwater zone is not within 1 per cent of normal
Fd	Finds the value of X in the Einstein-Barbarossa equation (Equation 4.5) when flow is not fully turbulent rough.
Freynolds	Finds the friction coefficient for a smooth wall; explicit function of Reynolds number (Equation A1.9)
Header	Prints out header of results file; lists initial geometric, hydraulic, and sediment transport values and control variables.
Initialization	Computes normal depth and sediment discharge and initial backwater profile showing effects of changing the water surface elevation at the downstream boundary.
Inputdata	Receives input data for the program

Loadr	Computes sediment transport per unit width using the Parker equation (Equation 4.4).
Results	Prints results at designated times. Includes bed and water surface elevation, depth, and sediment transport value for each node and the location and elevations of the shock face (if modeled).
Setbed	Computes the elevation and width associated with the distance nodes for a new run.
Slophead	Calculates the Froude number, energy slope, and total energy head for a node. Using Correct, computes the dimensionless grain shear stress for each node.

Table A3.3 Listing of variables

Variable	Type	Global or in what procedure	Definition
ANSWER	INTEGER	GLOBAL	Response to input question
B	VECTOR	GLOBAL	Width, m
B0	REAL	GLOBAL	Uniform width, m
BBOMB	BOOLEAN	GLOBAL	Warning message - iteration scheme failed
BEND	REAL	GLOBAL	Width at most downstream node, m
BLIP	REAL	GLOBAL	Width of shock, m
BOMB	BOOLEAN	CORRECT,CALCH, DELTAMOVE	Warning message. Iteration scheme failed
BWLM	INTEGER	GLOBAL	Initial backwater zone length is lengthened BWLM times
CB	REAL	CORRECT	Bed friction coefficient
CBK	INTEGER	CORRECT	Convergence check for C_b
CBT	REAL	GLOBAL	Trial value for C_b
CBUSTAR	REAL	CORRECT	C_bu^*
CCONV	BOOLEAN	DEPTH	If true, iteration scheme converges
CD	REAL	CORRECT	Bedform drag coefficient
CDT	REAL	GLOBAL	Trial value for C_d
CF	REAL	GLOBAL	Friction coefficient
CG	REAL	CORRECT	Grain friction coefficient
CGINV	REAL	CORRECT	Inverse of grain friction factor
CGK	REAL	CORRECT	Convergence check for C_g
CGT	INTEGER	GLOBAL	Trial value for C_g
CGUSTAR	REAL	CORRECT	C_gu^*
COEFF	REAL	GLOBAL	Coefficient in Equation (4.4)
CONV	BOOLEAN	CORRECT,CALCH, DELTAMOVE	Convergence flag
CRIT	REAL	BACKWATER	Critical depth, m
CRITICAL	REAL	GLOBAL	Critical depth, m
CTEST	REAL	CORRECT	Sum of CBT, CGT,CWT, and HK
CW	REAL	CORRECT	Wall friction coeffiecient
CWK	INTEGER	CORRECT	Convergence check for C_w
CWT	REAL	GLOBAL	Trial value for C_w
D1	REAL	DELTAMOVE	Height of shock, m
D50	REAL	GLOBAL	Median sediment diameter, m
D50DEL	REAL	FD	d_{50}/δ in determination of X in Einstein-Barbarossa equation
DDT	REAL	DELTAMOVE	Function describing how far the shock moves, m
DELT	REAL	DELTAMOVE	Guess of how far shock moves, m
DELTA	BOOLEAN	GLOBAL	If true, a shock exists

DN	REAL	DELTAMOVE	Next guess of how far shock moves, m
DNODE	INTEGER	GLOBAL	Node number at which shock is first located
DPDT	REAL	DELTAMOVE	Derivative of function describing how far the shock moves
DT	REAL	GLOBAL	Time step, seconds
DX	REAL	GLOBAL	Distance step, m
DXIEND	REAL	GLOBAL	Total change in downstream water surface, m
DXX	REAL	BACKWATER	Distance step for backwater calculations, m
ER	REAL	CORRECT,CALCH, DELTAMOVE	Difference between successive guesses in iteration schemes
ETA	VECTOR	GLOBAL	Bed elevation, m
ETALIP	REAL	GLOBAL	Elevation of top of shock, m
ETALIPOLD	REAL	GLOBAL	Elevation of top of shock for previous time step, m
ETAOLD	REAL	GLOBAL	Bed elevation one node upstream of shock for previous time step, m
ETATOE	REAL	GLOBAL	Elevation of bottom of shock, m
ETC	REAL	BACKWATER	Bed elevation used in backwater scheme m
EXTENDRUN	BOOLEAN	GLOBAL	If true, this is a continuation run
FC	REAL	CORRECT	Equation A1.18
FCG	REAL	CORRECT	CGT/FC
FCW	REAL	CORRECT	CWT/FC
FDELTA	REAL	CORRECT	Equation A1.13
FIRSTTIME	BOOLEAN	GLOBAL	If true, new run or first time to calculate backwater profile for a time step
FLUME	BOOLEAN	GLOBAL	If true, run is for a flume
FR2	REAL	GLOBAL	Square of Froude number
FRE	REAL	CORRECT	Darcy-Weisbach friction coefficient
FX	REAL	DELTAHT	Bed elevation 6 nodes upstream or downstream of initial shock location, m
FX1	REAL	DELTAHT	Bed elevation 16 nodes upstream or 5 nodes downstream of initial shock location, m
G	CONSTANT	GLOBAL	Gravitational constant, m/sec^2
H	VECTOR	GLOBAL	Water depth, m
HBEND	REAL	GLOBAL	Water depth at downstream boundary, m
HFLUME	REAL	INITIALIZATION	Normal depth in flume, m
HGUESS	REAL	INITIALIZATION	Guess of normal depth in flume, m

HIN	REAL	GLOBAL	Normal depth, m
HK	INTEGER	CORRECT	Convergence check for depth
HLIP	REAL	GLOBAL	Water depth above shock, m
HN	REAL	BACKWATER,CORRECT	Next guess for water depth, m
HT	REAL	BACKWATER	Trial guess of water depth, m
HTT	REAL	CORRECT	Trial value of water depth in normal depth iteration, m
HYRADIUS	REAL	CORRECT	Hydrauic radius, m
I	INTEGER	RESULTS,SETBED,BACKWATER, EXTENDBACKWATER, INPUTDATA, DUMPR,CHECKDELTA	Counter
IB	INTEGER	BACKWATER,EXTENDBW	Counter
IEND	INTEGER	DUMPR	Most downstream node for adjusting bed elevations
INITIAL	BOOLEAN	GLOBAL	If true, compute normal depth
INITIALDEPTH	REAL	GLOBAL	Initial depth at downstream boundary before raising or lowering occurs, m
J	INTEGER	GLOBAL	Time step counter
K	INTEGER	CORRECT,CALCH, DELTAMOVE, CHECKDELTA	Counter in iteration schemes
KK	INTEGER	DEPTH	Counter
KS	REAL	GLOBAL	Roughness height, m
LIMIT	INTEGER	GLOBAL	Node beyond which conditions do not change
LMULT	INTEGER	GLOBAL	Largest number of computational reach lengths allowed
LOCDELTA	REAL	GLOBAL	Location of shock, m
M	REAL	GLOBAL	Rate of divergence in flume
MULT	INTEGER	GLOBAL	Number by which distance and time steps are multiplied after a shock has been fit
N	INTEGER	GLOBAL	Total number of distance increments
N1	REAL	DELTAMOVE	Elevation of top of shock, m
N3	REAL	DELTAMOVE	Elevation of bottom of shock, m
NB	INTEGER	BACKWATER,EXTENDBW	Number of distance increments in diverging portion of flume
NEARNORMAL	BOOLEAN	GLOBAL	If true, water depth is within one percent of normal
P	REAL	CORRECT	Wetted perimeter, m
POR	REAL	GLOBAL	Porosity

QDOWN	REAL	GLOBAL	Sediment transport per unit width at downstream end of reach, m^2/sec
QS	REAL	GLOBAL	Sediment transport, m^2/sec
QSIN	REAL	GLOBAL	Steady sediment input rate, m^2/sec
QSLIMIT	REAL	GLOBAL	Sediment transport per unit width past the last node for computations, m^2/sec
QT	REAL	GLOBAL	Total water discharge, m^3/sec
QUP	REAL	GLOBAL	Sediment transport per unit width at upstream end of reach, m^2/sec
QW	REAL	BACKWATER	Water discharge per unit width, m^2/sec
R	REAL	GLOBAL	Submerged specific gravity
RE	REAL	CORRECT	Reynolds number
S1	REAL	DELTAMOVE	Channel slope immediately upstream of shock
S2	REAL	DELTAMOVE	Channel slope immediately downstream of shock
SD	REAL	BACKWATER	Energy slope at downstream end of reach
SDUMMY	REAL	INITIALIZATION	Channel slope
SF	REAL	GLOBAL	Energy slope
SG	REAL	GLOBAL	Specific gravity of sediment
SHOCK	BOOLEAN	GLOBAL	If true, a shock will be fit to the bed if appropriate
SINIT	REAL	GLOBAL	Normal slope
SU	REAL	BACKWATER	Energy slope at upstream end of reach
TAU	VECTOR	GLOBAL	τ/ρ, m^2/sec^2
TAUG	REAL	GLOBAL	τ/ρ, m^2/sec^2
TAUMIN	CONSTANT	GLOBAL	Value of TAUG below which there is no transport
TAUSR	REAL	GLOBAL	Critical bed shear stress in Equation (4.4)
TEMP	REAL	GLOBAL	Water temperature, degrees Celsius
THD	REAL	BACKWATER	Total energy head at downstream end of reach, m
THU	REAL	BACKWATER	Total energy head at upstream end of reach, m
TIME	REAL	GLOBAL	Accumulated simulation time, sec
TOTTIME	REAL	GLOBAL	Total simulation time, sec
TOTX	REAL	GLOBAL	Length of backwater zone, m
TP	REAL	GLOBAL	Accumulated time between printing results, sec
TPRINT	REAL	GLOBAL	Time between printing results, sec
TSTART	REAL	GLOBAL	Time at start of simulation, sec

U	REAL	CORRECT	Mean cross-sectional velocity, m/sec
UNODE	REAL	GLOBAL	
VISC	REAL	GLOBAL	Kinematic viscosity of water, m^2/sec
VMOVE	REAL	DELTAMOVE	Volume of sediment available for moving the shock, m^3
VSFILL	REAL	GLOBAL	How much the layer upstream of shock has been filled, m^3
VSIN	REAL	DELTAMOVE	Volume of sediment passing last node upstream of shock, m^3
VSVOID	REAL	GLOBAL	Volume of layer upstream of shock resulting from raising node immediately upstream, m^3
W	REAL	CORRECT	Channel width, m
W1	REAL	DELTAMOVE	Width of shock, m
WARNING	BOOLEAN	GLOBAL	If true, flow conditions are in upper regime flat bed
X	VECTOR	GLOBAL	Distance associated with nodes, m
XB	REAL	GLOBAL	Distance at which flume begins to diverge, m
XDAM	REAL	GLOBAL	Location of dam, m
XDUMMY	REAL	SLOPHEAD	Normal depth, m
XEND	BOOLEAN	CHECKDELTA	If true, counter is less than 6
XETA	REAL	SLOPHEAD	Bed elevation, m
XH	REAL	SLOPHEAD	Water depth, m
XIEND	REAL	GLOBAL	Water surface elevation at downstream boundary of model, m
XIENDF	REAL	GLOBAL	Final elevation of water surface at downstream boundary, m
XL	REAL	GLOBAL	Length of backwater zone input by user, m
XM	REAL	DELTAMOVE	Rate at which flume diverges
XQ	REAL	SLOPHEAD	Water discharge per unit width, m^2/sec
XS	REAL	SLOPHEAD	Energy slope
XSLOPE	REAL	CHECKDELTA	Channel slope between 2 nodes
XT	REAL	LOADR	Dimensionless grain shear stress
XTH	REAL	SLOPHEAD	Total energy head, m
XW	REAL	SLOPHEAD	Channel width, m
XX	REAL	LOADR	Dimensionless sediment transport